

**ROLE OF MAGNETIC RESONANCE IMAGING IN
DIAGNOSIS OF PEDIATRIC INTRACRANIAL
TUMORS**

Thesis

**Submitted in Partial Fulfillment of The M.D Degree in
Radiodiagnosis**

BY

Mokhtar Ragab Ramadan Mahmoud
Assistant Literature of Radiodiagnosis ,Al Azhar University

Supervised By

Prof. Dr. Hesham A. Al- Razik Ahmed Galal
Professor of Radiodiagnosis Faculty of Medicine
Al Azhar University

Prof. Dr. saalah El Din Mohamed Korayem
Assistant Professor of Radiodiagnosis Faculty of
Medicine, Al Azhar University

Prof. Dr. Shehab Mohamed EL Khadrawy
Profeeor of Neurosurgery Faculty of Medicine,
Al Azhar University

Faculty of Medicine
Al Azhar University
2003



To

my family

Mokhtar Ragab

ACKNOWLEDGEMENT

First and foremost thanks to GOD, to whom I related any success in achieving any work in my life.

I would like to express my deepest gratitude to PROF. Dr. Hesham A AL- Razik Ahmed, proffesor of Radiodiagnosis, Faculty of Medicine, Al Azhar University. For his kind supervision, sincere cooperation and incomparable support throughout the whol work.

I wish to express my thanks to Prof. Dr. Salah Mohamed Korayem, Assistant Prof of Radiodiagnosis, Faculty of Medicine, Al Azhar University. For his most useful help and contineous encouragement for the completion of this study.

Also I wish to expressmy thanks to Prof. Dr. Şhehab Mohamed EL – Khadrawy, Prof of neurosurgery, Faculty of Medicine. Al Azhar University. for his most useful helpful, sincere cooperation and contineous encouragement for the completion of this study.

Finally, I would like to record my appreciation and gratitude to every kind hand that helped me to accmplish this work.

CONTENTS

<i>Title</i>	<i>Page</i>
* <i>Introduction and Aim of The Work</i>	1
* <i>Review of Literature</i>	3-112
- Gross anatomy of the brain	3
- MRI anatomy of the brain	23
- Pathology of pediatric intracranial tumors ...	43
- Other modalities of diagnosis	80
- Basic physical principle of MRI	84
- MR Manifestations of intracranial tumors ...	93
* <i>Material and Methods</i>	113
* <i>Results</i>	117
* <i>Illustrated cases</i>	131
* <i>Discussion</i>	171
* <i>Summary and Conclusion</i>	188
* <i>References</i>	191
* <i>Arabic summary</i>	

LIST OF ABBREVIATIONS

- ACA : Anterior cerebral artery.
- AcoA : Anterior communicating artery.
- AVMS : Angiomatous malformation.
- B A : Basilar artery.
- CC : Corpus callosum.
- C H : Cerebral hemisphere.
- CNS : Central nervous system.
- CPA : Cerebello pontine angle.
- CSF : Cerebrospinal fluid .
- CT : Computarized tomography.
- EAM : External auditory meatus.
- FID : Field induction decay.
- Gd- DTPA : Gadolinium diethylene- triamine penta acetic acid.
- ICA : Internal carotid artery.
- IHF : Interhemispheric fissure.
- ISS : Inferior sagittal sinus.
- IV : Intravenous.

- MCA : Middle cerebral artery.
- MR : Magnetic resonance .
- MRA ; Magnetic resonance angiography.
- MRI : Magnetic resonance imaging .
- MRV : Magnetic resonance venography
- NICU : Neonatal intensive care unit .
- NF1 : Neurofibromatosis type 1.
- NF2 : Neurofibromatosis type 2.
- PCA : Phase contrast angiography.
- PCA : Posterior cerebral artery.
- PCAs : Posterior cerebral arteries.
- PcoA : Posterior communicating artery.
- RF : Radio frequency.
- S : Syphon.
- SS : Straight sinus.
- SSS : Superior sagittal sinus.
- T : Tesla (unit of magnetic field intensity).
- T1- W : T1- weighted image.

T2- W : T2 – weighted image.

TE : Echo time.

ToF : time of flight.

ToNE : Tilted optimized non – saturated excitation.

TR : Repitition time.

**INTRODUCTION
AND
AIM OF THE WORK**

Introduction and aim of the work

In the diagnostic work up of intracranial tumors, the primary role of imaging studies are to detect the abnormality, localize and determine the extent of the lesion and provide a list of differential diagnosis or if possible, the specific diagnosis [Ann et al, 1990].

Because of its unique features of exceptionally high soft tissue contrast and ability to image in any pre determined orientation, MRI has been considered a major step forward in medical imaging. [Mauricio Costillo et al, 1998].

Magnetic resonance [MR] is the imaging modality of choice in most disorders that affect the paediatric brain.

Intracranial tumors are the most frequent type of solid tumors and the second most common form of malignant disease in children under the age of 16 years, being exceeded by leukaemia, These tumors constitute the second commonest cause of cancer death in children of this age group [Pierre et al, 1997].

Over 90 percent of primary CNS tumors in children are located within the intracranial cavity. They primarily involve the brain, meninges, pineal gland, optic nerves, or parasellar region with tumors of the cranial nerve roots being rare. Many of the older statistical studies analysing distribution of CNS tumors in children, have ephasised their predilection for posterior fossa

structures, however, more recent analysis have demonstrated that about half of the pediatric brain tumors occur in the supratentorial region [Higano et al, 1997].

Supratentorial tumors are more common in infants and children up to the age of 3 years, however, from 4 to 11 years of age there is an infratentorial predominance [Markow, 1989].

Neuroepithelial tumor, mainly glial tumor, as a group represent the majority of neonatal tumors [Eric N faerber et al, 1997].

MRI is a sensitive technique for delineation of brain morphology in the axial, coronal and sagittal planes without changing patient position or any known biological hazard [Markow, 1989].

The aim of this work is to throw some light on the value of magnetic resonance imaging [MRI] in the evaluation of pediatric intracranial tumors.

ANATOMY

The cranial cavity is separated into supratentorial and infratentorial compartments by a rigid sheet of dura [tentorium cerebelli], the supratentorial compartment is the larger one and occupied by the cerebral hemisphere [Gado and Tobben,1992].

The brain is consists of three major components and each of which is composed of several parts:

1- Fore brain [prosencephalon] :

* Telencephalon.

* Diencephalon.

2- Mid brain [mesencephalon].

3- Hind brain [rhombencephalon] :

- Pons and medulla.

- Cerebellum. [Gado and Tobben,1992].

A) Telencephalon :

Consists of the two cerebral hemispheres that occupy most of the cranial cavity. They are separated by the longitudinal interhemispheric fissure which is interrupted by the fibers that

extend into the white matter of both hemispheres [Gado and Tobben, 1992].

The surface of the cerebral hemispheres describe convolutions caused by overgrowth of the cerebral cortex [gray matter] compared to the underlying white matter [centrum semiovale].

The convolutions [gyri] are separated by depressions [sulcci] [Gado and Tobben, 1992].

Each cerebral hemisphere has three surfaces, lateral, medial and inferior surfaces separated by the superomedial, superolateral, inferomedial and inferolateral borders [Gado and Tobben, 1992].

The three surfaces of the cerebral hemisphere contain numerous sulcci that separate the cerebral gyri. Four of these sulcci are helpful in dividing each cerebral hemisphere into its constituent lobes [frontal, temporal, parietal and occipital lobes], they are, the lateral sulcus [sylvian fissure], the central sulcus [Rolandic fissure], the parieto-occipital sulcus and the calcarine sulcus [Gado and Tobben].

B) Diencephalon :

It consists of several structures that lie around the third ventricle and connect the midbrain on one side to the cerebral hemisphere on the other side. This structures are:

1- The thalami :

They are two ovoid masses small in size anteriorly and more voluminous posteriorly. The small anterior end forms the posterior boundary of the foramina of Monro, the voluminous posterior end is the pulvinar. The medial surface of the thalamus forms the lateral wall of the third ventricle and is separated from the opposite thalamus by the third ventricle itself [Truwit and Lempert, 1994].

2- The geniculate bodies :

They are medial and lateral on each side, all four structures constitute the metathalamus. The lateral geniculate bodies are connected by the superior brachium to the superior colliculus and serve as a part of the auditory pathways [Truwit and Lempert, 1994].

3- The epithalamus :

The habenula, the pineal body and the posterior commissure constitute the epithalamus. The stalk which attaches the pineal gland consists of superior and inferior lamina. The superior lamina is formed by the habenula while the inferior lamina is formed by the posterior commissure. Between the two laminae is the pineal recess of the third ventricle [Schnitzlein and Murlagh, 1990].

4- The hypothalamus:

The mamillary bodies, the tuber cinereum, the infundibulum, the hypophysis and the optic chiasma, constitute the hypothalamus. The majority of the ventral external surface of the diencephalon is formed by the hypothalamus, it also form the floor and lateral wall of the third ventricle [Truwit and Lempert,1994].

5- The subthalamus:

It is located lateral and caudal to the hypothalamus. Functionally it is a part of the extrapyramidal motor system [Truwit and Lempert,1994].

The Midbrain [Mesencephalon]

The midbrain (mesencephalon) is a short segment of the brainstem. it connects the pons and cerebellum on the one hand with the forebrain on the other hand. The brain stem thus consists of the midbrain, the pons and the medulla. The latter two are part of the hindbrain. [Hirsch , et al, 1989].

The midbrain consists of a smaller dorsal portion called the tectum and a larger anterior portion formed by the cerebellar peduncles. Between the tectum and the cerebellar peduncles, the central gray substance of the midbrain surrounds the aqueduct which connects the fourth and third ventricles. The cerebellar

peduncles are viewed on the ventral surface of the brain as two prominent ridges, diverging as they approach cerebral hemispheres. Thus a triangular area, the interpeduncular fossa, separates the two cerebral peduncles. The floor of the interpeduncular fossa is the posterior perforated substance. [Lockhart et al, 1974].

The tectum:

The tectum of the midbrain consists of four rounded prominences, the corpora quadrigemina or colliculi. The superior colliculi are continuous on both sides with the superior brachia, each connects one superior colliculus to the ipsilateral lateral geniculate body where the ipsilateral optic tract ends. Thus the fibres of the superior brachium connect the superior colliculus and the visual cortex. Likewise, the inferior brachia extend from the inferior colliculi to the medial geniculate bodies connecting the inferior colliculus and auditory cortex. [Hans et al 1984].

Each cerebral peduncle consists of a ventral part, the crus (or basis pedunculi), and a dorsal part, the tegmentum of the midbrain. The superior cerebellar peduncle (brachium conjunctivum) penetrates deeply into the tegmentum of the inferior part of the midbrain from the dorsal aspect on each side of the midline.

The Hindbrain:

The hind brain consists of two parts. The anterior part is the medulla oblongata inferiorly and the pons superiorly. The posterior part is the cerebellum. Between the anterior and posterior parts of the hind brain is the fourth ventricle. This communicates with the third ventricle through the aqueduct of Sylvius and the extraaxial CSF space, the subarachnoid cistern, via its midline foramen of Magendi and the two lateral recesses, the foramina of Luschka. [Carpenter, Sutin , 1983].

The Meulla Oblongata :

The medulla oblongata is contineous inferiorly with the spinal cord and superiorly with the pons. It measures 3cm in length. its cross sectional dimensions are 2cm from side to side and 1.25 cm anterioposteriorly. There are two midline grooves, a ventral and a dorsal. Anteriorly, the ventral median fissure starts below at the pyramidal decussation and ends superiorly at the inferior border of the pons. The dorsal median sulcus present only on the dorsal aspect of the inferior half of the medulla and stops at the superior half, where the dorsal surface of the medulla forms the floor of the fourth ventricle. These two midline grooves thus bisect the medulla. Each half furthemore shows two longitudinal grooves, the ventral lateral sulcus and the dorsal lateral sulcus. [Hans, 1984].

The two lateral sulci enable several structures to be identified on the surface of each lateral half of the medulla. Anteriorly, the pyramid lies between the ventral median fissure and the ventral lateral sulcus. The olive lies between the two lateral sulci. Behind the dorsal lateral sulcus and lying between it and the dorsal median fissure are the cuneate and gracile tubercles. [Hans , 1984].

The upper half of the dorsal surface of the medulla show two diverging prominences forming the lateral boundaries of the floor of the fourth ventricle. These prominences contain the inferior cerebellar peduncles (retiform bodies), which connect the spinal cord and medulla with the cerebellum.

The Pons:

The pons connects the medulla below with the midbrain above. It forms a massive protuberance, with well-defined borders, on the ventral surface of the brain stem. This protuberance is separated from the medulla oblongata by the inferior pontine sulcus and from the cerebral peduncles of the midbrain by the superior pontine sulcus. There is a shallow midline depression on the ventral surface of the pons, the basilar sulcus. The basilar artery lies in this depression. In addition to the massive ventral component of the pons, which is also called the basis pontis, there is a smaller dorsal component, the tegmentum

of the pons. The dorsal surface of the tegmentum forms the upper half of the floor of the fourth ventricle, so the floor of the fourth ventricle is formed in part by the dorsal aspect of the medulla and in part by the dorsal aspect of the pons. These two components form the rhomboid fossa. [Hans , 1984].

The Cerebellum :

The cerebellum occupies the greater part of the posterior cranial fossa. It is located on the dorsal aspect of the pons and medulla, separated from these two structures by the cavity of the fourth ventricle. The upper surface of the cerebellum lies under the tentorium cerebelli, which separates it from the occipital lobes. The posterior surface of the cerebellum lies against the inner table of the occipital bone. The cerebellum is attached to the brainstem by three cerebellar peduncles. The superior peduncle (brachium conjunctivum) connects it with the midbrain, the middle peduncle (brachium pontis) connects it with the pons, and the inferior peduncle (restiform body) connects it with the medulla. The cerebellum consists of a narrow median portion, the vermis, and two hemispheres which extend laterally and posteriorly. [Courchesne E, et al, 1989].

The superior part of the vermis begins at the anterior medullary velum, which forms the superior part of the roof of the fourth ventricle. The farthest anterior part of the superior vermis

is the lingula, which can be visualized from the ventral aspect of the cerebellum after removal of the brain stem. The part of the superior vermis behind the lingula is the central lobule, and farther posterior is the culmen. when viewed from the superior aspect, the cerebellum has a midline shallow concavity anteriorly (the anterior cerebellar fissure) and a narrow deep groove posteriorly (the posterior cerebellar fissure), The anterior part of the culmen appears at the bottom of the shallow anterior cerebellar fissure, and the folium lies at the bottom of the narrow and deep posterior cerebellar fissure. Between the culmen and folium is the declive. When viewed from the dorsal aspect, the culmen, declive, and folium of the superior vermis appear in continuity with the tuber, pyramid, and uvula of the inferior vermis. The farthest forward structure of the inferior vermis is the nodulus, this cannot be visualized from the dorsal aspect of the cerebellum but only from the ventral aspect after removal of the brainstem. [Press et al, 1989].

The cerebellar tonsils are the most anterior inferior structures of the cerebellar hemispheres. The rest of the cerebellar hemispheres on the inferior aspect consist of the biventral lobules, followed posteriorly by the inferior semilunar lobules. The horizontal fissure separating the inferior semilunar lobule from the superior semilunar lobule is best visualized on the dorsal view of the cerebellum. The superior surface of the cerebellar

hemisphere is formed at its posterior end by the superior semilunar lobule. In front of the superior semilunar lobule and separated from it by the superior posterior fissure is the lobule simplex, which in turn is separated from the quadrangular lobule by the primary fissure. [Press et al, 1990].

Blood Supply Of The Brain

A) Arterial Supply:

Three arterial stems ascend to form the main blood supply of the brain, these are the right and left internal carotid arteries and the basilar artery [formed by the union of the vertebral arteries]. [Anderson, 1983].

The right and left internal carotid arteries are termed the anterior circulation while the basilar artery is termed the posterior circulation. Both anterior and posterior circulations are join in an arterial circle around the optic chiasma and infundibulum of the pituitary stalk at the ventral surface of the brain. This arterial circle is called the circle of willis [Gray,1977].

The circle of Willis (Fig 1)

It is an interconnecting arterial polygon. The following vessels comprise the circle of Willis:

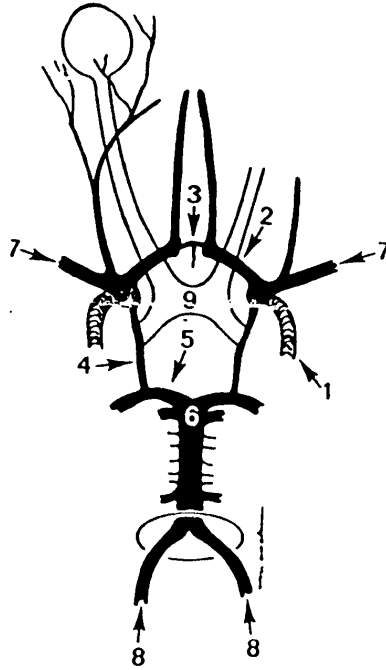


Fig (1) : Illustration of the circle of Willis (Osborn , 1994).

- 1- The two internal carotid arteries.
- 2- The horizontal segment of both anterior cerebral arteries.
- 3- The anterior communicating artery.
- 4- The posterior communicating artery.
- 5- The horizontal segment of both posterior cerebral arteries.
- 6- The basilar artery. [Osborn,1994].

Internal carotid artery [ICA]:

It begins at the bifurcation of the common carotid A opposite to the thyroide cartilage and ends by dividing into ACA and MCA. Anatomically the artey is dividing into four portions;

I. The cervical portion:

In which the artery ascend in front of the upper cervical transverse processes to enter the carotid canal in the petrous portion of the temporal bone. This portion of the artery gives no branches [Gray,1977].

II. The petrous portion:

In the carotid canal, the artery curves forward and inward then it ascends to leave the canal and enter the skull cavity. This portion of the artery gives the tympanic A [Gray, 1977].

The cavernous portion:

In this portion the artery is situated between the layers of the dura matter forming the cavernous sinus. The artery ascend anterior then curves upward percing the dura and forming the roof of the cavernous sinus. The artery is surrounded by sympathetic nerves and in relation to 3,4,5and 6 cranial nerves. The artery in this portion has an S shaped course which called the carotid syphon. This portion of the artery gives the anterior meningeal vessel and the ophthalmic artery [Gray, 1977].

The cerebral portion:

The artery passes to the inner extremity of the lateral sulcus where it gives the posterior communicating artery, in the anterior choroidal A, the ACA and the MCA [Martin, 1989].

The anterior cerebral artery [ACA] : (Fig 2)

It is the smaller of the two terminal ICA branches and ends near the callosal genu by two terminal branches the pericallosal and callosomarginal arteries, anatomically it is divided into:

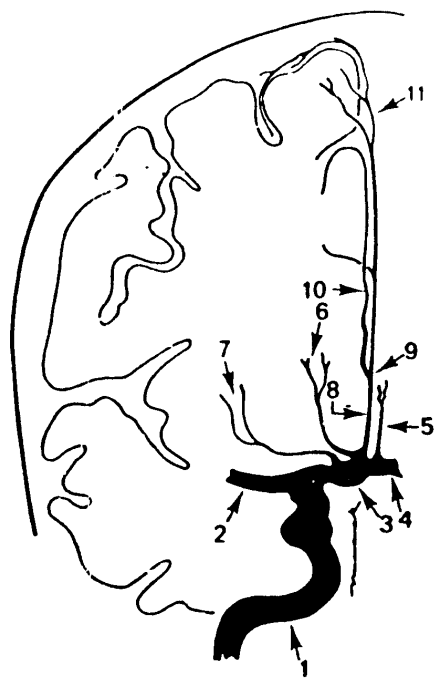


Fig (2) : The anterior cerebral artery.

A₁ (Horizontal) segment :

Extends from the ACA origin to its junction with the anterior communicating A. Deep perforating branches and the medial lenticulostriate artery arise from this segment to supply the head of the caudate nucleus and anterior limb of the internal capsule [Ghika et al, 1990].

A₂ segment :

This segment includes the artery from its junction with the anterior communicating A to its bifurcation.

The A₂ segment courses cephalad in the cistern of the lamina terminalis and curves around the corpus callosal genu where it gives the two terminal branches. (Ghika et al, 1990).

A₃ cortical branches:

Classically, cortical ACA branches are supply the anterior two thirds of the medial hemispheric surfaces plus a small superior area that extends over the convexities [Nathal et al,1992].

The middle cerebral artery (MCA) :

The MCA is the largest of the two ICA branches, the artery is divided into:

Horizontal (M₁) segment :

It extends laterally from its origin to its bifurcation at the sylvian fissure. Deep perforating branches and lateral lenticulostriate arteries.

Arise from this segment to supply the lentiform nucleus, caudate nucleus and part of the internal capsule [Nathal et al, 1992].

Insular [M₂] segment :

It is the MCA segment which gives the insular branches that loop over the insula and then passes laterally to exit from the sylvian fissure [Nathal et al,1992].

Opercular [M₃] segments :

These are the MCA branches as they emerge from the sylvian fissure and ramify over the hemispheric surface (Nathal et al, 1992).

Posterior cerebral artery (PCA) :

It originates from the basilar artery bifurcation, the PCA segments and branches are:

Precommunicating (P1) segment :

Extends from the PCA origin to the junction with the posterior communicating artery, the posterior thalamoperforating and medial posterior choroidal arteries are the main branches of this segment [Gerber et al, 1989].

Ambient (P2) segment :

The lateral posterior choroidal artery and thalamogeniculate artery are the main branches of this segment [Gerber et al, 1989].

Quadrigeminal (P3) segment :

The inferior temporal artery, parietooccipital artery and the posterior pericallosal artery are the important branches from this segment [Gerber et al, 1989].

The basilar artery (B A) :

It is about 3 cm in length and 1,5-4 mm width, the BA is formed by the union of both vertebral arteries in front of the pons and terminates in the interpeduncular cistern by dividing into the PCAs [Osborn, 1994].

B) Venous Drainage :

The cerebral venous system is composed of dural sinuses, superficial and temporal cerebral veins [Osborn, 1994].

Dural sinuses :

1- Superior Sagittal Sinus (SSS) :

The SSS is a midline structure situated between the inner table of the skull superiorly and the falx cerebri laterally. It originates near the crista galli anteriorly and extends posteriorly to its confluence with the straight and lateral sinuses [Osborn, 1994].

2- Inferior Sagittal Sinus (ISS) :

It runs in the inferior free margin of the falx cerebri and joins with the vein of galle to form the straight sinus [Osborn, 1994].

3- Straight Sinus (SS) :

The SS is enclosed by the confluence of the dura from the falx cerebri and tentorium cerebelli. It curves backward toward the SSS where they form the trochlear herophili [Osborn, 1994].

4- Transverse and occipital sinuses :

The trochlear herophili divides into the transverse sinus which course laterally around the tentorial attachment to the calvarium, and the occipital sinus which courses antero-inferiorly to the foramen magnum [Nathal et al, 1992].

5- Sigmoid sinus:

It is the continuation of the transverse sinus near the posterolateral wall of the petrous temporal bone. It joins the inferior petrosal sinus at the skull base [Osborn, 1994].

6- Cavernous sinus:

It is a highly variable collection of venous channels. The sinus receive the superior and inferior ophthalmic veins and communicate with the periclival venous plexus and the sigmoid sinus. The ICA,3,4,5 and 6 cranial nerves are in its lateral dural wall [Gerber et al, 1989].

7- Superficial cerebral veins:

They are small and variable, most of which are unnamed, though the following three veins are often identified:

- a- Superficial middle cerebral vein courses along the sylvian fissure.
- b- Vein of Troland courses from the sylvian fissure to the SSS.
- c- Vein of Labbe courses posterolaterally from the sylvian fissure to the transverse sinus. [Osborn, 1994].

8- Deep cerebral veins:

Medullary veins :

They originate 1-2 cm below the cortex and drain the subcortical and deep white matter to the subependymal veins [Osborn, 1994].

Subependymal veins :

They surround the cerebral ventricles and receive venous blood from the medullary veins. The thalamostriate vein and septal vein are join near the foramen of monro to form the internal cerebral vein. [Osborn, 1994].

Basal veins :

They course postero- superiorly in the ambient cisterns and join with the internal cerebral veins to form the vein of Gallen (Osborn, 1994).

Vein of Gallen : (Great cerebral vein).

It is a prominent venous channel that curves posteriorly under the splenium of the corpus callosum and unit with the inferior sagittal sinus to form the straight sinus [Osborn,1994].

MR Sectional Anatomy of the Brain

Detailed sectional anatomy of the brain has been described in various planes (Young et al, 1982).

1- Axial Sectional Anatomy:

Six axial planes parallel to the canthomeatal line are presented. It is convenient to describe these planes in four levels: (Fig. 3, 4).

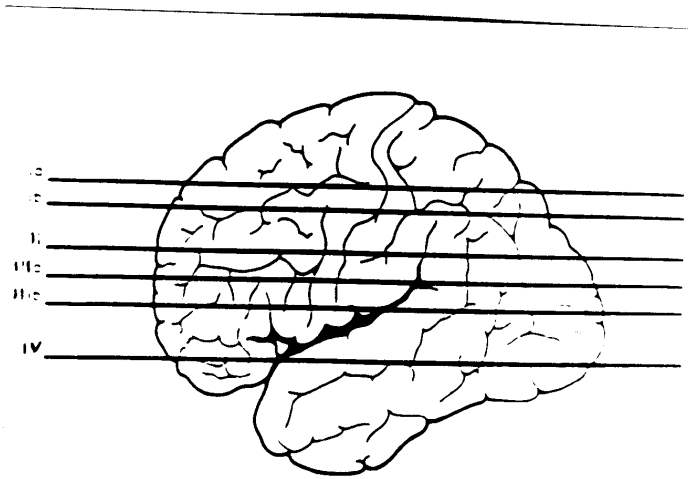


Fig. (3) : Levels of the selected axial sections on a diagram of the lateral surface of the cerebral hemisphere .

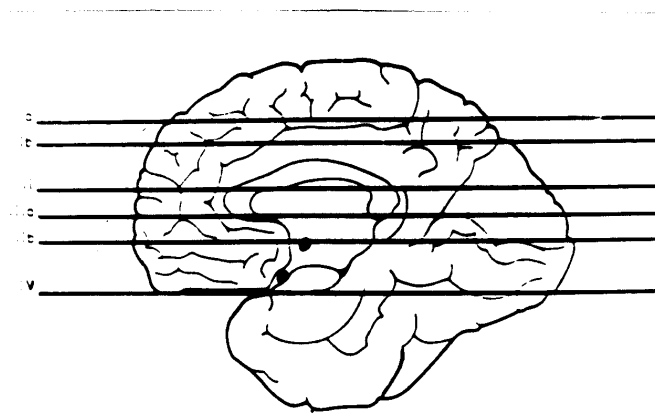


Fig.(4) : levels of the selected axial sections on a diagram of the medial surface of the cerebral hemisphere.

Ia, Ib, supraventricular level.

II, high ventricular level.

IIIa, IIIb , Low ventricular level.

IV, Infraventricular level.

Adapted from (Gado, 1992)

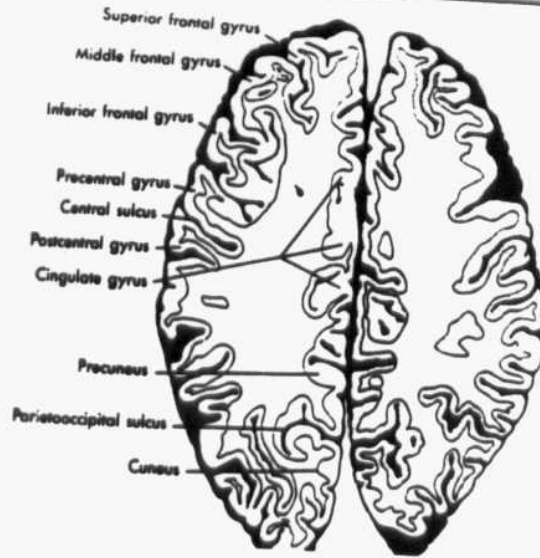
1- Supraventricular Level : (Fig. 5)

Examples of this level include the sections situated 6 to 7cm above the center of the external auditory meatus [EAM]. In this section, each cerebral hemisphere is represented by a central core of white matter and a peripheral array of convolutions of gray matter. A higher plane in this level transects the paracentral lobule on the medial surface of the cerebral hemisphere while, a lower plane transects the cingulate gyrus. On the lateral surface, both planes transect the frontal, the precentral and postcentral gyri. Each cerebral hemisphere shows a curved lateral border and a flat medial border (Drayer et al, 1986).

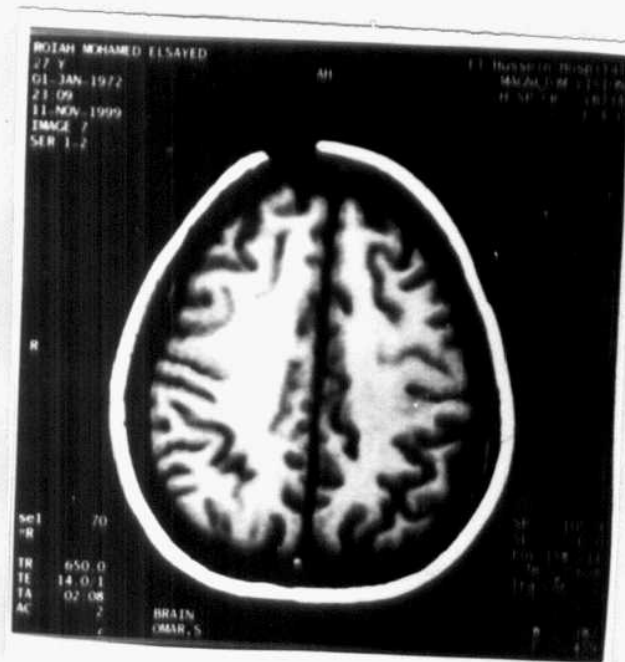
2- High ventricular level : (Fig. 6)

Sections at this level transect the bodies of the lateral ventricles examples of this level include the sections situated 4 to 7 cm above the EMA on the lateral surface of the cerebral hemisphere from front to back, the plane of the section transects the frontal gyri, the precentral, the postcentral, supramarginal and angular gyri. On the medial surface from front to back, the plane of the section transects the supramarginal gyrus, cingulate gyrus, corpus callosum [C.C], precuneus of the parietal lobe and cuneus of the occipital lobe. The IHF, is interrupted in its middle third by the C.C, which occupies the midline. On each side of the C.C, the body of the lateral ventricle appears as an elongated CSF filled

space. The tail of the caudate nucleus forms a narrow strip of gray matter along the lateral wall of the body of the lateral ventricle. Anterior to the C.C, the medial border of each cerebral hemisphere consists of the cingulate gyrus followed by the medial surface of the superior frontal gyrus which extends into the lateral surface. The frontal gyri and the precentral gyrus form less than half of the lateral border of the cerebral hemisphere [Schnitzlein and Murlage, 1990].



A

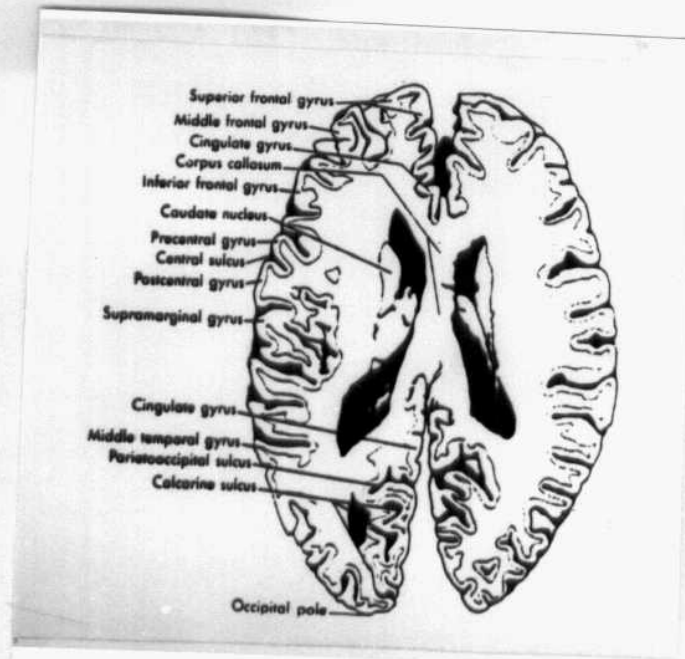


B

Fig.(5) : Supraventricular Level.

A) Line drawing of the axial section. Adapted from (Gado, 1992).

B) Axial T1- weighted image of a normal subject, obtained at the same level.



A



B

Fig.(6) : High ventricular level.

A) Line drawing of the axial section. Adapted from (Gado, 1992) .

B) Axial T1- weighted image of a normal subject at the same level.

3- Low ventricular level : (Fig. 7 &8).

Sections at this level transect the lateral ventricles below the body. Examples of this level are sections situated 3 to 4 cm above the EAM in these sections, the genu of the C.C, the frontal horns of the lateral ventricles and the third ventricle together form a prominent feature. Posterior to the third ventricle in the midline is the splenium of the C.C, or the tectum of the midbrain depending on the level of the section, on both sides the third ventricle is surrounded by the thalami. The lentiform nucleus is lateral to the head of the caudate nucleus and the thalamus, it consists of a large gray matter mass [putamen] and a smaller one [globus pallidus]. Another prominent feature is the insula, which is a part of the cerebral cortex that has been buried by overgrowth of the neighbouring cortex. The white matter between the putamen and insula divided by the claustrum [third part of the lentiform nucleus] into internal and external capsules. On the lateral aspect of the section, the sylvian fissure divides the lateral border into anterior half formed by the frontal gyri as well as the frontal and parietal opercula, and posterior half formed by the temporal gyri and the occipital lobe [more posterior], the anterior part of the medial border of the cerebral hemisphere is formed by the superior frontal gyrus and cingulate gyrus while the posterior part is formed by the occipital lobe separated from the splenium of C.C by the isthmus of the cingulate gyrus [Gado and Tobben, 1992].

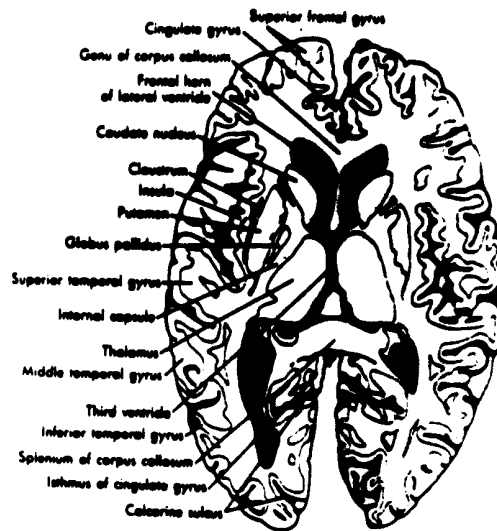


Fig.(7) : Low ventricular level.

Line drawing 4. 1 cm above the EAM., (IIIa). Adapted from (Gado, 1992).

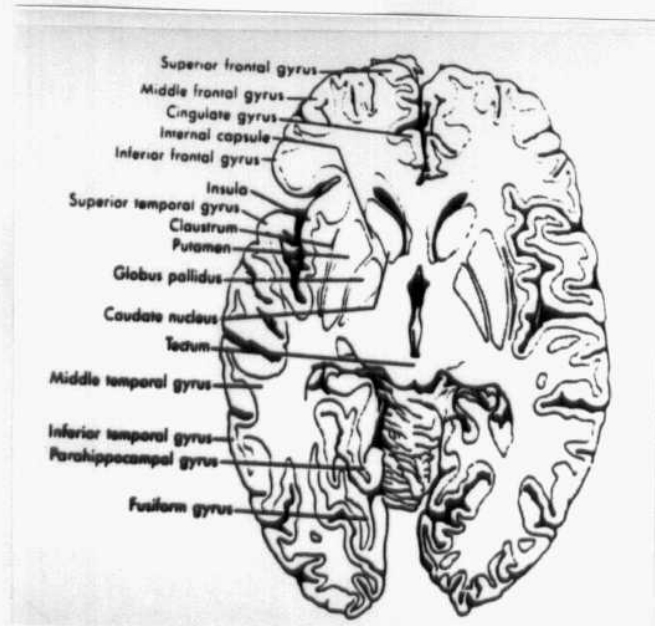


Fig. (8) : Low ventricular level.

Line drawing 3.5 cm above the EAM., (IIIb) . Adapted from (Gado, 1992).

Axial T1- weighted image of a normal subject, obtained at the same level.

4. Infraventricular Level : (Fig. 9).

Examples of this level include the sections situated 2cm above the EAM. This section does not contain parts of the frontal horn, trigone or the body of the lateral ventricle, it may contain part of the temporal horn.

On each side, the lower parts of the frontal and temporal lobes are separated by the sylvian cisterns. The frontal lobe is formed by the gyrus rectus medially and the orbital gyri laterally. The medial border of the C.H is formed by the inferior surface of the fusiform gyrus and para hippocampal gyrus. Anteriorly, the medial surface of the uncus abuts on the suprasellar cistern where hypothalamic structures [optic tract, hypothalamic gray matter, and the mammillary bodies] can be identified [Gado and Tobben, 1992].

Coronal Sectional Anatomy : (Fig. 10 & 11)

Coronal sectional anatomy will be presented in four selected planes perpendicular to the canthomeatal line:

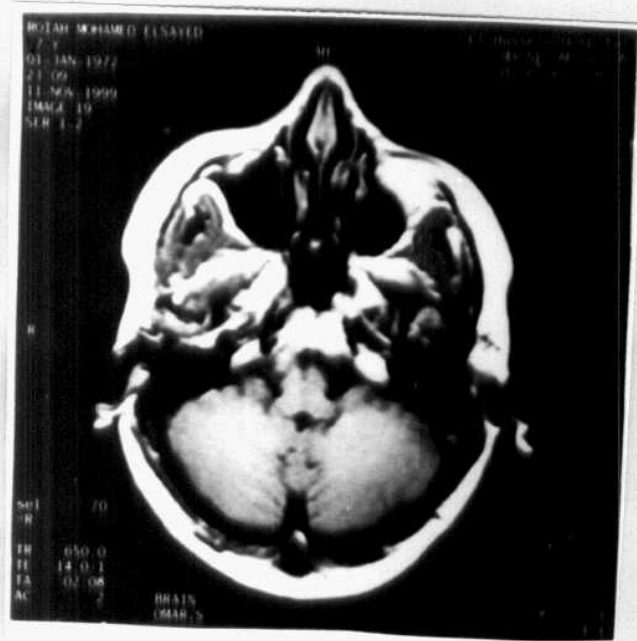
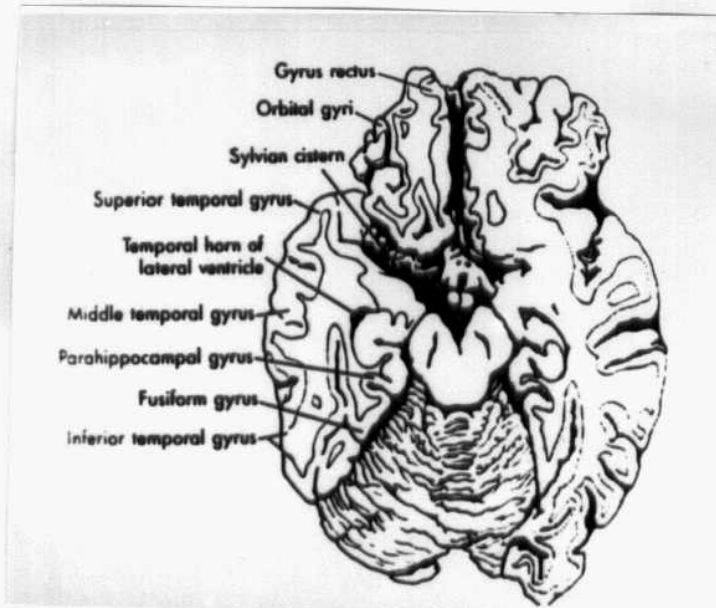


Fig.(9) : Infraventricular level.

- A) Line drawing of the axial section. Adapted from(Gado, 1992).**
- B) Axial T1 – weighted image of a normal subject, obtained at the same level.**

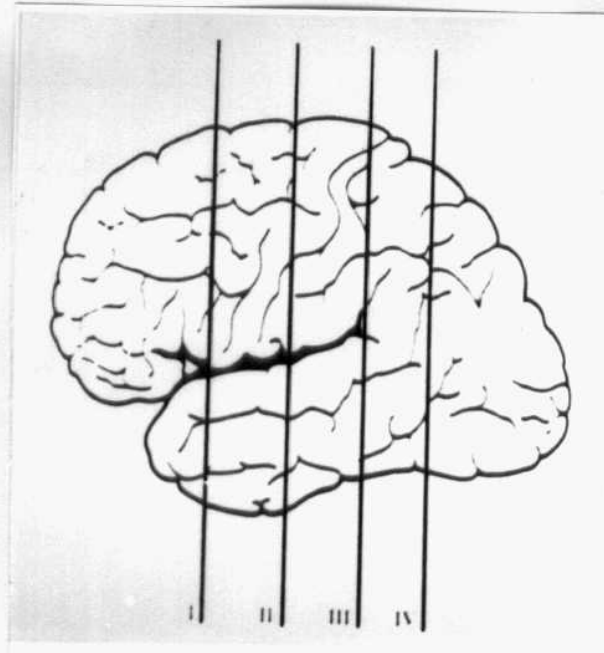


Fig.(10): Levels of the selected coronal section on a diagram of the lateral surface of the cerebral hemisphere.

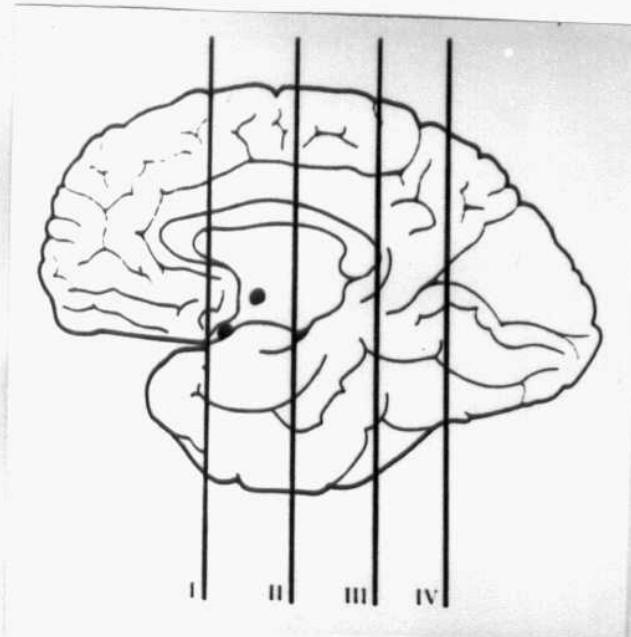


Fig. (11): Levels of the selected coronal sections on a diagram of the medial surface of the cerebral hemisphere.

I, Midfrontal plane.

II, Midthalamic plane.

III, Plane of splenium and pineal body.

IV, Plane of temporo-parieto-occipital junction.

Adapted from (Gado, 1992)

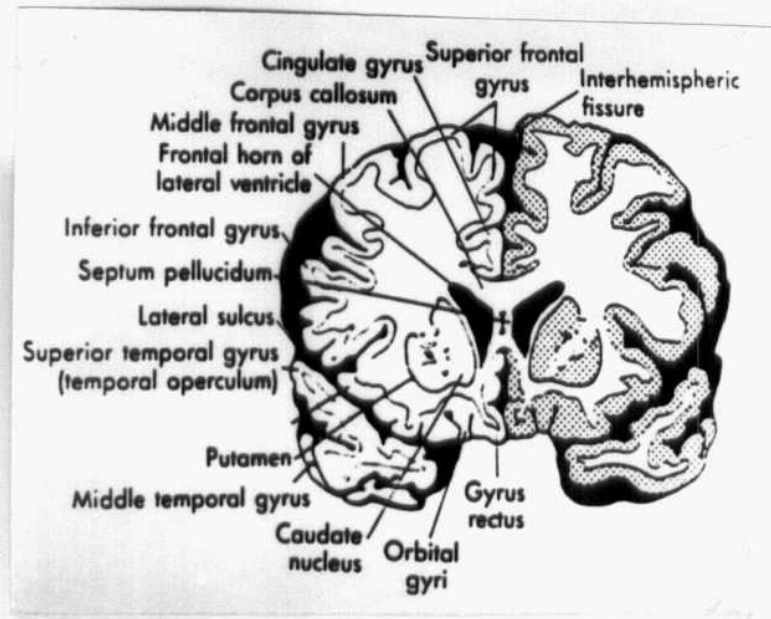
Mid frontal plane: (Fig. 12)

This plane lies approximately 3cm anterior to the EAM. On the medial surface, the plane of this section transects the superior frontal gyrus, cingulate gyrus, C.C and gyrus rectus. The frontal lobes abut on one another at the IHF whereas the temporal lobes are separated from one another by a gap occupied by the sella turcica and cavernous sinuses. On the lateral surface, the plane of this section transects the frontal gyri, the lateral sulcus and the lateral surface of the anterior part of the temporal lobe. The lateral sulcus is a prominent structure separating the hemisphere into a greater superior part formed by the temporal lobe. The insula lies at a deeper plane between the insula and the frontal horns, the caudate nucleus and the putamen form the masses of gray matter and together are called the corpus striatum [Young et al, 1982].

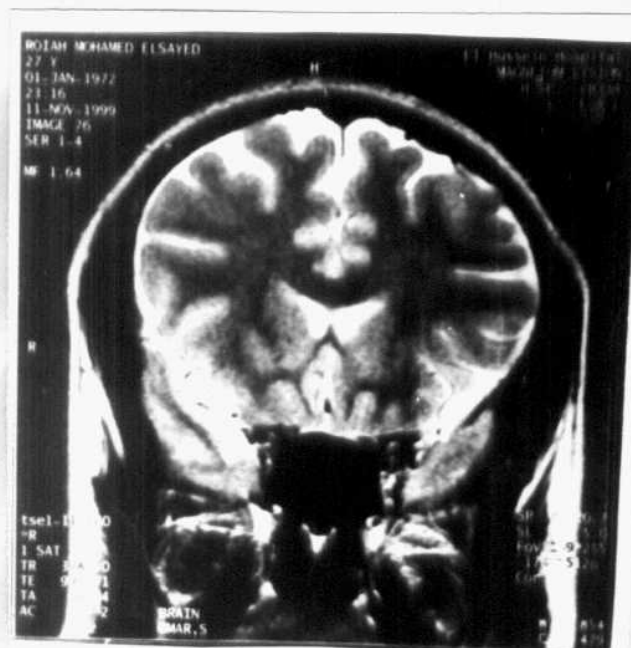
Mid thalamic Plane (Fig. 13)

An example of this plane is section of the brain approximately 5mm anterior to the EAM. On the medial surface, the plane of this section transects the posterior end of the superior frontal gyrus, cingulate gyrus, C.C and third ventricle. The IHF occupies only the upper part of the midline and the C.C lies at its bottom. The bodies of the lateral ventricles lies above the third ventricle which surrounded on both sides by the thalami on the lateral surface, the plane of this section transects the lateral

surface of the superior frontal gyrus, precentral gyrus, postcentral gyrus, sylvian fissure and the lateral surface of the temporal lobe. The lateral border is separated by the central sulcus and sylvian fissure into upper, middle and lower thirds formed by the frontal, parietal and occipital lobes respectively. The lentiform nucleus form a large mass of gray matter separated from the thalamus by the white matter of the posterior limb of the internal capsule [Nadichi et al, 1987].



A

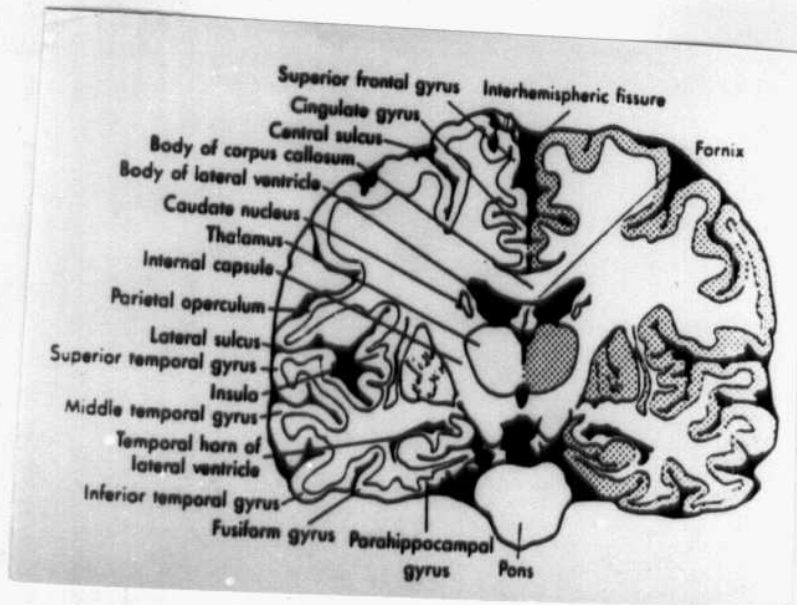


B

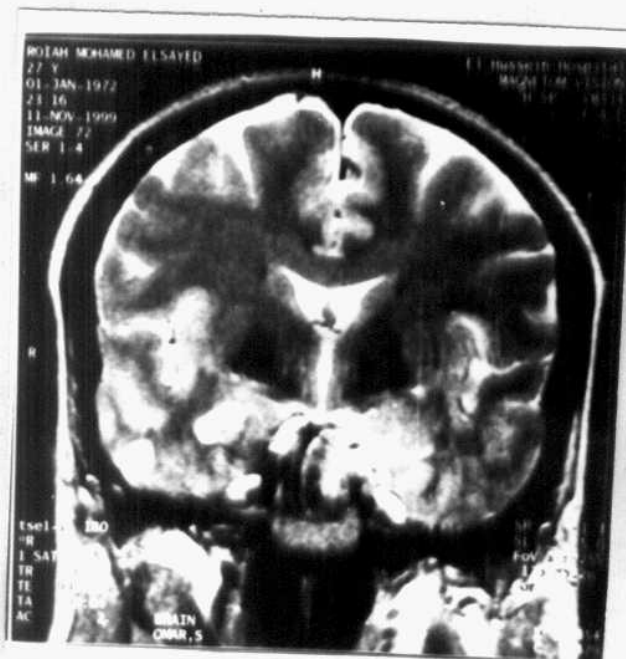
Fig.(12) : Midfrontal plane.

A) Line drawing coronal section. Adapted from (Gado,1992).

B) Coronal T2-weighted image of a normal subject, obtained at the same level.



A



B

Fig. (13) : Midthalamic plane.

A) Line drawing coronal section. Adapted from (Gado, 1992).

B) Coronal T2- weighted image of a normal subject, obtained at the same level.

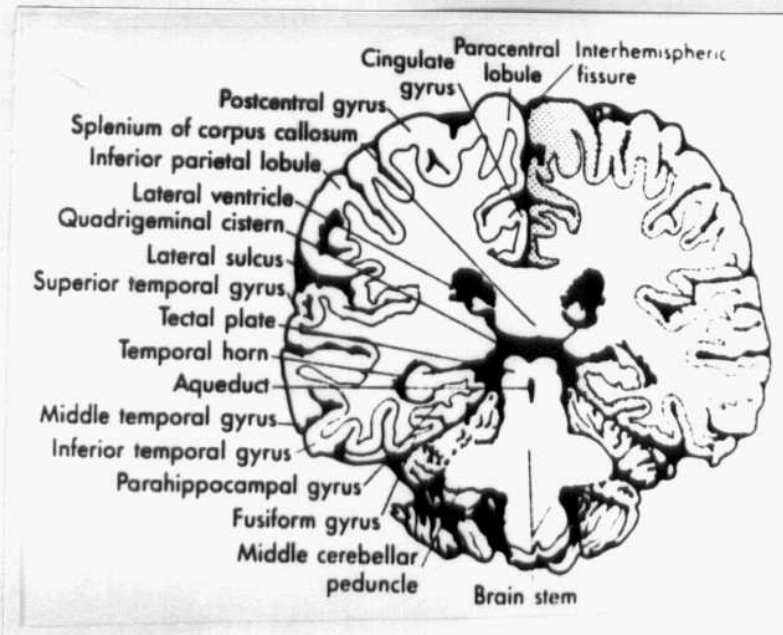
Plane of the splenium and pineal body: (Fig. 14)

This plane lies approximately 2cm posterior to the EAM. On the medial surface, the plane of this section transects the paracentral gyrus, cingulate gyrus and the splenium of the corpus callosum [C.C]. The IHF is seen in the upper part of the midline and the splenium of the corpus callosum [C.C] lies at its bottom below the splenium, the CSF space of the quadrigeminal cistern separates the splenium from the tectum of the midbrain which appears as a column of brain tissue continuous with the remainder of the brain stem below. Two lateral extensions formed by the middle cerebellar peduncles are noted. On the lateral surface, the plane of this section transects the upper end of the central sulcus, the postcentral gyrus and the lateral surface of the temporal lobe. The lateral border is formed by the parietal and temporal lobes separated by the lateral sulcus. The inferior surface of the temporal lobe is formed by the inferior temporal, fusiform and parahippocampal gyri. (Schnitzlein and murlagh, 1990).

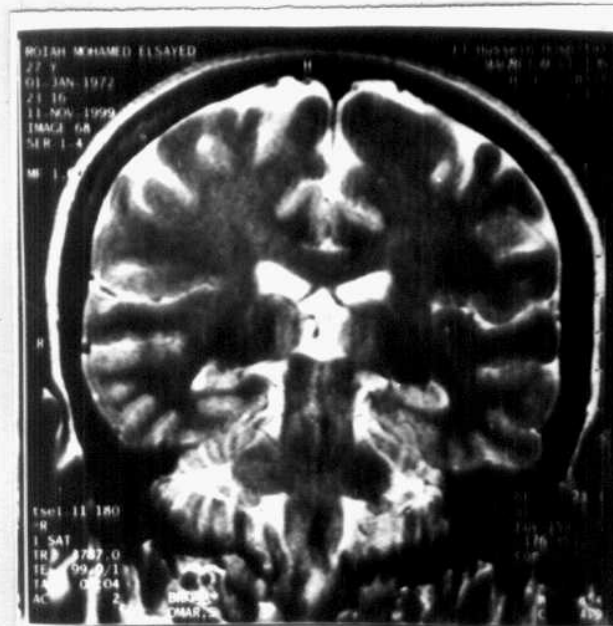
Plane of the temporo-parieto-occipital junction: (Fig. 15)

This plane lies approximately 3 to 5cm posterior to the EAM. On the medial surface, the plane of this section transects the precuneus of the parietal lobe and the cuneus of the occipital lobe. The medial border of the cerebral hemisphere is a continuous line and IHF separates the two hemispheres

completely with no crossing fibers of the C.C in between. The falx cerebri and tentorium cerebelli are in continuity at this level. The inferior surface of the hemisphere is formed by the temporooccipital junction [from medial to lateral, the lingual, the fusiform and inferior temporal gyri]. On the lateral surface, the plane of this section transects the superior parietal lobule, the temporo-parietal junction and the lateral surface of the temporal lobe. The upper two thirds of the lateral border of the cerebral hemisphere are related to the temporal lobe [Gado and Tobben, 1992].

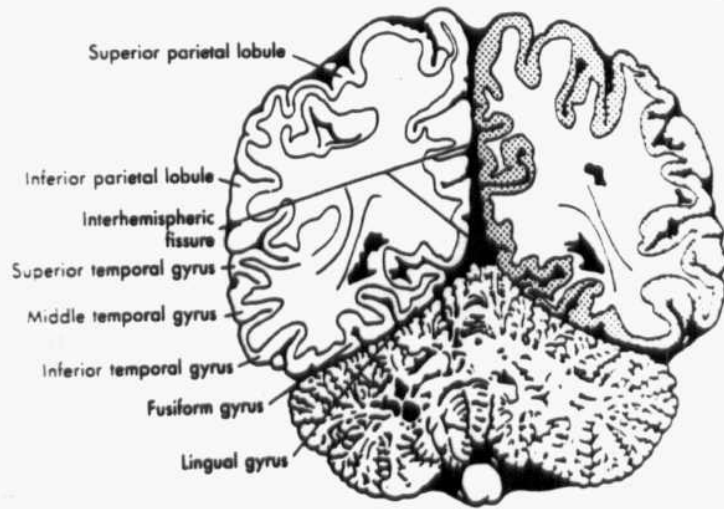


A



B

Fig. (14): Plane of splenium and pineal body.
 A) Line drawing of coronal section. Adapted from (Gado, 1992).
 B) Coronal T2- weighted image of a normal subject, obtained at the same level.



A



B

Fig. (15) : Plane of temporoparietooccipital junction.
A) Line drawing of coronal section. Adapted from (Gado, 1992).
B) Coronal T2- weighted image of a normal subject, obtained at the same level.

PATHOLOGY

Incidence of brain tumors in children:

C.N.S tumors are the second most common form of neoplasm to affect the pediatric population. Brain and spinal cord tumors account for 20% of all pediatric malignancies [Vast, 1997].

Tumors in children under 2 years of age represent slightly more than 10 percent of all childhood brain tumors and the types of tumors vary from those in older children. The most common tumors are ependymomas and low grade supratentorial astrocytomas [Duffner and Cohen, 1986].

In children, the incidence of intracranial tumors, their site and distribution differ from that found in adults, approximately 80 percent of all intracranial tumors in childhood are gliomas, compared with only 40 percent in adults. Low- grade astrocytomas make up the majority of gliomas in children whereas the principle glioma in adults is the high- grade astrocytoma. Additionally, benign tumors such as meningiomas, neurinomas, and pituitary adenomas which constitute about one third of all intracranial tumors in adult life, are rare in children.

TUMORS	%
GLIOMAS: 75 %	
Astrocytoma	50%
Cerebellar	30%
Brain stem	10%
Oligodendroglioma	<1 to 2%
Ependymoma	8%
Medulloblastoma	20 to 25 %
Non Glioma:	
Meningioma, schannoma, hemangioblastoma, sarcoma	Rare
Germ cell tumor	2 to 4 %
Dermoid, epidermoid	1 to 2 %
Craniopharyngioma	5 to 10 %
Pituitary adenoma	Rare
Others	

This table shows the primary intracranial tumors in children (less than 15 years old).

Quated from [Hauro Okazaki, 1989].

Table 0-4. Patterns of cellular Response to Injuries Within the Central Nervous System

Cell Types	Types Of Reaction		
	Regressive/Degenerative	Progressive/Hypertrophic-Hyperplastic (excluding neoplasia)	
Functional			
Neuron	Many specific and nonspecific alterations	None	
Interstitial (Glia)			
Oligodendroglia (Schwann cell)	Limited	None (Limited)	
Astrocyte	Limited	Scar formation (astrocytosis)	
Ependymal cell Epithelial cell of choroid plexus	Limited	None	
Microglia	Limited	Inflammatory reactions, phagocytosis	Neoplasia
Mesodermal (mesenchymal) connective tissue			
Hematogenous cells (Leukocytes)		Inflammatory reactions, phagocytosis	
Blood Vessels and connective tissue	Limited (edema)	Scar formation (Limited)	

Quated from [Hauro Okazaki, 1989].

The vast majority of brain tumors arise from the neuroglia [which consists of astrocytes, oligodendrocytes, microglia, ependymoma and choroid epithilium] and are included under the broad term of gliomas [Burger et al, 1994].

Histological classifications of pediatric intracranial tumors:

Tumors of the neuroepithilial tissue :

- Supratentorial astrocytoma.
- Oligodendroglioma.
- Cerebellar astrocytoma.
- Ependymoma.
- Brain stem glioma.
- Optic chiasmal glioma.
- Thalamic glioma.

Choroid plexus and related structures tumors :

- Choroid plexus papilloma and carcinoma.
- Colloid cyst.
- ***Embryonal tumors:***
 - Neuroblastoma.

- Tumors of the meninges:

- Meningioma.

- Reticulo endothelial system tumors :

- Primary lymphoma.
- Metastatic lymphoma.

- Pineal region tumors :

- Germinoma.
- Pineocytoma.
- Pineoplastoma.

- Tumors of maldevelopment :

- Craniopharyngioma. - Dermoid.
- Epidermoid - Lipoma.
- Neurofibromatosis. - Hamartoma.

Primitive neuroectodermal tumors:

- Medulloblastoma.
- Metastatic tumors.

Classifications of paediatric intracranial tumors according to the site [A. James Barkovich, 1994].

Supratentorial paediatric intracranial tumors:

- Supratentorial Astrocytomas [Hemispheric Astrocytomas, chiasmatic and hypothalamic astrocytomas].
- Choroid plexus tumors [papillomas and carcinomas].
- Pineal region tumors [germinomas, teratomas, pineocytomas and pineoblastomas].
- Sellar region tumors [craniopharyngiomas and less common pituitary adenomas].
- Oligodendrogliomas.
- Lipomas.
- Hamartomas.
- Dermoids and epidermoids.
- Gangliomas and Gangliocytomas.
- Metastasis and lymphomas.

Infratentorial paediatric intracranial tumors [Posterior Fossa Tumors] :

- Cerebellar Astrocytomas.
- Medulloblastomas.
- Ependymomas.
- Brain stem gliomas
- Hemangioblastomas.
- Oligodendrogliomas.
- Gangliomas and Gangliocytomas.
- Dermoids and Epidermoids.
- Meningiomas.
- Metastasis and Lymphomas.

Aetiology of brain tumors:

The vast majority of intracranial tumors occur sporadically and their cause is unknown. According to Cohnheim's theory of craniogenesis, (the real cause of subsequent development of tumors should be sought in an anomaly of the embryonic life). Cohnheim went to say, (tumors often develop at sites where certain complications have occurred at some stages of embryonic development). This theory of (misregeneration) would seem to provide a logical explanation for the origin of certain congenital tumors, such as craniopharyngioma, which arise along embryonic closure lines.

Some recent studies proved relations between some external factors and the aetiology of brain tumors in children. Kristensen et al, 1996 reported that use of pesticides are associated with cancer at an early age, whereas factors in animal husbandry, in particular poultry farming, are associated with cancer in later childhood.

In addition, occupational exposures of parents might be related to cancer in their offspring, the evidence was for childhood nervous system cancers and paternal exposure to paints in Cott's, and Blair's study (1998). Parents who worked in the chemical industries were at risk of having had children with astroglial tumors, while children of fathers as electrical workers

were at increased risk of developing brain tumors of any histological type (Mc Kean et al, 1998).

Cordier et al, 1997 said, astroglial tumors are more frequent among children of mothers in health services and maternal exposure to solvents at high level is associated with an increased risk of astroglial and PNET. (Lennart et al, 1996).

Paternal preconception smoking is related to a significantly elevated risk of childhood cancers by inducing genetic damage that, in turn, acts as the predisposing factors for cancer (Ji et al, 1997).

Also there are some relations proved between hormonal replacement therapy, like the growth hormone therapy, it might either increase the risk of cancer recurrence in a child who has previously been treated for a brain tumor or leukaemia, or induce de novo cancer (Shalet et al, 1997).

In addition, recent advances in molecular biology and cytogenetics have begun to identify possible sites of oncogenesis. Chromosomal abnormalities associated with brain tumors include deletions of chromosome 22,9 (meningiomas, acoustic neurinomas), alterations of chromosome 17 (medulloblastoma, astrocytoma), and loss of chromosome 10 (glioblastoma) (Wisoff, 1995).

Gliomas [tumors of neuroglial cells]:

Glial origin tumors account for 70 to 80 percent of primary intracranial neoplasms in the pediatric population, and astrocytomas account for 21 to 45 percent of this group [Watanabe et al, 1992].

Pediatric central nervous system neoplasms include a spectrum of both glial and non glial tumors that differ significantly in location and biological behaviour from those of adults.

Brain tumors in infants and children most often arise from central neuroepithelial tissue, whereas a significant number of adult tumors arise from C.N.S coverings (meningioma), adjacent tissue (pituitary adenoma), or metastasis [Yachins, 1997].

The great majority of tumors of neuroepithelial tissue are derived from the neuroglia : astrocytes, oligodendrocytes, and ependymal cells, or their precursors. The corresponding tumors are astrocytoma, oligodendroglioma, ependymoma and glioblastoma, and are often referred to, collectively, as the gliomas. [Koba and Kyritsis, 1997].

A. Astrocytoma:

This type of glioma is composed of neoplastically transformed astrocytes, which vary in their degree of histologic

resemblance to normal astrocytes, some can be readily identified as astrocytes [well differentiated or benign], and others show a great deal of anaplasia [undifferentiated or malignant].(Hauro Okazaki,1989).

Kernohan and his associates at the Mayo Clinic simplified previously complicated nomenclatures of astrocytic neoplasms by dividing them into four numerical grades on a benignancy – malignancy scale. The system shown in Table 7 – 1.

Table 7-1. Classification of astrocytomas

<i>Grade of Malignancy</i>				
<i>Histologic Features</i>	<i>1</i>	<i>2</i>	<i>3</i>	<i>4</i>
<i>Constituent cells</i>				
<i>Cellularity</i>	<i>Normal to slightly increased</i>	<i>As in grade 1</i>	<i>Increased (by 50% or more)</i>	<i>Markedly increased (up to three times as many cells)</i>
<i>Degree and frequency of anaplasia</i>	<i>None to early in a small number of cells</i>	<i>Early in roughly half of cells</i>	<i>Moderate in roughly half of cells</i>	<i>Pronounced in most cells</i>
<i>Mitotic figures</i>	<i>None</i>	<i>None</i>	<i>One in every high-power field on average</i>	<i>Numerous- four to five per high-power field on average</i>
<i>Giant cells</i>	<i>None</i>	<i>None</i>	<i>Occasional</i>	<i>Frequent</i>
<i>Necrosis</i>	<i>None</i>	<i>None</i>	<i>Frequent</i>	<i>Frequent</i>
<i>Blood vessels</i>				
<i>Numbers</i>	<i>Normal or near normal</i>	<i>As in grade 1</i>	<i>Increased</i>	<i>Markedly increased</i>
<i>Endothelial and adventitial proliferation</i>	<i>None</i>	<i>Minimal</i>	<i>Quite prominent</i>	<i>Markedly increased</i>

Table 7-1 quoted from Hauro Okazaki,1989.

Astrocytomas of grade 3 and 4 correspond to the age-honored term (glioblastoma multiforme). Some authors favor dividing glioblastomas into two categories : 1) anaplastic astrocytomas or secondary glioblastomas and 2) primary glioblastomas.(Hauro Okazaki, 1989).

With respect to general histologic features, in better – differentiated (or so – called low – grade) astrocytomas the following sutypes of component cells are commonly recognized :

Fibrillary. Elongated cells with little visible cytoplasm and long glial fibres. This is the predominant cell type. When thses fibres form parallel rows or trabeculae, the term piloid or pilocytic (hair like) is applied.

Protoplasmic. Stellate cells with delicate processes that have few or no staiable neurologic fibrils, formin a fine cobweb matrix.

Gemistocytic. Plump cells with abundant eosinophilic cytoplasm, one or more eccentric neuclei, and short glial fiibes.

In mor malignant (anaplastic or high- grade) forms 99 glioblastoma multiform), the bulk of the tumor consists of 1) small, round, 2) spindle or fusiform, or 3) giant, pleomorphic cells alone or in varying combinations.(Hauro Okazaki,1989).

The average age incidence of astrocytomas is 7 to 8 years, being slightly more common in males. [Zimmerman, 1985].

1- Cerebellary astrocytoma :

Cerebellar astrocytoma account for about 11 percent of primary central nervous system [CNS] tumor in children and carries an excellent prognosis after surgical resection of up to 94 percent at 10 years. Approximately one-third of childhood posterior fossa tumors are cerebellar astrocytomas, with no definite sex predilection. [Schneider et al, 1992].

These tumors commonly occur in the first two decades, with a peak late in the first decade and early in the second decade. Cerebellar astrocytomas commonly harbor cysts, are well circumscribed, and are relatively surgically resectable. [Russell, Rubenstein, 1989].

Cerebellar astrocytoma may occur in the cerebellar vermis or hemispheres in children, older patients tending to have eccentric hemispheric lesions. Extension into or origin within the vermis is common, although cerebellar astrocytoma infrequently presents within the fourth ventricle. [Gusnard, 1990].

Cerebellar astrocytoma is well defined grossly, and up to 80 percent are frankly cystic, with hemispheric tumor more commonly cystic than its vermian counter part. A solitary cyst peripheral to a neoplastic mural nodule tends to be composed of gliotic tissue from degenerated glial cells, although biopsy is

required to exclude active tumor. The cysts contain highly proteinaceous yellow or brown fluid. Infrequently a predominantly solid tumor is identified. Cystic or solid forms diffusely infiltrate adjacent tissues or leptomeninges on microscopic appearance. [Duffner et al, 1985].

Although marked variation occurs histologically within these tumors, the most common or [juvenile] type is a mixed tumor with compact areas of fibrillary cells and spongy areas with microcysts and stellate astrocytes. [Naidich , Zimmerman , 1984].

These characteristics closely resemble those of juvenile pilocytic astrocytoma of the third ventricular region. A less common form, occurring in approximately 15 percent of cerebellar astrocytomas and particularly in adolescence, is the diffuse astrocytoma with fibrillary stellate or piloid cells and few microcysts. These diffusely infiltrating astrocytomas are the ones most commonly implicated in anaplastic change and have a less favorable prognosis than the more common juvenile cerebellar astrocytoma. [Zimmerman et al, 1978].

2- Brain Stem Glioma :

Brain stem gliomas are primarily pediatric lesions, accounting for 10 to 15 percent of CNS tumors in children. [Epstein, Wysoff, 1988].

Most are either astrocytoma or glioblastoma multiforme. The peak age of presentation is 5 to 14 years, although, these have been described in children under 1 year of age and in late adulthood. A slight male sex predominance had been noted. [Bilaniuk et al 1980].

Most brain stem neoplasms are of astrocytic origine, and fibrillary or pilocytic types are common. The cells themselves are fibrillated, with the pilocytic pattern of growth imposed by insiulation within preexisting pontine tracts [Cohen, 1984].

Up to 40% [percent] are frankly malignant, as in glioblastoma multiforme. Brain stem gliomas may be eccentric or may involve virtually the entire brain stem diffusely. Those involving the pons and medulla tend to be more aggressive than those of the midbrain. [Smith , 1990].

Extension into the adjacent thalamus from midbrain tumors is common, while those of the pons and medulla eccentrically infiltrate into the cerebellum. [Smith , 1990].

3- Deep Basal Ganglia and Thalamic Glioma :

Primary tumors of the deep structures of the brain excluding the relatively benign hypothalamic- chiasmal group are uncommon, accounting for approximately 6 percent of primary brain tumors in children. The biologic behaviour and patient

survival rates vary with the degree of malignancy, although these generally are more aggressive than their midline counterparts arising in the hypothalamus and optic chiasma. [Kollias, et al 1991].

The full range of astrocytic tumors occur in the deep structures, with approximately an equal distribution between benign pilocytic and malignant astrocytoma-glioblastoma multiforme. Both benign and malignant forms extend by direct infiltration along white matter pathways, especially in the subependymal location in the CSF. [Cohen, et al, 1984].

1- Hypothalamic-optic-chiasmal Glioma :

Hypothalamic and optic chiasmal origin tumors are usually low-grade midline tumors that carry a better prognosis than other supratentorial astrocytomas [Devi et al, 2001]. These are grouped together since they may be indistinguishable clinically, radiographically, and pathologically. The optic chiasm and hypothalamus are in close anatomic proximity, and neoplasms of this area rapidly extend along normal neural tracts between those tissues. Gliomas originating in the optic pathways represent 3 to 5 percent of intracranial tumors in children. Approximately half the children with optic glioma have neurofibromatosis, while about 3 to 10 percent of children with neurofibromatosis have optic pathway glioma [Russel et al, 1989].

These tumors usually are juvenile pilocytic astrocytomas and rarely are histologically malignant in children, although malignancy has been described in adults. They are composed of mature astrocytes without anaplasia. Pilocytic forms develop when fibrillary astrocytomas are forced into elongated parallel forms owing to constraints by the surrounding tissues, such as white matter tracts. Microcysts and spontaneous hemorrhage are infrequently noted without histologic evidence of malignancy. Although grossly these tumors are well defined, direct infiltration into adjacent deep gray matter and infiltration of the meninges are common pathologically. [Russell et al, 1989].

2- *Hemispheric Supratentorial Astrocytoma :*

Supratentorial tumors of the pediatric population account for up to 55 percent of CNS primary tumors, and most of these are astrocytoma. Deep midline tumors have a slightly better prognosis than hemispheric tumors. Prognosis varies with the location and degree of malignancy of these neoplasms. Gross examination of hemispheric astrocytoma reveals a diffusely infiltrating, ill defined tumor of white and gray matter, or a discrete mass, perhaps with one or more cysts. A particularly well-defined cystic benign astrocytoma with a mural tumor nodule

carries an excellent prognosis after resection analogous to its counterpart in the cerebellum [Davis, 1990].

Hemispheric astrocytomas may occur anywhere in the supratentorial region, although relatively few involve the occipital lobes. [Davis, 1990].

Apparent multiplicity has been reported in 5 to 15% of cases, this may be due to multifocal anaplasia in a diffusely infiltrating benign tumor or to clearly separate foci of anaplasia. [Hauro Okazaki, 1989].

Necrosis and hemorrhage occur in proportion to foci of anaplasia within the tumor. [Allen, et al 1991].

Low-grade tumors are usually fibrillary in nature, although focal areas of pilocytic or gemistocytic astrocytomas are common. Microscopically, most astrocytomas are inhomogenous, often including non astrocytic elements such as oligodendroglioma.

Protoplasmic astrocytes are generally restricted to gray matter, especially of the cerebral cortex. Astrocytes that have a swollen cytoplasm with short thick processes are referred to as gemistocytic and generally cannot a more aggressive tumor. Piloid or pilocytic tumors are typical of midline astrocytomas rather than hemispheric lesions. [Russell, et al 1989].

Protoplasmic astrocytoma is uncommon in relatively pure form, with the exception of superficial temporal lobe masses, it commonly contains foci of cystic degeneration. Fibrillary astrocytomas are more commonly hemispheric in adults than in children. Foci of anaplasia are common microscopic findings within an otherwise low-grade astrocytoma, and may evolve over time. Associated with anaplasia are necrosis, spontaneous hemorrhage, nuclear pleomorphism, frequent mitotic figures, and increased cellularity. [Russell et al, 1989].

Medulloblastoma: [Primitive neuroectodermal tumor]

These tumors are now recognized as arising exclusively in the cerebellum. the majority occurs in childhood, some 75% occur before the age of 15, 50% in the first decade. A male predominance (2 or 3:1) is noted. Considered primitive tumors, they are thought to arise from the residual germinative cells that have persisted at some stage in the genesis of the external granular layer, which would normally disappear during the first year of life [Hauro okazaki, 1989].

There are two subgroups :

- 1- Midline tumors (the most frequent type, about 75% occurring mostly in children) are friable, homogenous, pale gray tumors that arise in the roof of the fourth ventricle, are

relatively well circumscribed, and often completely fill the fourth ventricle. They frequently extend into the cisterna magna. Further spread over the cerebellar folia and beyond is a relatively early event.

- 2- Lateral tumors (the minority, mainly in adults) are smooth or lobulated masses on the surface of a cerebellar hemisphere (usually dorsal) with firm, homogeneous surfaces when cut, they occasionally spread en plaque on the surface of the hemisphere and are at times largely extracerebellar in location (Huro Okazaki, 1989).

Medulloblastoma is one of the few malignant brain tumors known to metastasize systemically, and this is usually to bone, occurring in about 5% of cases. Calcifications are rare and cystic changes are also uncommon. [Deutsch, 1988].

Medulloblastoma appears well circumscribed on gross examination, the adjacent tissues are diffusely invaded on microscopic views. Histologically, medulloblastoma appears as an extremely cellular tumor of predominantly hyperchromic small cells with frequent mitoses and leptomeningeal invasion [Zulch, 1986].

Ependymoma and Ependymoblastoma :

Ependymoma account for approximately 5 to 10 percent of all intracranial tumors and approximately 6 percent of all gliomas. The mean age of incidence is 5 to 7 years with a peak in the first 2 years of life. Ependymomas occur in both sexes but a male predominance of 1,7 to 1 has been described for ependymoblastoma. [Kune et al 1988].

It arises from differentiated ependymal cells of any ependymal cell-lined surface. Rests of ependymal cells in the lateral recesses of the fourth ventricle, at other points of sharp angulation of the ventricular surfaces, and at variable distances from the ventricles in the adjacent white matter may account for the common occurrences of ependymoma in the fourth ventricle and in the supratentorial periventricular white matter . About 40 percent arise in the supratentorial space and 60 percent in relation to the fourth ventricle. [Diebler, et al, 1987].

Intracranial ependymomas are categorized histologically as epithelial, papillary, and cellular, all with a similar prognosis. On microscopic examination, ependymomas typically contain ependymal epithelium, ependymal rosettes, and perivascular pseudorosettes. Ependymoma may be extensively cystic, with calcification present in 44 percent. [Barkovich, Edwards , 1990].

Histologically noted malignancy such as anaplasia, pleomorphism, and high mitotic rates are uncommon, account for approximately 5 percent of intracranial ependymomas. More mature malignant forms are termed malignant ependymoma, although the histologic appearance does not reliably correlate with survival.

Anaplastic or malignant ependymomas show histologic evidence of ependymal differentiation and is not synonymous with the embryonal or undifferentiated form of ependyoblastoma. [Centeno, et al, 1986].

Ganglioglioma and Gangliocytoma:

Ganglioglioma is a rare tumor containing exclusively mature ganglion cells in a stroma of spindle cells with calcospherites. Masses of histologically similar appearance that contain a mixture of mature ganglia and astrocytic cells are termed ganglioglioma. These tumors account for approximately 4 percent of primary CNS tumors in children. [Benitez et al 1990].

Ganglioglioma is much more common than gangliocytoma (3% of all pediatric brain tumors), has an equal incidence in the sexes, occurs between the ages 9 to 18 years.

Frequent locations include the temporal lobe and floor of the third ventricle, although examples have been described in virtually all locations [Russel, et al, 1989].

Ganglioglioma and gangliocytoma tumors contain cells of neuronal origin, with Nissl substance and neurofibrils on a scanty background of supporting tissue.

Microscopic evidence of Nissle substance and neurofibrils is necessary of identification of a ganglion origin cell, and engulfment of ganglial cells by another tumor type must be excluded. The cells generally are well differentiated, and mitoses are notably absent [Russell, et al, 1989].

Oligodendroglioma:

Oligodendroglioma is an uncommon glial neoplasm of the cerebral hemispheres that occurs at all ages, but accounts for less than 1 percent of CNS tumors in children, These tumors occurs mainly in adults, with a peak incidence in the 35to 40 age group. Oligodendrogliomas are histologically mixed gliomas with a predominance of oligodendroglial elements. They may grossly be firm in appearance or have necrotic, cystic, friable or frankly calcified components. Calcifications occasionally are inapparent radiographically , but are virtually always noted on histological examination. Spontaneous hemorrhage may have catastrophic

consequences. Common sites include frontal and temporal lobes, with rare cerebellar and spinal origins. [Bakovich , Edwards, 1990].

Microscopically, these tumors appear as compact masses containing swollen oligodendroglia with a sparse supporting matrix. Calcifications are generally located in proximity to the blood vessels, and may progress to frank bone formation with a lamellar organization. A general lack of correlation exists between histologic evidence of aggression and the clinical behaviour of the tumor. Part of this difficulty stems from the reporting of malignant oligodendrogliomas as glioblastoma multiforme. [Russel, et al, 1989].

Choroid plexus papilloma and carcinoma :

Choroid plexus papilloma and carcinoma are uncommon neoplasms, accounting for less than 1 percent of all CNS primary tumors. They occurs in both children and adults, approximately 40 to 50 percent present during the first decade. About 20 percent are identified in children under 1 year of age. A male predominance has been reported. [Diebler, et al, 1987].

32 percent arise from the lateral ventricle, 60 percent from the fourth, and 8 percent from the third. In children, most arise from the choroid plexus of the lateral ventricles [particularly the

left], while in adults a fourth ventricular or cerebellopontine angle origin is more common. [Russell, Rubenstein, 1989].

Uncommonly these tumors are bilateral or extend through the choroidal fissure into the quadrigeminal plate cistern. Malignant forms are uncommon [10 to 20 percent], tending to occur in younger pediatric patients. [Russell, Rubenstein, 1989].

Choroid plexus papillomas arise and are attached to choroid plexus epithelium, and thus have a pink or reddish-gray globular or cauliflower like appearance on gross examination. Approximately one-fourth have focal areas of ependymal differentiation, occasionally making it difficult to distinguish these tumors pathologically from ependymoma [David Sutton, 1998].

Dense calcification is not unusual. Benign forms are slow-growing masses that characteristically expand the adjacent ventricular walls without invasion of the adjacent parenchyma.

Microscopically, papillomas are characterized by arborizing front like papillae with collagen in their stroma, lined by single-layered or pseudostratified cuboidal to columnar epithelium. Occasional mitotic figures, atypia, microscopic infiltration, and ependymal differentiation are present in benign papilloma, which may not adversely affect the prognosis. About 10 percent of choroid plexus papillomas are malignant. [Mc Girr, et al, 1988].

Pineal region tumors :

Pineal region masses are conveniently grouped into several categories :

1. Germ cell tumors, including germinoma, benign teratoma, malignant teratoma, embryonal carcinoma, choriocarcinoma and chorioepithelioma.
2. Pineocytoma [formerly called pinealoma].
3. Pineoblastoma.
4. Glial tumors such as astrocytoma and glioblastoma multiforme.
5. Others : hamartoma, lipoma, meningioma arising from the tentorium or velum interpositum, and non- neoplastic cysts [Russell, et al, 1989]. These are tumors represent 0.4- 1.0 % of all intracranial tumors [Tien et al, 1990].

Germinomas :

Germinomas probably account for more than 50% of the neoplasms arising in or near the pineal gland and appear in the second and third decades of life. Germinomas are histologically malignant and infiltrative but are highly radiosensitive [Tien et al, 1990].

Germinomas are usually seen as a homogenous mass, isointense relative to white matter on T1- weighted images and slightly hyperintense on T2- weighted images. Intense homogenous enhancement has been noted [Tien et al, 1990].

Teratomas :

These tumors are composed of well differentiated tissues from all germinal layers. Intracranial teratoma is the most common intracranial tumor in the newborn. Pineal region teratomas are heterogenous mass with cystic portion hypointense on T1- weighted images and hyperintense on T2- weighted images [Tien et al, 1990].

Pineocytoma : This slowly growing tumor of mature pineocytes can present at any age and affects both sexes equally. Pineocytoma is usually well defined cyst like pattern homogenous hypointense on T1- weighted images and hyperintense on T2- weighted images [Nakagawa et al, 1990].

Pineoblastoma :

This malignant tumor of primitive pinealocytes is most often seen in children with male predominance. These tumors are often illdefined,

Lobulated hypointense on T1- weighted images and hyperintense on T2- weighted images associated with ventricular and leptomeningeal spread. [Chiechi et al, 1995].

Tumors of maldevelopment :

Lipomas : Are very rare intracranial tumors, half of these tumors are located in the midline between the frontal lobes and are associated with partial or complete agenesis of the corpus callosum. They are composed of a dipose tissue and a variable amount of vascular elements, collagen and muscle fibers, glial cells, and ganglion cells, which are indicative of their malformative nature, calcifications and ossification are not infrequent. [Hauro Okazaki, 1989].

Dermoids and Epidemoids : Represen approximately 1% of all primary intracranial tumors, they are less common tumors that originate from the inclusion of epithelial cells and skin appendages(Tampier et al, 1989) . They are more frequently located in the midline, commonly in the pineal and parasellar regions. Anterior lesions may be associated with a midline bone or skin defect, posterior lesions may be associated with an occipital encephalocele. (Smith et al, 1991).

Hamartoma :

Intracranial hamartomas are unusual tumors that may be divided into two groups, the first is the hamartomas that is generally attached by a thick stalk to the tuber cinereum or mammillary bodies. The second group is the presence of multiple lesions in association with phakomatosis. Hamartomas are rounded, may be large masses, isointense with the brain on T1- weighted images and slightly hyperintense on T2- weighted images. The tumor shows no enhancement after injection of contrast agent [Boyko et al, 1991].

Neurofibromatosis :

Two distinct forms of neurofibromatosis have been recognized, neurofibromatosis type 1 [NF-1, Von Recklinghausens disease] and neurofibromatosis type 2 [NF-2, bilateral acoustic neurofibromatosis].

The neoplasms of NF-1 are those of astrocytes and neurons while in NF-2 are those of the covering of the brain and nerve [neoplasm of the meninges and schwann cells].

Patients with NF-1 have a high incidence of optic pathway gliomas [10-70%] but may be asymptomatic.

Hyperintense areas within the cerebellum, brain stem, basal ganglia and cerebral white matter have been seen on T1 and T2 weighted images in patients with NF-1, these foci of abnormal signal appear to represent areas of hamartomatous tissue or gliosis.

The unusual appearance of choroidal calcification is feature of neurofibromatosis [Aokis et al, 1989].

Tumors of meningeal and related tissues :

Meningioma : This is rare in children with an incidence of 2.4% of all primary intracranial tumors, with many of them arising in arachnoidal granulation (Erdinler et al, 1998). They occur mainly above the tentorium cerebelli in relation to venous sinuses and occasionally they occur within a lateral ventricle (one quarter of paediatric meningiomas are intraventricular). The absence of dural attachment is more common in children than in adults.

Meningiomas vary greatly in appearance, some being soft and fleshy while others are hard and gritty. Sometimes the tumor grows as a thick sheet on the surface of the brain, this being referred to as meningioma en plaque. The meningiomas often also evoke reactive changes in the adjacent bone to produce hyperostosis.(Mallucci et al, 1998).

Histological appearances : there are several named types of meningiomas based on their histological appearances. Meningiotheliomatous meningioma, the most frequently type seen in children, is composed of polygonal cells with poorly defined cell boundaries. There is frequently considerable pleomorphism of these cells and there are often compact groups of closely packed smaller cells within the tumor.(Mallucci et al, 1998).

Other rare types of meningioma are the haemangioblastic meningioma and the anaplastic meningioma(Adams et al, 1988).

Pituitary Tumors:

Pituitary adenomas may be classified as non functioning or functioning because non functioning adenomas are noted when they cause signs or symptoms secondary to either local mass effect or pituitary failure, they are usually macroadenomas. Pituitary microadenomas [10mm or less] are more common than macroadenomas [Scotti et al, 1988].

Pituitary adenomas: These vary greatly in size and appearance from microadenomas no more than 1-2 mm in diameter (occurring as an incidental finding in 10-15 percent of pituitary glands if examined routinely post-mortem) to

lesions several centimeters in diameter (Horvath and Kovacs, 1986).

Histological appearances: These vary greatly, the great majority of adenomas are composed of trabeculae of oval or polygonal cells with single nuclei. In tumors devoid of any evidence of endocrine activity, the cytoplasm is often scanty, but in other adenomas, there may be a considerable amount of cytoplasm and in active adenomas, binucleate cells are frequently present. The stroma varies considerably in amount, but in prolactinomas it often contains amyloid (Scheithauer, 1984).

Suprasellar lesions:

Craniopharyngioma:

It is a primarily tumor of childhood and the most common supratentorial tumor of non glial origin in children. Fifty percent of suprasellar tumors in the paediatric age group are craniopharyngioma (Harlod et al, 1992).

It affects boys and girls equally and most frequently presents in patients between 5 and 8 years of age. At time of diagnosis, 70% of these tumors are both intrasellar and suprasellar, 10% are purely intrasellar, and 20 % are suprasellar and parasellar in

location. Tumors rarely present purely within the third ventricle, in the sphenoid wing or in the nasopharynx (James and Edwards, 1985).

They arise in the region of the pituitary stalk from ectopic nests of squamous epithelial cells derived from Rathkes pouch or from cells in the pars tuberalis of the pituitary gland that have undergone squamous metaplasia. In children, the craniopharyngioma usually has adamantinomatous structure. It is encapsulated and sharply circumscribed from the adjacent brain tissue, much of the tumor is usually cystic. [Balakrishna et al, 1997].

The solide areas are rather gray or white and there is usually considerable calcification that can be seen in plain x-ray of the skull. The solide parts of th tumor are composed of keratinising stratified squamous epithelium, and despite the apparent encapsulation of the tumor macroscopically, small cell nests are often seen infiltrating for 1 or 2mm into the adjacent brain [William and Simon, 1992].

Vascular lesions:

Aneurysm:

Intracranial aneurysms may present clinically in three different ways. The commonest mode of presentation is by

subarachnoid hemorrhage. The second method of presentation is pressure upon the cranial nerves, the third cranial nerve is the commonly involved one. Finally in a few cases the aneurysm may reach a very large size and simulate an intracranial tumor [Martin, 1989].

Angiomatous malformation [AVM] :

These lesions are of congenital origin and should be differentiated from the simple arteriovenous fistula which is usually due to trauma, rupture of the wall of an aneurysm or diseased artery into an adjacent or adherent vein. The typical clinical presentation, jacksonian epilepsy, headache, a small but significant proportion of cases presented by rupture of an angioma and subarachnoid hemorrhage (Terest and Davis, 1992).

MRA is used to evaluate the feeding artery and the draining vein. Most AVMS are supratentorial with a large component of the AVM located superficially in the pia. 3D TOF MR angiography can identify the arterial supply to the AVM, define the location and morphology of the venous drainage and attempt to detect the presence of fistula within the AVM. The ability to define the size and location of AVM nidus is essential for the proper selection of patients for surgery, endovascular or radiation therapy. AVM nidus greater than 0.36 cm could be

reliably identified by 2D TOF MR angiography (Kovwenhouen et al, 1994).

Primary malignant lymphomas :

Primary C.N.S. lymphomas most commonly arise in the supratentorial region.

Multiple lesions have been reported in 16% to 60% of patients. The primary lymphoma of the C.N.S. is similar morphologically to non-Hodgkin's lymphoma arising outside the C.N.S. (Leibel and Sheline, 1987).

They occur intrinsically within the brain and there may be no evidence of systemic lymphoma, although in some cases the brain appears to be affected as a part of a generalized process. Intrinsic cerebral lymphomas vary greatly in appearance, some are well defined, rather fleshy masses whilst others are ill defined, sometimes rather granular lesions. Occasionally the appearances are very similar to those of astrocytoma, including cyst formation with multicentric deposits not being uncommon. Deposits of lymphoma often seem to replace brain tissue rather than acting as expanding lesions, and there is therefore often no evidence of a raised intracranial pressure (Leibel and Sheline, 1987).

Histological appearances : The main part of the tumor is usually richly cellular, being composed of round or oval cells

with a distinctly lymphoid appearance and usually containing oval or slightly twisted nuclei. Mitotic figures and varying degrees of pleomorphism may be present and there are sometimes foci of necrosis. Throughout the tumor, enlarged astrocytes and hypertrophied microglia are often conspicuous. The edge of the tumor is very poorly defined and cells similar to those in the main tumor surround the immediately adjacent brain blood vessels. A characteristic feature is cocentric reduplication of reticulin around the blood vessels within the tumor, and in the blood vessels surrounded by tumor cells in the adjacent brain. Nearly all intrinsic cerebral lymphomas are diffuse, non-Hodgkin lymphomas, composed of B-lymphocytes, but Hodgkin's disease is very rarely seen within the brain (Adams et al, 1988).

Metastatic brain tumors:

Metastatic disease accounts for 15% to 25% of intracranial tumors. The involvement of the brain takes many forms, ranging from hematogenous metastases to the brain meninges, direct spread to the brain and meninges from primary tumors of the skull base and face, or intracranial dissemination of primary and secondary brain tumors via CSF pathways (Russell et al, 1989).

Hematogenous metastasis to brain parenchyma are uncommon in the pediatric population, most commonly resulting from hematopoietic malignancies. Skull metastasis to the bone or

adjacent dura arise in neuroblastoma, lymphoma and leukemia. Uncommon skull primary tumors and tumors arising adjacent to the skull base (orbit, nasopharynx, middle ear) may invade the CNS, as in chondrosarcoma, osteosarcoma, rhabdomyosarcoma and nasopharyngeal malignancy.

Leptomeningeal seeding in the intracranial space or spinal canal results from systemic disorder generally of the hematopoietic system, e.g, leukemia and lymphoma, or from CNS primary tumors. The more common CNS primary tumors associated with metastasis in the subarachnoid space include medulloblastoma, pineal germ cell tumors, pineoblastoma, ependymoma and malignant astrocytoma. (Curnes, et al, 1986).

All the areas of the brain may be affected : the corticomedullary junction appears to be the favored (but certainly not exclusive) starting point. Extensive hemorrhage into metastatic nodules may occur, most characteristically with metastatic melanomas (frequent) and choriocarcinomas (with a low overall incidence).

Other Modalities Of Daiagnosis Of Pediatric Intracranial Tumors

Ultrasonography: [Fig 16 & 17]

US has emerged and remains the modality of choice for neuroradiology in premature neonates. [Ambrosino , et al 1992.]

Major advantages of US include its portability, allowing examination of the infant in the NICU, lack of ionizing radiation, multiplanar capability, ability to display and quantitate flow in vascular structures, and relatively low cost. The small size of the premature neonates head is well suited to the geometry of US imaging, allowing use of high- frequency, high resolution transducers. Limitations of US include difficulty in imaging the periphery of the brain through the anterior fontanelle, limited differentiation of gray and white matter structures, relative insensitivity to calcification and edema, operator influence on image quality, and potential for images in non standard scan planes. [Blickmann, et al 1991].

Technique:

Using a 7.0 or 7.5 MHz transducer, the brain is examined through the anterior fontanelle, which conveniently is usually widely patent in premature neonates. We perform a standardized set of a minimum of six coronal followed by six parasagittal scans in each infant (Fig.). Abnormalities are documented with additional scans. Axial images are not routinely obtained, nor do we routinely scan through the posterior fontanelle or use Doppler for screening head US. [Barkovich, 1988].

If the ventricles are enlarged, we measure the transverse width of the frontal horns in the coronal plane at the level of the foramina of Monro. [Liao , 1986].

Computed Tomography:

CT was first used to examine the brain of the premature neonates in the later 1970s. [Flodmark, et al 1980]. [Early studies showed that CT was at least as good as US in detecting ventricular enlargement and hemorrhage. CT surpasses US, however, in its ability to detect blood, fluid, and other abnormalities in the periphery of the brain, the posterior fossa, and the extraaxial spaces. [Foldmark , et al 1990].

The use of CT is less convenient and potentially more hazardous than US in imaging premature neonates.

Isotopic Scanning:

Nuclear medicine of the neonatal brain has limited application. The portable nuclear medicine camera allows performance of brain flow studies in the documentation of brain death. Nuclear medicine SPECT scans of the brain are possible with agents that reflect distribution of cerebral blood flow. Little has been reported using this application for premature neonates. [Denasy , et al, 1993].

Angiography:

Angiography is an invasive technique seldom used in the 1990s in the premature neonate. Evaluation of the vascular structures is now possible with MR angiography, obviating the need for conventional catheter angiography in most situations [Medlock , et al 1992].

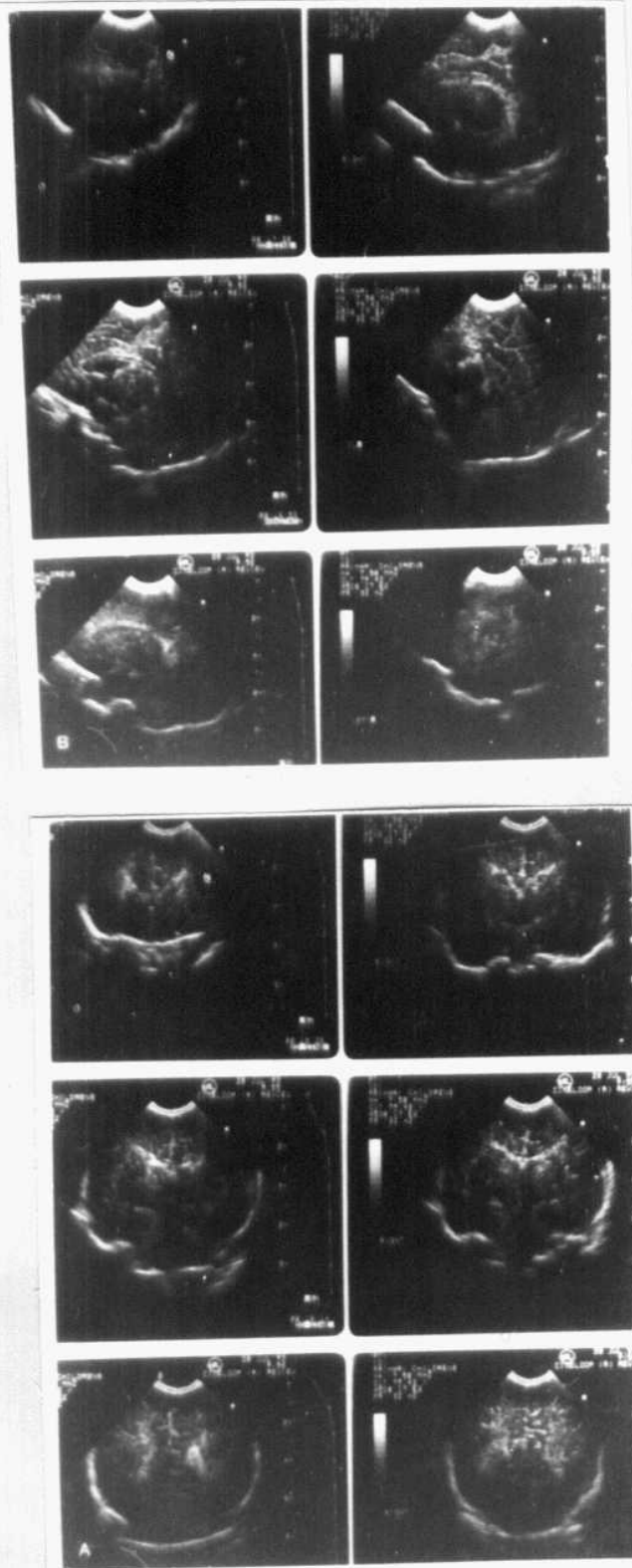


Fig.(16,17) : U S coronal and sagittal planes.
(Quoted from Barkovich AJ,1994).

Basic principle of MRI

The atoms consists of a nucleus and a shell (made up of electrons). In the nucleus there are protons that have a positive electrical charge and they are constantly spinning around an axis. This moving electrical charge is nothing more than an electrical current, and the latter always include a magnetic field so, every proton has it,s little magnetic field (Wehrli, 1988).

The nuclei suitable for MRI are those which have an odd (unpaired) number of protons, the hydrogen atoms which are single proton(H1) are particularly useful for illustrating the MR phenomenon because of their strong signal and abundance in human tissues(Wehrli, 1988).

When the patient is present in the MR magnet (external magnetic field) the protons align with the external magnetic field by two ways, parallel and antiparallel according to the amount of energy needed (energy level), this type of movement is called precession and its speed is measured by precession frequency (how many times the protons precess per second).

This precession frequency is not constant and can be calculated according to larmor equation:

$$\omega_0 = \gamma B_0.$$

ω_0 : precession frequency in HZ or MHZ.

γ : constant called gyromagnetic ratio.

B_0 : strength of the external magnetic field which given in Tesla or Gauss where : Tesla= 10000 Gauss(Makow, 1989).

Magnets used for imaging mostly have field strength between 0.5- 1,5 Tesla, there are different types of magnets :

Permanent Magnets:

Do not use any energy for work, possible disadvantages are thermal instability, limited field and its weight (Wehrli, 1988).

Resistive Magnets [Electromagnet]:

There is a resistance to the flow of electricity through the wire, these magnets get warm when in operation and have to be cooled [Wehrli, 1988].

Super Conducting Magnets :

Are the most widely used in MR machines at the present time. Helium and nitrogen are used for cooling so called cryogenes.

Advantage:

High field strength and excellent magnetic field homogeneity.

Disadvantages :

High costs and use of expensive cryogens (Wehrli, 1988). The radiofrequency coils are necessary to send in the radiofrequency (RF) pulse, to excite the protons and to receive the resulting signal. A variety of coils are in use :

Volume coils :

Are used in all MR units and completely surround the part of the body that is to be imaged (Makow, 1989).

Shim coils :

Used for electrical and mechanical adjustments of the magnetic fields homogeneity (Shimming) (makow, 1989).

Gradient coils :

Produce additional linear electromagnetic fields thus making slice selection and spatial information possible they are the cause of noise that you can hear during MR examination (Makow, 1989).

Surface coils :

Are placed directly on the area of inserte and have different shapes corresponding to the part to be examined they are receiver coils only (Makow, 1989).

Resonance phenomenon :

At equilibrium, the protons magnetic field is longitudinal to the external field of the MR machines magnet, when this protons exposed to RF pulse, some of them pick up energy and go from lower to higher energy level which result in decreasing the magnetization along the Z axis (longitudinal magnetization) with establish of new magnetization along the X Y axis (transverse magnetization).

When the RF pulse is turned of the excited protons relax and return to their equilibrium orientation and loss the excess energy, this explain the resonance phenomenon (Wehrli, 1988).

Relaxation Times :

At equilibrium, the longitudinal magnetization (MZ) is equal to the net magnetization(M_0) and the transverse magnetization (M_{xY}) is zero. Following RF excitation, MZ decrease and M_{xY} increase. At a flip angle of 90 all MZ existing immediately prior to the RF pulse is rotated into the transverse plane. When the RF pulse is turned off the excited nuclei relax and return to their equilibrium orientation, they loss the excess energy by emitting electromagnetic radiation of the same frequency as the applied pulse, this emitted radiation (electromagnetic wave) is the source of the MR signal which can be detected by a receiver coil. The

emitted signal is called the free induction signal or the free induction delay (FID). The length and magnitude are determined by the relaxation times which are two related constant times that characterize the process of relaxation :

1. The spin lattice :

The characteristic time constant for the magnetization to return to the longitudinal axis after being excited by an RF pulse, also called : the longitudinal relaxation time or the relaxation time (Wehrli, 1988).

2. The spin-spin:

The characteristics time constant for loss of phase coherence among spins(due to the interaction between spins) and the resulting loss in transverse magnetization, also called : the transverse relaxation time or T2 relaxation time(Wehrli, 1988).

T₁ relaxation time:

When the RF pulse is switched off, the net magnetization take some of time to fully return to equilibrium or relax to the original longitudinal orientation, the process by which this happens is known as the spin latic relaxation(this is because of the fact that the excited nuclei can return to the original state only by dissipating their excess energy to their surroundings (their latic). T1 relaxation time is vary across different tissues, fat has a

short T1 relaxation time (fast relaxation) while the water has long T1 relaxation time (slow relaxation) (Bydder et al, 1985).

T₂ relaxation time:

With a certain type of RF pulse, the transverse magnetization increase while the longitudinal magnetization decrease, the transverse component of the net magnetization can induce a measurable signal in the receiver coil. This signal is seen to quickly decay, this is because the transverse magnetization is composed of microscopic individual spins which are synchronous immediately after being tipped into the transverse plane after that they quickly loss phase coherence with subsequent loss of transverse magnetization. The T2 relaxation time describe the exponential loss of transverse magnetization as a result of local field inhomogenities in the tissues being studied, T2 relaxation time is not field dependant (Bydder et al, 1985).

Echo Formation:

Immediately after an RF pulse, transverse magnetization is maximal and then quickly decays at a rate indicated by the time constant T2. Direct detection of the FID signal immediately formed after the 90 pulse, most MRI pulse sequences form an echo of the original FID, which is the signal that is collected. (Makow, 1989).

Gradient Echo:

In the MR system, the dominant sources of extrinsic magnetic field imperfection are the gradient fields lead to variation in spin frequencies in the same direction of the gradient, this is the basis for image reconstruction but however, this also lead to dephasing of transverse magnetization which can be prevented by another gradient of identical amplitude but opposite polarity (Wehrli, 1988).

Spin Echo:

Another, more popular method for echo formation in which 180 rephasing pulse is used instead of the gradient used in the gradient echo (Bydder et al, 1986).

MR Angiography:

MRA is the modality of choice for the evaluation of neurovascular lesions and based on the flowing blood had MR properties different from those of stationary tissue. Two distinct types of flow related processes were recognized :

1-Time of flight (ToF) MR angiography:

ToF MR angiography based on inflow enhancement (spins moving into a slice would have bright signal intensity compared

with the surrounding stationary tissue) (Kouwenhoven et al, 1994).

The basic concept of ToF are:

A) Saturation of stationary tissue :

For optimum display of the vessel containing free moving blood, all stationary tissue in the imaging volume should be saturated which is easily achieved by a gradient field echo sequence in gradient echo, repetition time is less than the relaxation time of the tissue, so, the longitudinal magnetization will not reach equilibrium before the next (RF) pulse on succeeding excitation, less and less longitudinal magnetization is present until steady state condition is reached, at which the tissue will be saturated (Sibert et al, 1992).

B) Enhancing signal from flowing blood:

Blood which had not received any RF pulses (Unsaturated blood) produce strong MR signal when excited by an RF, thus its signal will be strongly enhanced compared to the stationary saturated tissues.

2- Dimensional MRA:

A large flip angle(50-60) and thick slices are used, so, there is high contrast between the vessels and surrounding tissues

resulting in a projection image of the vessels against the background of the stationary tissues (Keller et al. 1992).

3-Dimensional MRA :

Using ToNE, tilted optimized non-saturated excitation, technique which depend on using a small flip angle (15-25), so, the contrast between the moving blood and the stationary tissue is high with easy detection of smaller vessels(Paker et al, 1991).

II- Phase contrast angiography(PCA) :

PCA, are a group of techniques that allowing the study of the morphological and haemodynamical properties of the vascular lesions. PCA is based on using two gradient (bipolar) pulses of equal magnitude and duration but with opposite polarity, this induce phase shift which proportional to position (position dependant phase shift) (Domalin, 1992) For protons moving during the interval between the gradient pulses, the phase shift induced by the first pulse will not be cancelled by those of the second pulse, thus, the moving protons acquire a net phase shift which is proportional to the velocity(Sibert et al, 1992).

MRI Characteristics And Manifestation Of Pediatric Intracranial Tumors

On MRI, neoplastic lesions are detected because of their long T1 and T2 relaxation times compared with those for brain parenchyma. This is because of the increased water content of the neoplastic tissue. Therefore, the tumor is seen as low signal intensity on T1 weighted images and high signal intensity on T2 weighted images (Kortman et al, 1988).

At times the tumor nidus is difficult to differentiate from the surrounding edema, as both exhibit prolonged T1 and T2 relaxation times. However, there is less prolongation of T1 and T2 in the tumor than in the surrounding edema, therefore, on the MRI the tumor is differentiated by its slightly greater intensity than the surrounding edema on T1 weighted images and slightly less intensity than the surrounding edema on T2 weighted images (Grossman et al, 1985).

MR Characteristics and Pathological Findings with Pediatric Intracranial Tumors :

Location:

Tumor location is important for brain tumor differential diagnosis and for determining MR imaging technique (Dropcho, 1989).

Multiplicity:

Intra-axial tumor multiplicity usually indicates metastatic disease. Multiple gliomas are rare. Multiple meningiomas have characteristic dural surface locations. Multiple sclerosis, emboli and cerebral abscesses are conditions associated with multiplicity that can mimic multifocal neoplasm (Dorpcho,1989).

Intensity :

Lesion intensity and degree of homogeneity are important clue to tissue type neoplasm. Neoplastic lesion intensities are detected because of their long T1 and T2 relaxation times compared with those for brain parenchyma(Fitz,1985).

Margination:

Smooth, sharply defined margination favors the diagnosis of benign lesions. While, irregular, poorly defined margins favor the diagnosis of malignant neoplasm(Leo et al, 1979).

Contrast enhancement:

Gd_DTPA (gadolinium diethylene triamine pentaacetic acid) is paramagnetic contrast agent which have excellent biologic tolerance, no significant complication or side effects have been reported. The agent is injected intravenously at dose of 0.1 mmol/Kg. The gadolinium contrast agents do not cross the intact blood brain barrier(BBB) if the (BBB) is disrupted by a disease process, the contrast agent diffuse into the interstitial space and shorten the relaxation time of the tissue resulting in increased signal intensity on T1 weighted images. The scan should be acquired between 3 and 30 minutes after injection for optimal results(Yuh et al, 1985).

Calcification:

Calcification produce signal void on MRI and so is more difficult to identify by it. Calcification occurs within many tumors and it may be punctate or diffuse and is best seen as high density with CT scanning(Paley et al, 1989).

Hemorrhage:

A large variety of primary and metastatic tumors may be presented with spontaneous hemorrhage. Hyperacute hemorrhage (oxyhemoglobin) exhibits iso to low signal intensity on T1 and

high signal intensity on T2. Acute hemorrhage (deoxyhemoglobin) exhibits iso to low signal intensity on T1 and low signal intensity on T2 while chronic hemorrhage (hemosidrin) appear of low signal intensity on T1 and T2 images.(Grossman et al,1985).

Edema:

One of the most serious side effects of brain tumors, it is of the vasogenic type: result from the absence of BBB in the tumor neovascularity, which allows leakage of proteins and other solutes into the surrounding extracellular space of the white matter (Elster et al,1989).

As edema is the primary cause of increased intracranial pressure and mass effect with tumors, it should be quantefied in the report. On MRI, it is hypointense on T1 and hyperintense on T2 weighted images.(Elster et al, 1989).

Displacement and obstruction :

The tumor mass effect results from the tumor mass itself plus the surrounding edema and possible associated ventricular obstruction. Mass effect may be present as a simple shift of midline structures, ventricular compression or sulcal effacement (Byrne et al,1989).

***MR Findings and Manifestations of The Pediatric
Intracranial tumors:***

1. Tumors of the neuroepithelial tissue:

Intracranial gliomas are more commonly seen in men. The peak occurrence is during middle adult life. Gliomas occur predominantly in the cerebral hemisphere, but the brain stem and cerebellum are frequent location of gliomas in children(Dean et al, 1990).

A strocytomas:

A strocytomas are a large group of gliomas and comprise 35% of all primary intracranial tuomrs. Astrocytomas are graded 1 to 4 according to the degree of anaplasia present which is a localized phenomenon within the tumor(Burger et al,1994).

A strocytoma is applied to grade 1 and 2 tumors that can be further divided into fibrillary and pilocytic types. These are usually slowly growing tumors but are poorly demarctaed from adjacent structures. This often result in incomplete surgical resection and a tendancy to recur (Burger et al,1994).

Astrocytomas of grade 3 and 4 correspond to the age-honored term (glioblastoma multiforme). Some authors favor dividing

glioblastomas into two categories : 1) anaplastic astrocytomas or secondary glioblastomas and 2) primary glioblastomas.(Hauro Kokazaki, 1989).

Glioblastoma usually occur late in adult life, with a peak occurrence between 45 and 60 years. The frontal lobes are a common site of involvement, and extension contralaterally through the corpus callosum may give rise to a butterfly pattern (Hicks et al,1990).

Supratentorial low grade astrocytomas:

These tumors include grade 1 and grade 2 astrocytomas. The tumors demonstrate high signal intensity on T2-weighted images and low signal intensity on T1-weighted images and tend to be well defined and non hemorrhagic with little mass effect and vasogenic edema. Calcification is most often seen as an area of decreased signal intensity, which is better appreciated on T2-weighted than T1 weighted images (Dean et al, 1990).

In low grade a strocytomas theris generally a relative intact BBB, so that there is only patchy or no enhancement(Hesselink et al, 1988).

Supratentorial high grade astrocytomas:

These tumors include grade 3 (anaplastic astrocytoma) and grade 4 (glioblastoma) [Hicks et al, 1990].

Anaplastic astrocytoma:

Are less well defined and demonstrate low signal intensity on T1-weighted images and high signal intensity on T2-weighted images with moderate amount of mass effect, heterogeneity and edema. Calcification is rare. The pattern of contrast enhancement is variable from fine rim to dense, thick irregular enhancement (Johnson et al, 1989).

Glioblastoma:

Are poorly defined and demonstrate varying degree of low signal intensity on T1-weighted images and high signal intensity on T2-weighted images with mass effect, edema and heterogeneity (representing necrosis, cystic changes and hemorrhage). Enhancement is usually ring like with thick irregular wall, nodularity and central non enhancing foci representing necrosis or cyst formation (Black et al, 1991).

Cerebellar astrocytoma:

Most (85%) cerebellar astrocytomas arise in the midline with secondary extension into the hemisphere or extrinsic obliteration of the fourth ventricle. About 15% of these tumors involve only the cerebellar hemisphere, a commoner location in the older patient (Maroldo, Barkovich, 1992).

The typical appearance of a cerebellar astrocytoma is that of a predominantly cystic lesion with a mural nodule. The cyst can be round or ovoid and is always unilocular. The tumor nodule is either rounded or plaque like and enhances homogeneously and intensely. Ten percent to 20% are calcified. (Gusnard, 1990).

The MR appearance of cerebellar astrocytomas parallels that of CT. Cysts are seen in 80% of pilocytic tumors. The cyst fluid itself tends to be slightly more proteinaceous than CSF, therefore compared with CSF signal intensity, cyst fluid tends to be slightly hyperintense on short TR/TE images and hyperintense on long TR, short TE pulse sequences. On T2-weighted images, the solid element tends to be hyperintense to gray matter. The solid juvenile pilocytic astrocytoma has bright T2 signal and almost always shows intense paramagnetic enhancement. (Zimmerman et al, 1992).

Diffuse /fibrillary low – grade astrocytomas are not readily differentiated from pilocytic tumors. Highly anaplastic astrocytomas and glioblastomas are occasionally encountered in the cerebellum. These lesions tend to have more mass effect than their benign counterpart, be widely infiltrative, and show various areas of necrosis. Most enhance.

Special Variant of a astrocytoma:

Giant cell astrocytoma:

Rare slow growing tumor, occur in 10 to 26% of patients with tubers sclerosis. The peak age of presentation is between 8-18 years. This tumor is benign and arising from the wall of the lateral or third ventricle (Waggenspack et al,1989).

The tumors are hypo to iso intense on T1 weighted images and hyperintense on T2 weighted images with unilateral dilatation of the lateral ventricle, but if the tumor is large both lateral ventricles may be dilated.. Calcification is frequent. The pattern of enhancement is homogenous (Braffman et al,1992).

Oligodendrogliomas:

Are relatively uncommon brain tumors that constitute 5-7% of all primary intracranial neoplasma. The peak incidence is in the

4th and 5th decades, and the vast majority of these tumors are located peripherally in the frontal and fronto-temporal regions (Atlas, 1990).

Oligodendrogliomas tend to be relatively superficial in location (cortical and subcortical) and appear hypointense on T1 weighted images and hyperintense on T2 weighted images with little edema. Calcification is present in 50-90%, gradient echo imaging is highly sensitive in demonstrating these calcifications. Following paramagnetic contrast agent infusion, enhancement may be homogenous, peripheral (cystic changes) or mixed. Thick rim like enhancement with central necrosis suggestive of malignant degeneration (Tice et al, 1993).

Ependymomas:

Ependymomas represent 5-6% of all gliomas. They occur most commonly in children, the majority of these tumors occur within the fourth ventricle, although 21% may be supratentorial, located along the walls of the lateral ventricles, the septum pellucidum is a common supratentorial location (Lee et al, 1985).

The tumor is seen as an irregular inhomogenous mass, hypointense on T1 weighted images and hyperintense on T2 weighted images. Cysts are common and calcification is seen in up to 44% of ependymomas. Little or no edema is typical,

however, if significant edema is present malignant transformation should be considered. Contrast enhancement is usually inhomogenous because of necrotic changes(Castillo,1994).

Medulloblastoma:

On MR images, the typical presentation is of a midline inferior vermian lesion extending into the fourth ventricle, at times into the fourth ventricular foramina (primarily foramen of Magendie). The lesions tend to have low-to-intermediate signal on short TR/TE images and be isointense to slightly hyperintense to cerebellar cortex on long TR/TE images(Meyers et al, 1992).

Their character on T2 – weighted images is typically homogenous with the exception of cystic or necrotic foci. Vascular flow voids and calcifications (seen as low T2 signal foci) contribute to the more heterogenous lesions. Homogenous enhancement of the solid portion is the rule on MR, although up to 10% of the lesions do not enhance on MR. (Zimmerman et al,1992).

Cerebellar tonsillar herniation is commonly observed(Meyers et al,1992).

Brain stem gliomas:

Brain stem gliomas constitute 25% of posterior fossa neoplasms in children.

Almost all brain stem gliomas are fibrillary high grade astrocytomas, anaplasia is present in 60% to 100% of lesions (Packer et al, 1992).

On MR, these lesions are hypointense on short TR/TE and hyperintense on long TR/TE images. Enhancement is present in 25% to 50% of cases and is usually limited to small foci within the lesion (Smith, 1990).

Tumors of the meninges :

Meningioma:

Meningiomas account for 15% of all intracranial tumors and are the most common extra-axial tumor. They originate from the dura or arachnoid and occur in middle – aged adults (Glasier et al, 1993).

Meningiomas in pediatric patients are unusual and associated with neurofibromatosis in 25% of cases. Pediatric meningiomas are more commonly seen in the posterior fossa or unusual sites such as intraventricular or intraparenchymal (Glasier et al, 1993).

The MR appearance of meningioma is a mass that is isointense to hypointense on T1- weighted scans and bright on T2-weighted scans. The tumor enhances brightly. Dense calcifications can be seen on MR as low- intensity areas within the mass. Hyperostosis related to meningioma is better seen by

CT. edema surrounding a meningioma is variable. Malignant sarcomatous changes is more common in children than adults, it is suggested by blurred borders and inhomogenous enhancement (Wilms et al, 1991).

Reticuloendothelial System Tumors :

Primary lymphoma:

Lymphomas typically appear as homogenous well demarcated mass. They are usually slightly hypointense relative to parenchyma on T1-weighted images and iso-to hyperintense on T2-weighted images. Most lymphomas have only a small amount of associated edema and mass effect. Intense homogenous enhancement is usually seen (Schwaighofer et al, 1989).

Metastatic lymphoma:

Secondary involvement of the CNS with lymphoma occurs much less commonly than the primary type and is seen almost exclusively with non hodgkin s lymphoma, with greater incidence of leptomeningeal involvement rather than brain parenchyma (Yuh et al, 1995).

The tumor is generally appears isointense to the gray matter on T1-weighted images and hyperintense on T2-weighted images. Parenchymal extension of the tumor, which may be multiple, are generally moderately hypointense on T1-weighted images and

hyperintense on T2-weighted images and usually enhance homogeneously but with irregular margins (Davis et al,1991).

Choroid plexus tumors :

On MR, the tumors are lobulated, well marginated mass with generalized hydrocephalus. They are of low signal intensity on T2-weighted images and may be of low signal intensity on T2-weighted images. Multiple areas of signal void may be noted related to calcification or hypertrophied vessels. Cyst formation is relatively common, edema is uncommon and it is a prominent feature of carcinomas. Invasion of the brain parenchyma and subarachnoid tumor seeding are also typical of carcinomas which are very heterogeneous. Following contrast infusion, the tumor show marked enhancement (Osborn, 1994).

Pineal Region Tumors:

Tumors in the pineal region are classified into three major groups based on their origin: germ cell tumors (germinoma and teratoma), pineal parenchymal tumors (pineocytoma and pineoblastoma) and parapineal tumors (glioma of the tectum, meningiomas arising within the quadrigeminal cisterns, dermoid, epidermoid and arachnoid cyst). These rare tumors represent 0.4-1.0% of all intracranial tumors (Tien et al,1990).

Germinomas:

Germinomas are usually seen as a homogenous mass, isointense relative to white matter on T1-weighted images and slightly hyperintense on T2-weighted images, intense homogenous enhancement has been noted(Tien et al,1990).

Teratomas:

These tumors are composed of well-differentiated tissues from all germinal layers. Intracranial teratoma is the most common intracranial tumor in the newborn. Pineal region teratomas are heterogenous mass with cystic portion hypointense on T1-weighted images and hyperintense on T2-weighted images(Tien et al, 1990).

Pineocytoma:

This slowly growing tumor of mature pineocytes can present at any age and affects both sexes equally. Pineocytoma is usually well defined, cyst like pattern homogenous hypointense on T1-weighted images and hyperintense on T2-weighted images(Nakagawa et al,1990).

Pineoblastoma:

This malignant tumor of primitive pinealocytes is most often seen in children with male predominance. These tumors are often

ill defined, lobulated hypointense on T1-weighted images and hyperintense on T2-weighted images associated with ventricular and leptomeningeal spread (Chiechi et al,1995).

Tumors of Maldevelopment:

Most lipomas are hyperintense on T1-weighted images and hypointense on T2-weighted images. A linear low intensity region may appear adjacent to the border of the mass, this region represent a chemical – shift artifact between fat and water(Zimmerman,1990).

Dermoids:

Dermoids are heterogenous masses isointense or slightly hypointense on T1-weighted images and hyperintense on T2-weighted images. Rupture of a dermoid and leakage of the cyst contents into the ventricles or subarachnoid spaces may produce a chemical ependymitis or meningitis.(Smith et al, 1991).

Epidermoid:

Epidermoids are iso intense to CSF on T1-weighted images and moderately hyperintense, heterogenous on T2-weighted images. The tumor margins are irregular and calcification present in 25% of cases, epidermoid tumors do not enhance after administration of contrast agents(Tampieri et al,1989).

Neurofibromatosis:

Two distinct forms of neurofibromatosis have been recognized, neurofibromatosis type 1 (NF-1, Von Recklinghausen's disease) and neurofibromatosis type 2 (NF-2, bilateral acoustic neurofibromatosis). The neoplasms of NF-1 are those of astrocytes and neurons while in NF-2 are those of the covering of the brain and nerves (neoplasm of the meninges and Schwann cells). Hyperintense areas within the cerebellum, brain stem, basal ganglia and cerebral white matter have been seen on T1 and T2 weighted images in patients with NF-1, these foci of abnormal signal appear to represent areas of hamartomatous tissue or gliosis. The unusual appearance of choroidal calcification is a feature of neurofibromatosis (Aokis et al, 1989).

Ganglion Cell Tumors:

Gangliocytomas:

These tumors have been observed in the temporal lobes and hypothalamic regions. Gangliocytomas are well circumscribed, occasionally cavitory and sometime heavily calcified masses. These tumors are iso intense on T1-weighted images and hypointense on T2-weighted images (Altman, 1988).

Gangliogliomas:

These lesions are manifested by areas of increased signal intensity on T2-weighted images. Multiple tumoral cysts may be seen and are reflected as foci of relatively decreased signal on T1-weighted images and increased signal on T2-weighted images. Focal calcification is a typical feature (Castillo et al, 1990).

Pituitary tumors:

On MRI, pituitary microadenomas are best detected by using thin sections (2-3mm) and detected as areas of low signal intensity on T1-weighted images. Immediately after IV contrast, small microadenoma (10mm or less) appears hypointense relative to the enhancement of the pituitary gland and the cavernous sinus. (Zimmerman, 1990).

Large pituitary adenomas (macroadenomas) tend to have signal intensity similar to those of the normal gland, about 22% show evidence of hemorrhage, cavernous sinus infiltration is caused by invasion laterally through the dura (Miki et al, 1990).

Craniopharyngioma:

Are benign slow-growing tumors that originate from remnants of Rathke's cleft in the pars tuberalis with peak incidence at 5-10 years of age. On T1-weighted images the solid

components of the tumor are hypointense, the cystic portions are usually slightly hyperintense relative to CSF, on T2-weighted images the solid components are hyperintense, calcification is common. Enhancement is heterogenous and intense (Pusey et al, 1987).

Chiasmatic and hypothalamic gliomas:

On MRI, these tumors are solid that appear hypointense or iso intense relative to normal brain on T1-weighted images. On T2-weighted images the tumors are hyperintense. These tumors show variable patterns of enhancement (Rodriguez et al, 1990).

Vascular lesions:

Aneurysm:

Conventional MRI is done in the first as a rule T1w and T2w, then MRA and 3D ToF MR angiography are done. They present as rounded or slightly lobular extraaxial masses with eccentric area of signal void and area of variable signal representing the associated clot. Calcification in the wall may be apparent as a thin, usually discontinuous rim of signal void (Potchen et al, 1996).

Angiomatous malformation(AVM):

MRA is used to evaluate the feeding artery and the draining vein. Most AVMs are supratentorial with a large component of the AVM located superficially in the pia. 3D ToF MR angiography can identify the arterial supply to the AVM. AVM nidus greater than 0.36 cm could be reliably identified by 2 D ToF MR angiography (Kouwenhoven et al,1994).

Metastatic brain tumors:

Metastases are most commonly imaged as multiple intraaxial lesions with a tendency to occur at the gray matter-white matter interface. These lesions are usually hypointense to iso intense relative to brain parenchyma on T1-weighted images and hyperintense on T2-weighted images, associated with surrounding edema. Metastatic melanoma demonstrate increased T1 signal intensity on non enhanced scan due to hemorrhage or the paramagnetic effect of melanin(Woodruff et al, 1987).

Many metastatic lesions have a round, homogeneously enhancing appearance on the enhanced scan, but the ring sign is also a frequent finding (Yuh et al,1995).

Materials And Methods

- In our study 50 cases of pediatric intracranial tumors were selected, 26 cases were females and 24 cases were males. Their age ranged between 30 days to 16 years. The studied cases were referred from the pediatric and neurosurgery departments to the MRI center of the AL_Husseini University Hospital (magnitom Semines 1,5 T), and one case from AL Salam International Hospital.

- The MRI findings in most cases were confirmed surgically and pathologically.

- The selected cases included in our study were subjected to the following:

a) Full clinical history including neurological symptoms, medical therapy, previous laboratory and radiological investigations and the previous operations.

b) Radiological examinations which include :

- CT scanning (in 25 cases) : axial pre and post I.V contrast 10mm cuts, additional coronal cuts were used for more evaluation. We found that, CT was superior to MRI in :

- Bone eroding and pathological calcifications producing tumors.

- Scanning facility including time and price.

All cases were evaluated by MRI examination. The procedure was started by a short explanation for the patient to inform him about this relatively new technique. This explanation was of particular importance in patients who might fear of closed places and in pediatric patients.

The patients were asked to remove the metallic objects before the examination, patients with cardiac pace makers, metallic aneurysmal clips and biomedical implants were excluded from the study.

Special needs of the premature neonate:

Special care must be taken in imaging of premature neonates, whether in the NICU [neonatal intensive care unite] or the radiology imaging departement [Barnes et al, 1992].

The premature neonate needs caeful monitoring of blood gases, heart and respirtatory rate, blood pressure, temperature, fluid balance and electrolytes [Teel, Share, 1991].

Many premature neonates are intubated and supported by mechanical ventilation and therefore may be paralyzed during their imaging study with a short- acting agent, such as vercuronium (norcuron, Organon), with good result.

Non intubated premature neonates usually require sedation for imaging studies other than US and CT (Barkovich, 1988).

Consultation with the neonatologist or pediatrician or careful chart review is critical to the radiologist ordering sedation in these neonates. After discussion with the primary care physicians, we prefer to have the neonate sedated in the NICU before coming to the imaging department. Our most commonly used sedative for premature neonates is chloral hydrate, usually given through a nasogastric or orogastric tube. We reduce our standard dose of 80 mg/kg to 60mg/kg in premature neonates.(McArdle, et al 1987).

Occasionally small intravenous dose of pentobarbital (1 to 3 mg/kg) is given to supplement chloral hydrate if sedation is not adequate.(McArdle, et al 1987).

The selected cases were examined as following :

- 1- Axial T1- weighted images TR < 1500mes. TE < 30 mes.
- 2- Axial T2 weighted and proton density images;
TR > 1500 mes. TE > 60 mes
TE > 30 mes.
- 3- Coronal T1 and T2 weighted images.
- 4- Sagittal T1 and T2 weighted images.
- 5- The same T1W images were repeated after I.V contrast.

Other sequences :

Additional sequences may be added as needed if the neonate is stable and a sleep or paralyzed. If there is concern for hemorrhage, a gradient recalled echo image (GRE) may be useful in detecting the field inhomogeneities of hemorrhage. If there is concern for a vascular lesion, MR angiography is useful. (Medlock, et al 1992).

Contrast Agents :

Gd- DTPA, [Gadolinium diethylene triaminic penta acetic acid] was the paramagnetic contrast agent for MRI. It was safe and clinically well tolerated with no significant complication or allergic reaction have been reported. The enhancement with contrast agents may be due to an alteration in the local vascularity and the B.B.B [blood brain barrier].

Gd- DTPA was available in 20ml vials (magnivist) and injected in a dose of 0.1 mm 01/kg body weight. The rate of injection was 10ml/min, followed by saline flush, the scan was obtained between 5 and 20 minutes postinjection.

Gd – DTPA was used in 40 cases.

MRA and MRV were done for one case.

Results

This study was performed on 50 pediatric patients, 26 girls and 24 boys. (as showing in the next table, which is the master table) :

No. of Cases	Sex	Age	Diagnosis	Clinical Pictures	Investigations	Contrast Enhancement	Associated Findings			
							Mass effect	Edema	Hydrocephalus	Hemorrhage/ Calcifications
1	Male	11years	Lt Fronto Temporal Astrocytoma	Headache Vomiting Convulsion	MRI	Heterogenous	Yes	No		
2	Male	15years	Rt High Parietal Astrocytoma	Headache Vomiting	MRI	Homogenous	Yes	No		
3	Male	12years	Recurrent Lt Temporo Parietal Astrocytoma	Headache	CT & MRI	Heterogenous	Yes	No		
4	Female	3years	Lt Temporo Parietal astrocytoma	Headache Convulsion	MRI	Ring Enhancement	No	Yes		
5	Female	5years	Lt High Parietal astrocytoma	Headache Vomiting	CT & MRI	Heterogenous	No	Yes		

No. of Cases	Sex	Age	Diagnosis	Clinical Pictures	Investigations	Contrast Enhancement	Associated Findings			
							Mass effect	Edema	Hydrocephalus	Hemorrhage/ Calcifications
6	Female	16years	Recurrent Lt Temporo Parietal Astrocytoma	Headache Vomiting Convulsion	MRI	Heterogenous	No	No		
7	Male	13years	Rt Temporal Astrocytoma	Convulsion	MRI	No Injection	Yes	Yes		
8	Female	7month	Rt Temporo Parietal astrocytoma	Gradual Increased Size of the Skull	CT & MRI	No Injection	No	No		
9	Female	3years	Lt Temporal Astrocytoma	Convulsion	MRI	No Injection	Yes	Yes		
10	Female	3years	Lt Frontal astrocytoma	Headache Vomiting	CT & MRI	Ring Enhancement	No	No		
11	Male	3years	Rt Temporo Parietal Astrocytoma	Headache Convulsion	CT & MRI	Heterogenous	Yes	No		

No. of Cases	Sex	Age	Diagnosis	Clinical Pictures	Investigations	Contrast Enhancement	Associated Findings			
							Mass effect	Edema	Hydrocephalus	Hemorrhage/ Calcifications
12	Male	9years	B Stem Glioma	Headache Facial Palsy Divergent Squint	MRI	Heterogenous	No	No		
13	Female	12years	B Stem Glioma	Unconsciousness Paraparesis	MRI	Heterogenous	No	No		
14	Female	14years	B Stem Glioma	Ataxia Facial Palsy	CT & MRI	No Injection	Yes	No		
15	Female	10years	B Stem Glioma	Headache Blurring of Vision	CT & MRI	No enhancement	No	No		
16	Male	11years	B Stem Glioma	Headache Unconsciousness	MRI	No Injection	No	No		
17	Male	9years	B Stem Glioma	Squint Headache	MRI	No Injection	No	No		

No. of Cases	Sex	Age	Diagnosis	Clinical Pictures	Investigations	Contrast Enhancement	Associated Findings			
							Mass effect	Edema	Hydrocephalus	Hemorrhage/ Calcifications
18	Female	9years	B Stem Glioma	Headache Nystagmus	MRI	Heterogenous	No	No		
19	female	10years	Cerebellar Astrocytoma	Headache 6 th Nerve palsy Papilledema	CT & MRI	Homogenous with Nidus	Yes	No	Hydrocephalus	Calcifications
20	Male	1Month	Haemorrhagic Cerebellar Astrocytoma	Gradual Increased Skull size Papilledema	CT & MRI	No Injection	YES	No		Haemorrhage
21	Female	9years	Cerebellar Astrocytoma	Headache Papilledema	CT & MRI	Homogenous	Yes	No	Hydrocephalus	
22	Male	4years	Cerebellar Astrocytoma	Headache Papilledema	MRI	Heterogenous	Yes	No	Hydrocephalus	
23	Male	8years	L1 Thalamic Glioma	Headache Blurring of Vision	MRI	No Injection	No	No		

No. of Cases	Sex	Age	Diagnosis	Clinical Pictures	Investigations	Contrast Enhancement	Associated Findings			
							Mass effect	Edema	Hydrocephalus	Hemorrhage/ Calcifications
24	Male	6years	Sellar & Suprasellar Craniopharyngioma	Headache Unilateral Hemianopia	CT & MRI	Heterogenous	Yes	Yes	Hydrocephalus	
25	Female	16years	Suprasellar Craniopharyngioma	Headache Blurring of Vision	MRI	Ring Enhancement	Yes	No	Hydrocephalus	
26	Female	3years	Sellar Craniopharyngioma	Headache Unilateral Hemianopia	CT & MRI	Heterogenous	No	No	Hydrocephalus	
27	Male	1,5year	Suprasellar Craniopharyngioma	Unilateral Hemianopia Papilledema Headache	MRI	No Injection	No	No		
28	Female	5years	Suprasellar Craniopharyngioma	Vomiting Blurring of Vision	CT & MRI	No Injection	Yes	NO		Calcifications

No. of Cases	Sex	Age	Diagnosis	Clinical Pictures	Investigations	Contrast Enhancement	Associated Findings			
							Mass effect	Edema	Hydrocephalus	Hemorrhage/ Calcifications
29	Female	3years	Sellar Craniopharyngioma	Headache Prosis Papilledema	MRI	Heterogenous	Yes	No		
30	Male	4years	Sellar & Suprasellar Craniopharyngioma	Bilateral hemianopia Papilledema	CT & MRI	Homogenous	No	No	Hydrocephalus	
31	Male	5years	Suprasellar Craniopharyngioma	Headache Vomiting	MRI	Heterogenous	Yes	No		Calcifications
32	Male	3years	Medulloblastoma	Vomiting Ataxia	MRI	Heterogenous	No	No		
33	Female	16years	Medulloblastoma	Headache Blurring of Vision Papilledema	CT & MRI	Homogenous	Yes	No	Hydrocephalus	

No. of Cases	Sex	Age	Diagnosis	Clinical Pictures	Investigations	Contrast Enhancement	Associated Findings			
							Mass effect	Edema	Hydrocephalus	Hemorrhage/ Calcifications
34	Male	16years	Medulloblastoma	Headache Ataxia	MRI	Heterogenous	Yes	No	Hydrocephalus	
35	Male	11years	Medulloblastoma	Headache Vomiting Blurring of Vision	MRI	Heterogenous	Yes	No	Hydrocephalus	
36	Female	4years	Medulloblastoma	Ataxia Papilledema	CT & MRI	Heterogenous	Yes	No		
37	Male	3years	Medulloblastoma	Headache	CT & MRI	Heterogenous	Yes	No		
38	Male	8years	Medulloblastoma	Ataxia Papilledema	MRI	Homogenous	No	No		
39	Male	14years	Medulloblastoma	Headache Blurring of Vision	CT & MRI	Homogenous	Yes	No	Hydrocephalus	
40	Female	3years	Ependymoma	Headache Blurring of Vision	CT & MRI	Homogenous	Yes	No	Hydrocephalus	

No. of Cases	Sex	Age	Diagnosis	Clinical Pictures	Investigations	Contrast Enhancement	Associated Findings			
							Mass effect	Edema	Hydrocephalus	Hemorrhage/ Calcifications
41	Female	15years	Ependymoma	Headache Vomiting ataxia	MRI	Homogenous	Yes	Yes	Hydrocephalus	
42	Female	4years	Ependymoma	Headache Vomiting	CT & MRI	Heterogenous	Yes	No		Calcification
43	Male	15years	Ependymoma	Headache Paraparesis	MRI	Homogenous	No	No		
44	Female	5years	Pinealoma	Headache Vomiting	CT & MRI	Homogenous Enhancement	Yes	No	Hydrocephalus	
45	Female	10years	Pineal Body Germinoma	Headache Vomiting	MRI	Intense Homogenous enhancement	No	No	Hydrocephalus	
46	Female	10years	Metastasis	Headache Convulsion	MRI	Homogenous	No	Yes	Hydrocephalus	

No. of Cases	Sex	Age	Diagnosis	Clinical Pictures	Investigations	Contrast Enhancement	Associated Findings			
							Mass effect	Edema	Hydrocephalus	Hemorrhage/ Calcifications
47	Male	3years	Metastasis	Headache Prosis	CT & MRI	Heterogenous	No	Yes		
48	Female	11years	Choroide Plexus papilloma	Headache Vomiting	CT & MRI	Intense Homogenous Enhancement	No	No		Haemorrhage
49	Male	7month	V. Of Galen Aneurysm	Gradual Increased Skull size.	CT, MRI MRA and MRV	Intense Homogenous Enhancement	No	No	Hydrocephalus	
50	Female	16years	C/P Angle Meningioma	Headache Convulsion	CT & MRI	Intense Homogenous Enhancement	No	No		

Table (1) The age distribution of the 50 patients of this study was as follows :

<i>Age group</i>	<i>No. of cases</i>
0 – 1,5 year	4
1,5 – 5 years	18
5 years –9 years	7
9 years – 12 years	10
12 years – 16 years	11

The ages of our patients ranged between 30 days and 16 years, with mean age at 9 years.

Table (2) The classification and No. of cases encountered in the study.

<i>Diagnosis</i>	<i>No. of cases</i>
<i>Gliomas :</i>	23
- Supratentorial astrocytoma	11
- Brain stem glioma	7
Cerebellar astrocytoma	4
Thalamic Glioma	1
<i>Craniopharyngioma</i>	8
<i>Medulloblastoma</i>	8
<i>Ependymoma</i>	4
<i>Pineal body tumors:</i>	2
- Germinoma	1
- Pindeloma	1
<i>Ch plexus papilloma</i>	1
<i>Meningioma</i>	1
<i>V. of Galen anurysm</i>	1
<i>Metastasis</i>	2

Table (3) The different clinical presentations encountered in the study.

<i>Symptoms</i>	<i>No.</i>	<i>Signs</i>	<i>No.</i>
Headache	24	Ataxia	6
Headache and vomiting	14	Facial Palsy	2
Convulsions	7	Papilledema	9
Ptosis	2	Nystagmus	1
Blurring of Vision	8	Unilateral hemianopia	5
Paraparesis	2	Increased Skull Size	3
Unconsciousness	2	Squint	2

The main presenting symptoms in these patients were the headache (24 cases), vomiting (14 cases) which usually associated with headache , and convulsions (7 cases).

<i>Contrast Enhancement</i>	<i>No. of cases</i>
<i>No Injection</i>	10
<i>No enhancement</i>	1
<i>Ring Enhancement</i>	3
<i>Homogenous Enhancement</i>	16
<i>Hetreogenous Enhancement</i>	20

This table shows the number of cases in relation to the given contrast media [Gd – DTPA] .

<i>Associated Findings</i>	<i>No. of cases</i>
<i>Mass Effect</i>	25
<i>Edema</i>	11
<i>Hydrocephalus</i>	13
<i>Haemorrhage</i>	2
<i>Calcifications</i>	4

This table shows the number of cases in relation to the associated findings .

Case No. [1]

Fig.(18)

A 3 years male patient, presented with a history of headache and convulsions.

A] Axial T1 – weighted image demonstrate right deep temporo parietal hypointense lesion with mixed cystic and solid components, associated with significant mass effect, in terms of compressing the ipsilateral lateral ventricle and dilatation of the contralateral side.

B] Coronal T2 – weighted image, the lesion becomes hyperintense with surrounding vasogenic oedema.

C] Coronal post contrast T1 – weighted image, the lesion shows irregular ring enhancement of the cystic component with homogenous enhancement of the solid portion.

Diagnosis :

RT deep temporo parietal grade 11 astrocytoma.

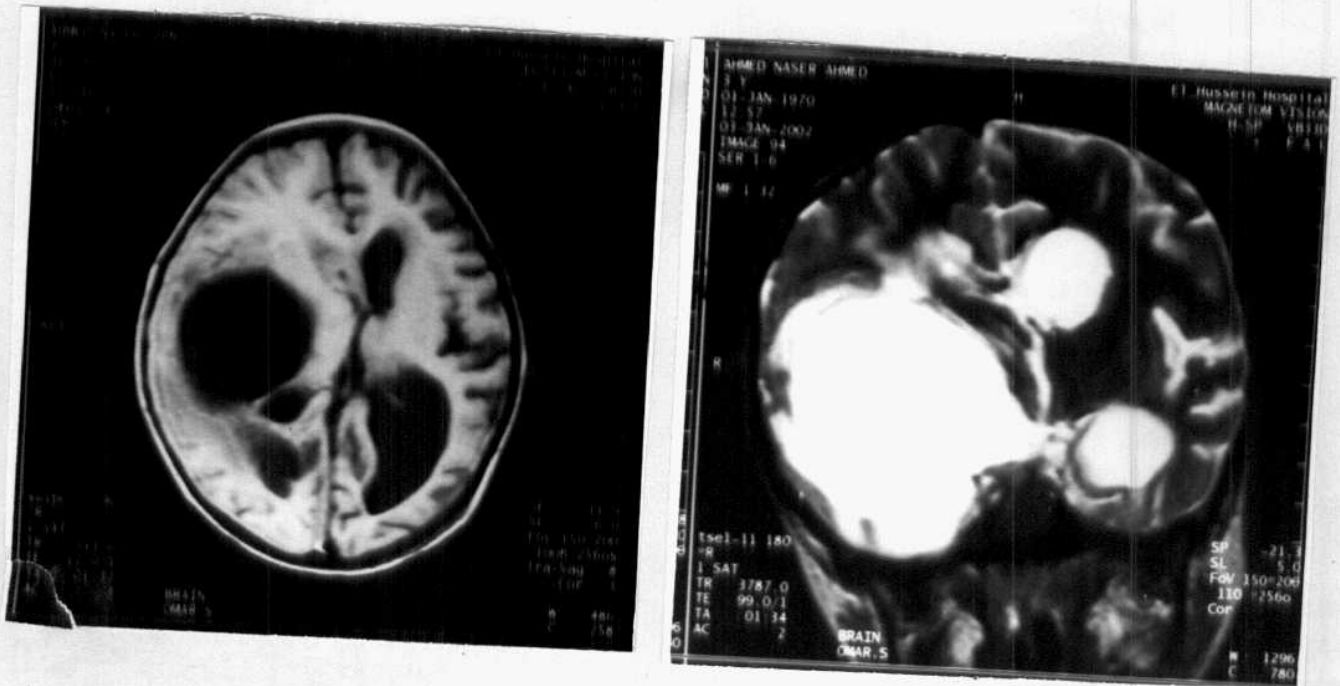


Fig.(18) Right deep temporo parietal grade II astrocytoma.

Case No. [2]

Fig. (19)

A 5 years female patient, presented with a history of epileptic fits and headach.

A] Axial T1 – weighted image demonstrate left high parietal hypointense lesion with no evidence of mass effect or brain oedema.

B, C] Axial and coronal post contrast T1 – weighted images, the mass Show hetrogenous enhancement of the solide portion, associated with mild surrounding edema.

Diagnosis :

Left high parietal low grade astrocytoma.



Fig. (19) Left high parietal low grade astrocytoma

Case No. [3]

Fig. (20)

A 3 years female patient, presented with a history of headach and epilptic fits.

A] Sagittal T1 – weighted image demonstrate large left tempro parietal hypointense lesion with cystic and solide components, associated with mass effect, in term of compressing the epsilateral lateral ventricle.

B] Coronal T2 – weighted image, the mass becomes hyperintense with brain oedema.

C & D] Sagittal and coronal post contrast T1 – weighted image, the mass lesion show homogenous uniform enhancement of the solid copmponent with faint marginal rim of enhancement of the cystic component.

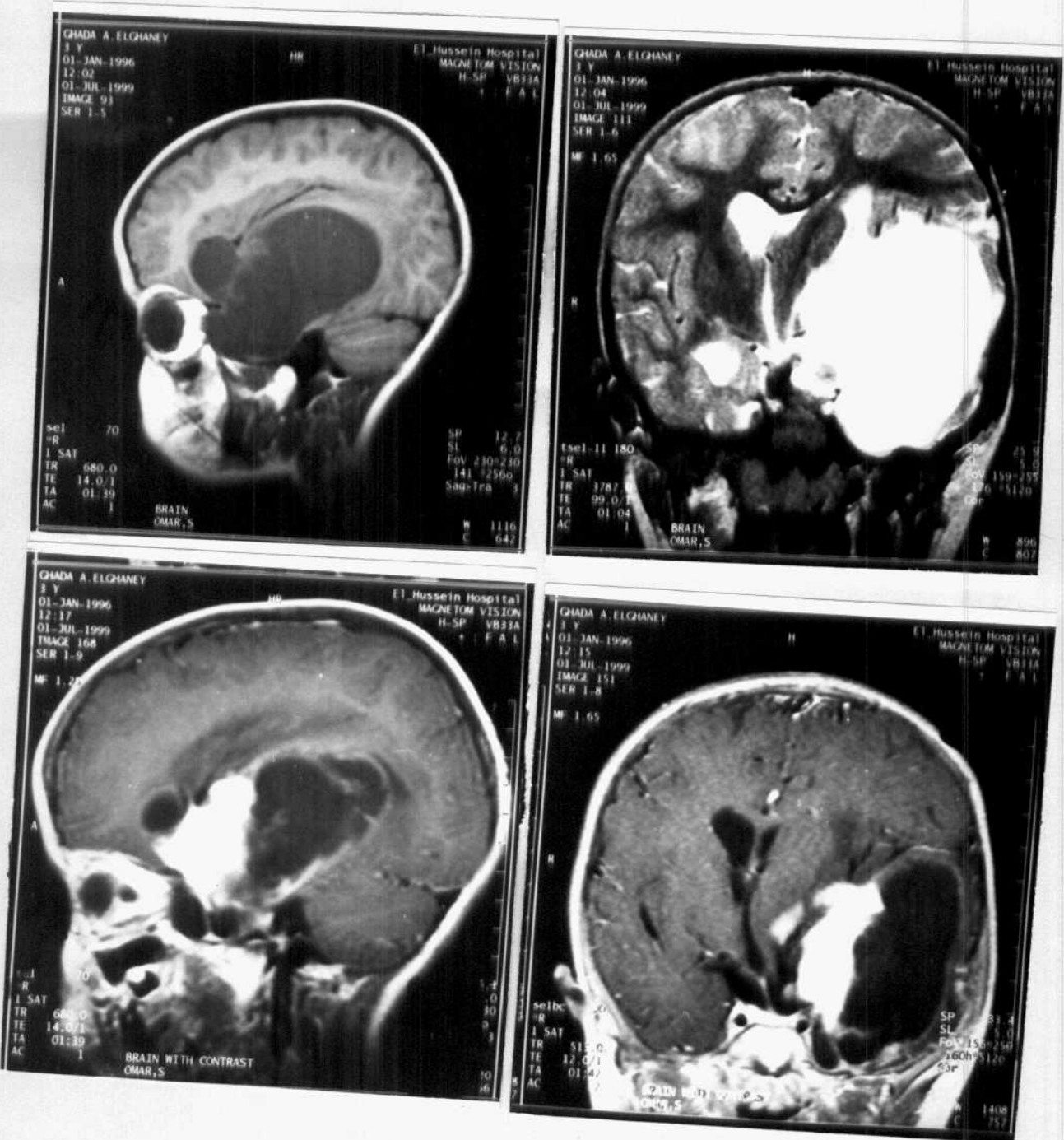


Fig. (20) Left temporo parietal astrocytoma.

Case No. (4)

Fig. [21]

A 16 years old male patient, presented with Headache and projectile vomiting [Recurrent left temporo parietal astrocytoma].

A] Axial T1 – weighted image demonstrate left fronto parietal mass of heterogenous low intensity.

B] Coronal T2 – weighted image, the mass appears of heterogenous hyperintensity with cystic components and mass effect in term of shift of the midline structures.

C, D] Axial and sagittal post contrast T1 – weighted images, the mass show homogenous enhancement at the solid portion while the cystic portion show ring, thick, irregular enhancement.

Diagnosis :

Recurrent left temporo parietal astrocytoma.

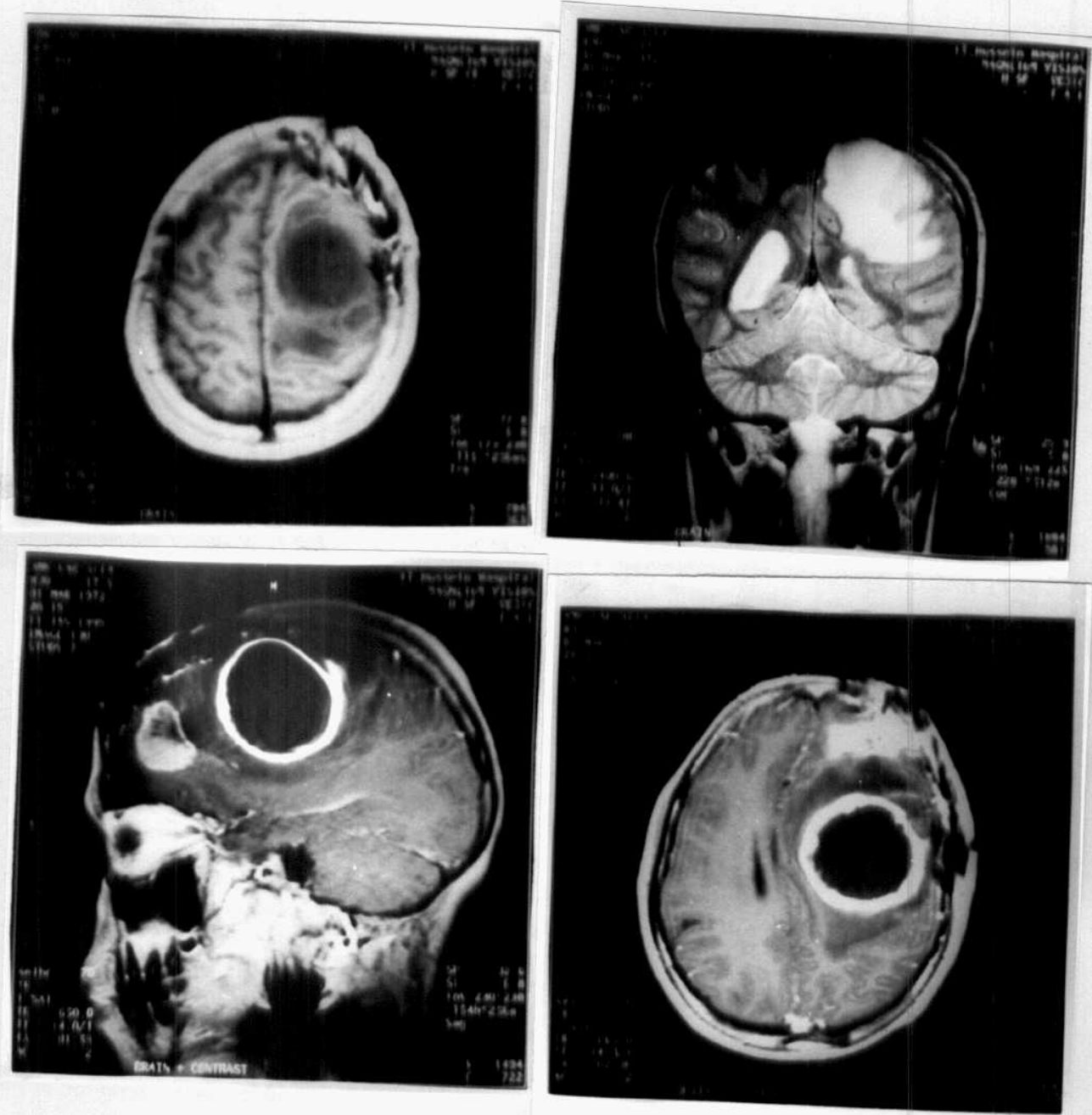


Fig. (21) Recurrent Left Temporo Parietal Astrocytoma.

Case No. [5]

Fig. (22)

A 12 years old male patient, presented with severe headache and vomiting [Recurrent left temporo parietal astrocytoma] .

A] Coronal T2 – weighted image demonstrate left temporo parietal hyperintense mass lesion with surrounding massive brain oedema and mass effect, in term of compressing the ipsilateral lateral ventricle.

B,C] Axial and sagittal post contrast T1 – weighted images, the mass Show heterogenous contrast enhancement.

Diagnosis :

Recurrent left temporo parietal astrocytoma.



Fig. (22) Recurrent left temporo parietal astrocytoma.

Case No. [6]

Fig. (23)

A 15 years old male patient, presented with headache and vomiting.

A] Axial T1 – weighted image demonstrate right high parietal isointense well defined mass lesion with mass effect, in term of shift of the midline structures.

B] Axial T2 – weighted image, the mass becomes slightly hyperintense with moderate vasogenic oedema.

C, D] Coronal and sagittal post contrast T1 – weighted images, the mass show homogenous enhancement.

Diagnosis :

RT high parietal astrocytoma.

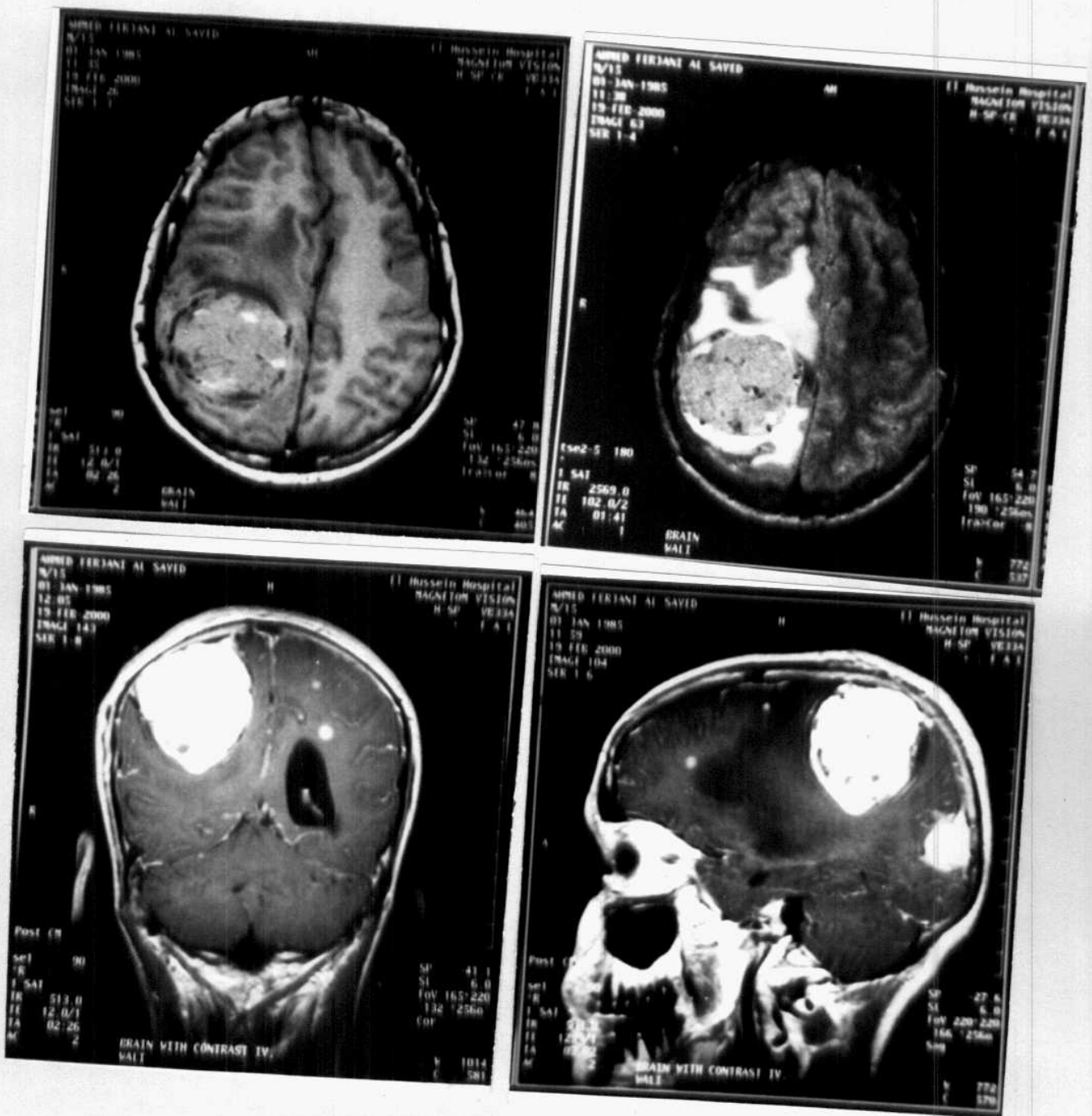


Fig. (23) Right high parietal astrocytoma.

Case No. [7]

Fig. (24)

A 11 years old male patient, presented with a history of headache, vomiting and convulsions.

A] Sagittal T2 – weighted image demonstrate a large hyperintense lesion occupying the left fronto parietal region with surrounding brain oedema and mass effect in term of comprising the ipsilateral frontal horn of the lateral ventricle.

B,C] coronal post contrast T1- weighted images, the lesion show heterogeneous contrast enhancement.

Diagnosis :

Left fronto temporal astrocytoma.



Fig. (24) Left fronto temporal astrocytoma.

Case No. [8]

Fig. (25)

10 years old femal patient, presented with headach , bilateral 6th nerve affection and bilateral 3rd degree papilloedema.

A] Axial C T scanning with and without show a hetrogenous right cerebellar mass lesion with solide and cystic components, with hetrogenous enhancement, the mass appears comprissing the fourth ventricle, resulting in obstructive hydrocephalus.

B] Coronal T1- weighted image shows a hypointense mass lesion of mixed intensity involving the right cerebellum and comprissing the 4th ventricle.

C] Sagittal post contrast T1 – weighted images, the mass revealed hetrogenous contrast enhancement.

Dignosis :

Right cerebellar astrocytoma.

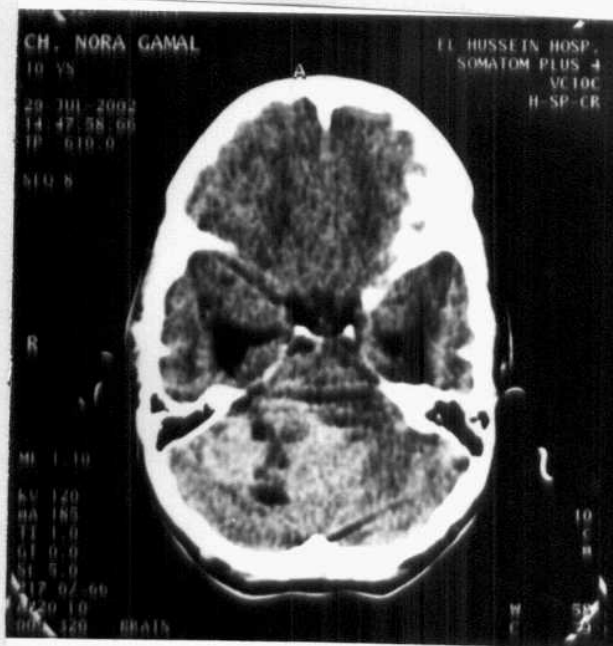


Fig. (25) Right cerebellar astrocytoma.

Case No. [9]

Fig. (26)

A 12 years old female patient, presented with a history of headache, facial palsy and divergent squint.

A,B] Sagittal and axial T1 – weighted images demonstrate a large hypointense mass lesion occupying the brain stem, compressing the fourth ventricle , resulting in supratentorial hydrocephalus.

C, D] Coronal and sagittal post contrast T1 – weighted image, the mass show heterogeneous enhancement.

Diagnosis : Brain stem glioma.

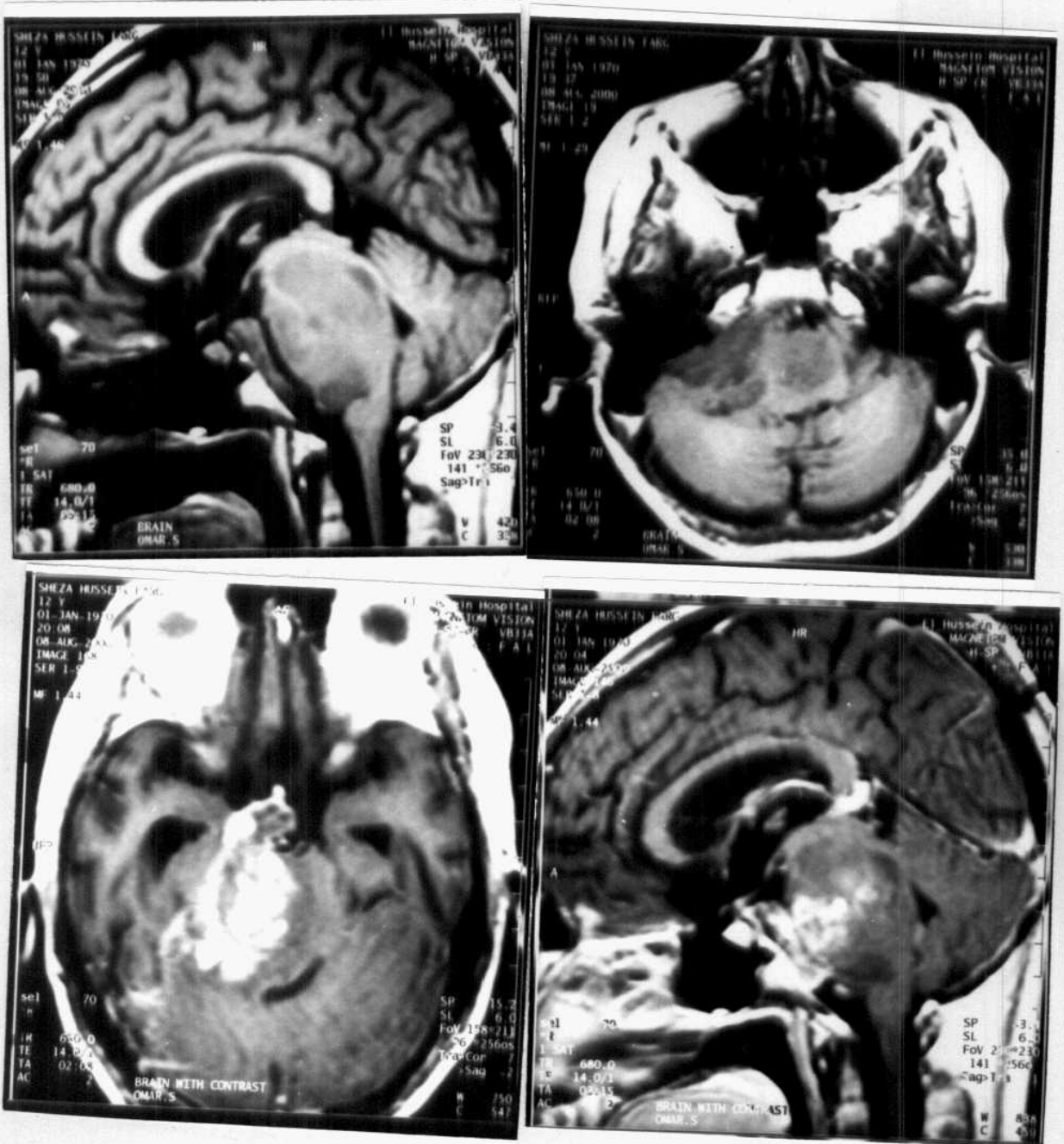


Fig. (26) Brain stem glioma.

Case No. [10]

Fig. (27)

A 9 years old male patient, presented with a history of headache, nystagmus and unconsciousness.

A & B] Axial and sagittal T1 – weighted image demonstrate hypointense lesion of the brain stem.

C] Coronal T2 – weighted image, the lesion becomes hyperintense with no evidence of brain oedema.

D] Sagittal post contrast T1 – weighted images, the mass show heterogenous contrast enhancement.

Diagnosis :

Brain stem glioma.

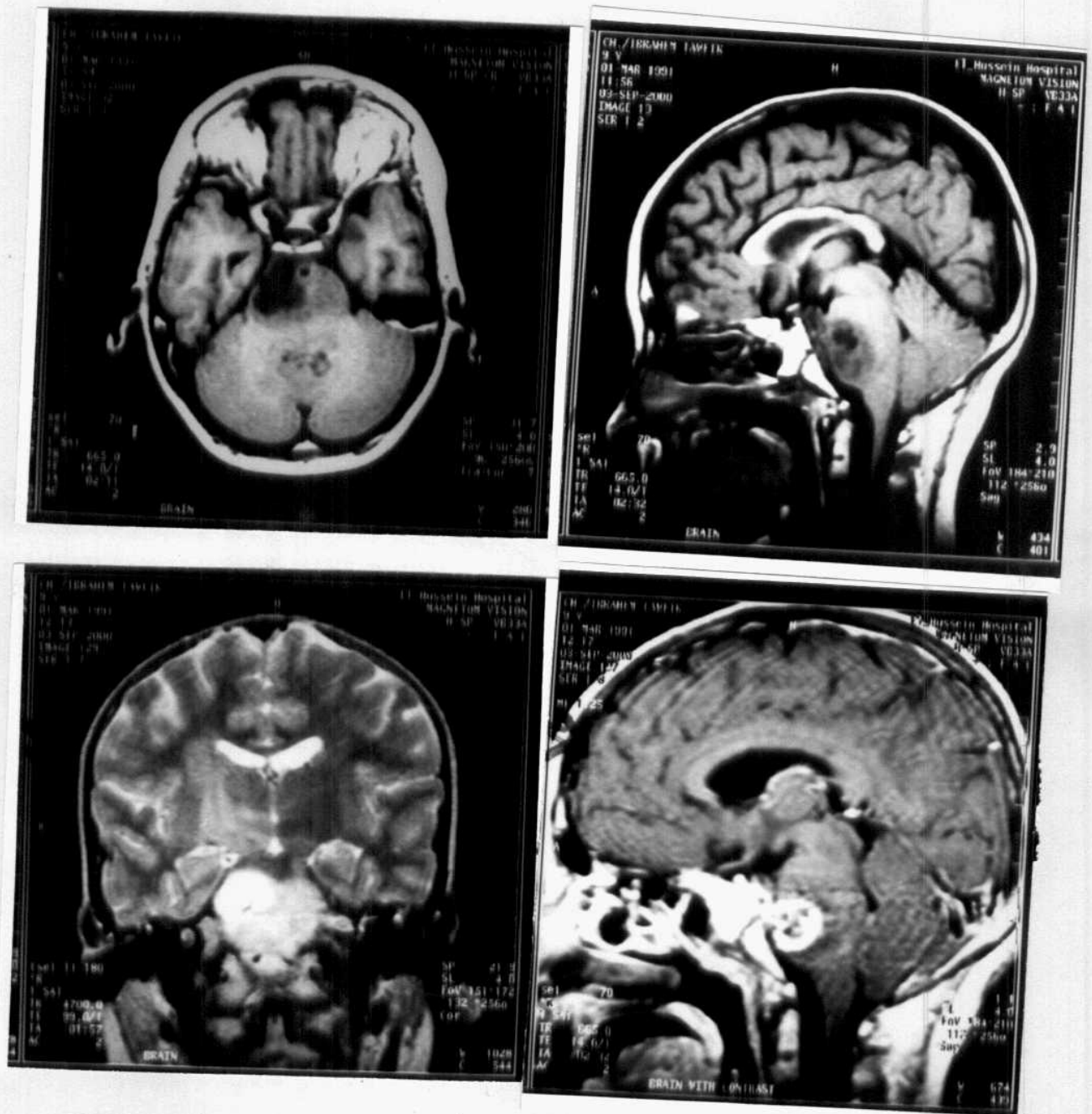


Fig. (27) Brain stem glioma.

Case No. [11]

Fig. (28)

A 3 years old female pateint, presented with a history of headach and unilateral hemianopia.

A] Coronal T1 – weighted image demonstrate a suprasellar hypointense mass lesion with solid and cystic components.

B] Coronal T2 – weighted image, the mass becomes hyperintense.

C] Coronal post contrast T1 – weighted image show ring enhancement of the cystic component and homogenous enhancement of the solid portion.

Diagnosis :

Suprasellar craniopharyngioma.

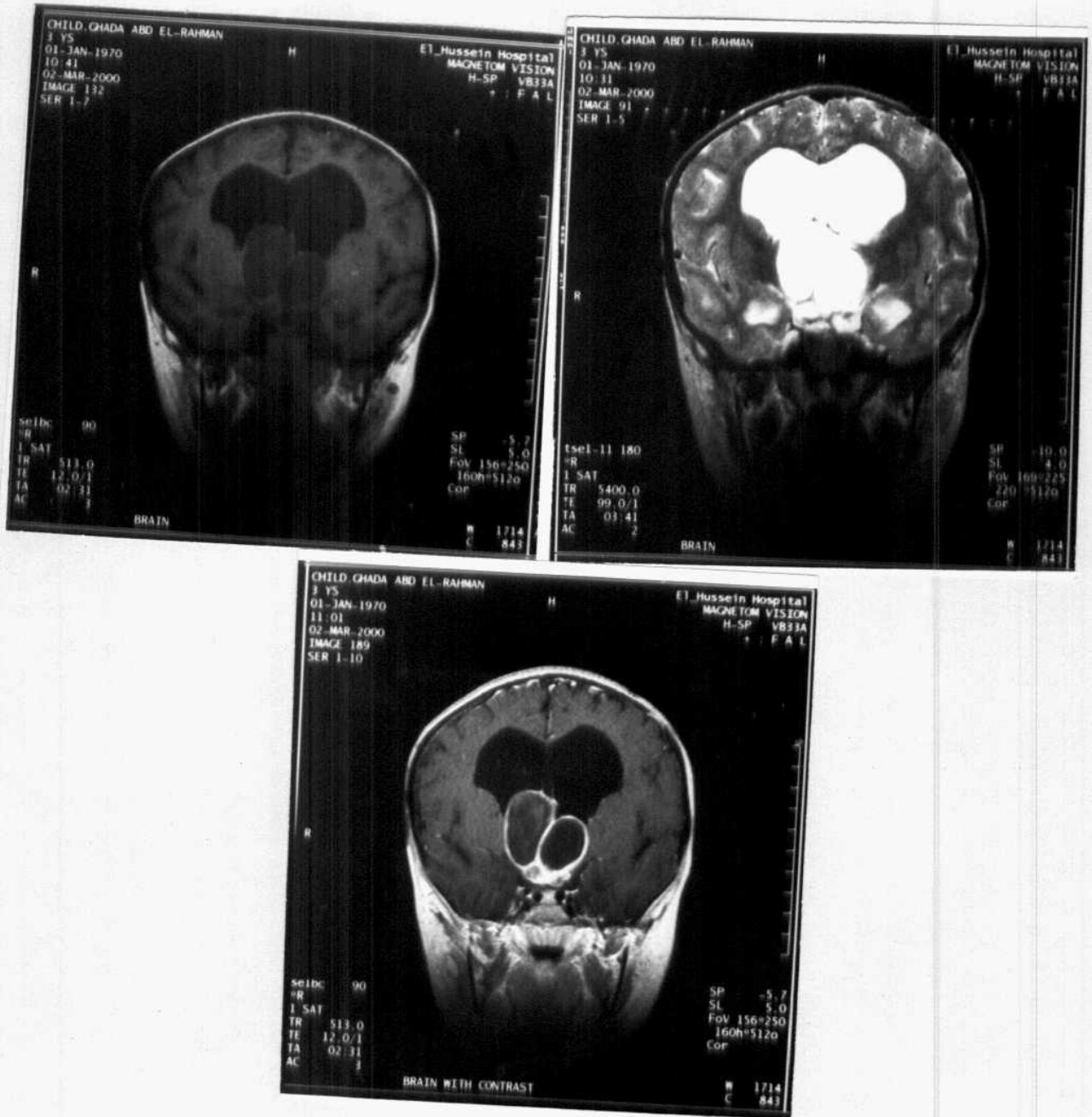


Fig. (28) Suprasellar craniophayngioma.

Case No. [12]

Fig. (29)

A 16 years old female pateint, presented with a history of headach and blurring of vision.

A] Axial T1 – weighted image demonstrate an isointense midline suprasellar mass lesion with a symmetrical right frontal horn dilataion of the lateral ventricle.

B] Coronal and sagittal post contrast T1 – weighted images show ring contrast enhancement.

Diagnosis:

Suprasellar craniopharyngioma.

Case No. [13]

Fig. (30)

A 6 years old male patient, presented with a history of headache, blurring of vision and vomiting.

A] Axial T1 – weighted image demonstrate a very large sellar and suprasellar hypointense mass [8 shaped configuration]. The mass extend to the parasellar region comprising the optic chiasm and superiorly to compress the right foramen of monro, resulting in a symmetrical dilatation of the left lateral ventricle.

B, C] Coronal and sagittal post contrast T1 – weighted images, the mass show intense enhancement of the solid component and non enhancement of the cystic portion..

Diagnosis :

Sellar and suprasellar craniopharyngioma.

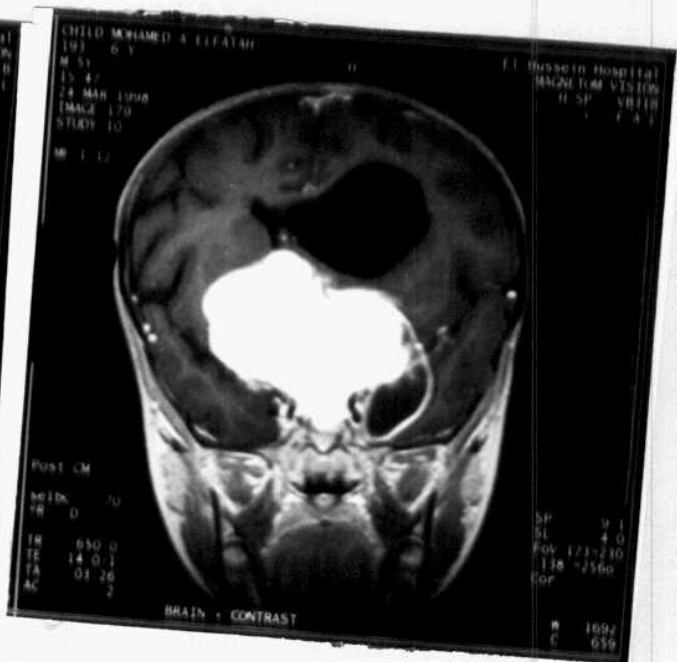
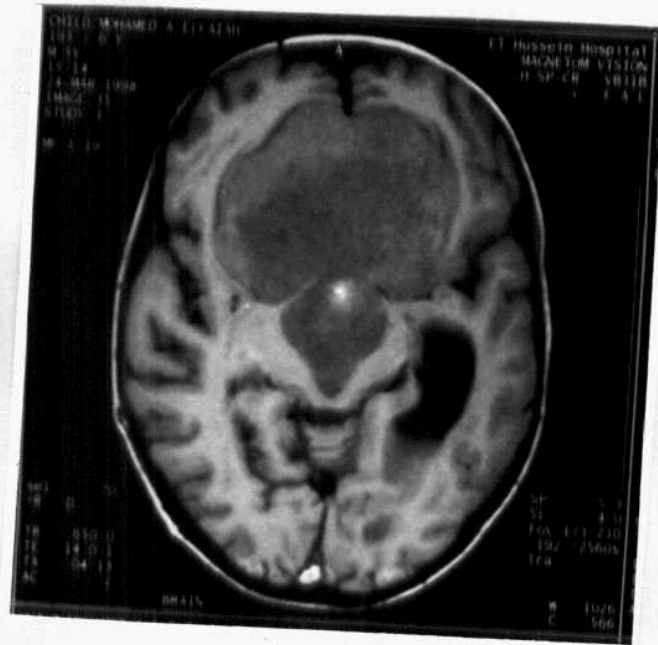


Fig. (30) Sellar and suprasellar craniopharyngioma.

Case No. [14]

Fig. (31)

16 years old female patient, presented with a history of headache and vomiting and ataxia.

A] Axial CT with contrast demonstrate a midline posterior fossa mass lesion arising from the roof of the fourth ventricle of heterogeneous contrast enhancement, extending to the cisterna magna with no caudal migration.

B] Axial T1 – weighted image demonstrate a fourth ventricular hypointense mass lesion.

C,D] Axial and sagittal post contrast T1- weighted images, the mass show homogeneous uniform enhancement.

Diagnosis :

Medulloblastoma.



Fig. (31) medulloblastoma .

Case No. [15]

Fig. (32)

A 3 years old male patient, presented with ataxia, headache and vomiting.

A] Sagittal T1 – weighted image demonstrate a midline posterior fossa mass lesion of hypointensity occupying the fourth ventricle and displacing the brain stem anteriorly with no caudal migration.

B,C] Axial and sagittal post contrast T1 – weighted images show heterogeneous contrast enhancement.

Diagnosis :

Medulloblastoma.

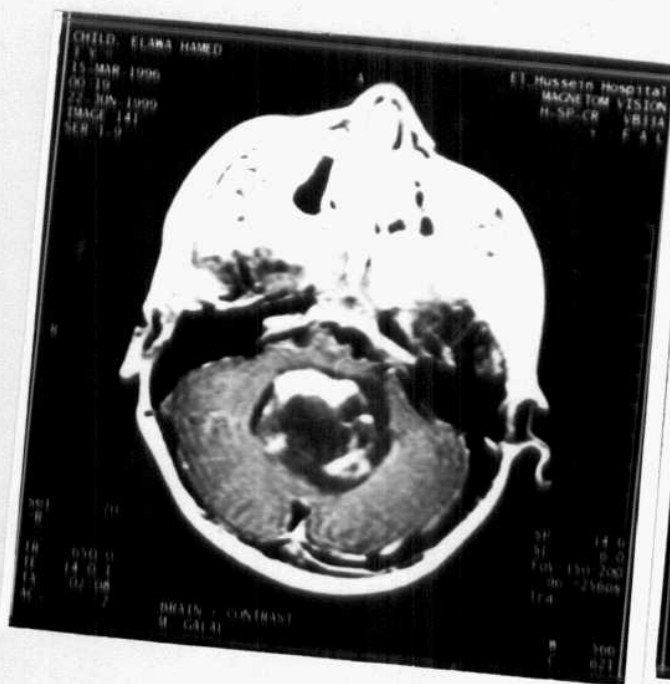
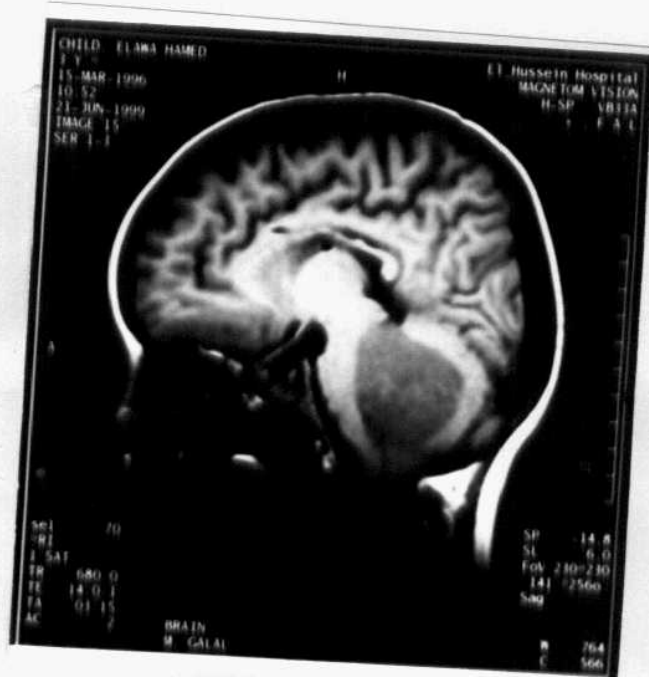


Fig. (32) Medulloblastoma.

Case No. [16]

Fig. (33)

15 years old female patient, presented with a history of headache, vomiting and ataxia.

A] Coronal T1- weighted image demonstrate a fourth ventricular posterior fossa hypointense mass lesion with supratentorial hydrocephalus.

B,C] Coronal and sagittal post contrast T1- weighted images show uniform homogenous contrast uptake with caudal migration.

Diagnosis :

Posterior fossa ependymoma.



Fig. (33) Posterior fossa ependymoma.

Case No. [17]

Fig. (34)

10 years old female patient, presented with a history of hydrocephalus and headache.

A] Coronal T1 – weighted image demonstrate a midline well defined slightly hypointense focal mass lesion related to the pineal region, encroaching upon the aqueduct of sylvius, resulting in bilateral symmetrical hydrocephalus.

B,C] Axial and sagittal post contrast T1- weighted image show uniform intense enhancement of the lesion.

Diagnosis :

Pineal body germinoma.

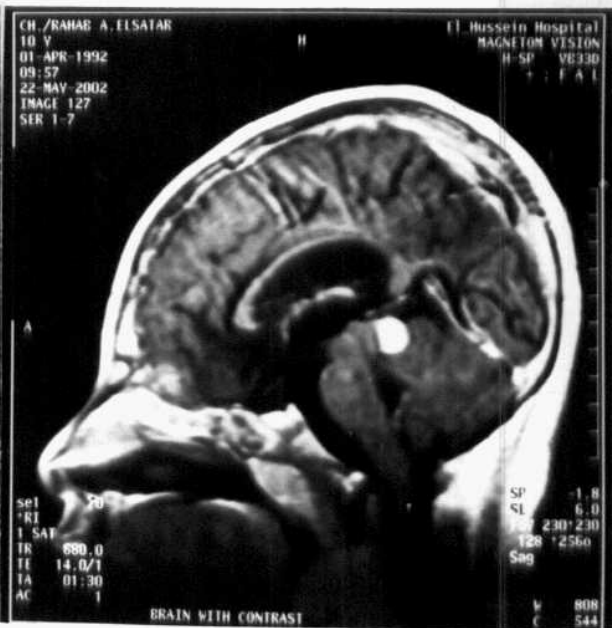


Fig. (34) Pineal body germinoma.

Case No. [18]

Fig. (35)

A 7 month old male patient presented with gradual progressive increased size of the skull with signs of hydrocephalic changes.

A] Axial post contrast T1- weighted image demonstrate a large midline lesion of double shadow [thrombus formation] and intense contrast enhancement, associated with marked supratentorial hydrocephalus as a result from compression of the aqueduct

B,C] MRA and MRV confirm the diagnosis.

Diagnosis :

Vein of Galen aneurysm.



Fig. (35) vein of Galen aneurysm.

Case No. [19]

Fig. (36)

A 10 years old male patient presented with epileptic fits, severe headache and vomiting [post operative surgically removed pineoblastoma].

A] Axial post contrast T1 – weighted images show multiple hyperintense focal lesions with intense enhancement involving the right cerebellum, midbrain and pons.

B,C] Sagittal post contrast T1- weighted images show the same findings demonstrated at A.

Diagnosis :

post operative brain metastasis

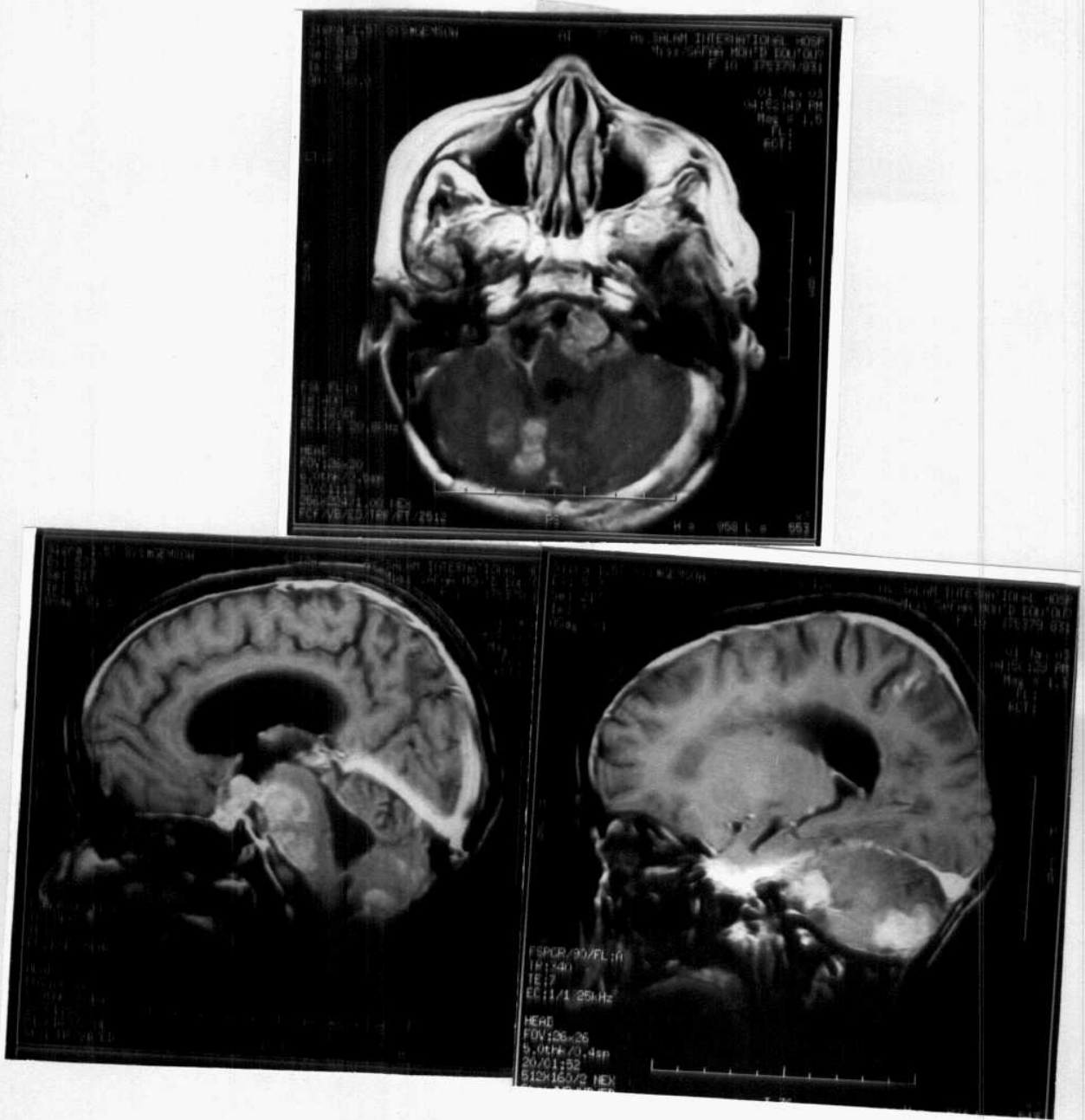


Fig. (36) Post operative brain metastasis.

Case No. [20]

Fig. (37)

11 years old female patient, presented with a history of headache and vomiting.

A] Axial T1 – weighted image demonstrate an intraventricular isointense mass lesion within the lateral ventricle with a peripheral hyperintense haemorrhagic foci.

B] Axial T2- weighted image, the lesion becomes slightly hyperintense.

C] Axial post contrast T1 – weighted image show intense enhancement of the above described intraventricular lesion.

Diagnosis:

Intraventricular choroide plexus papilloma.

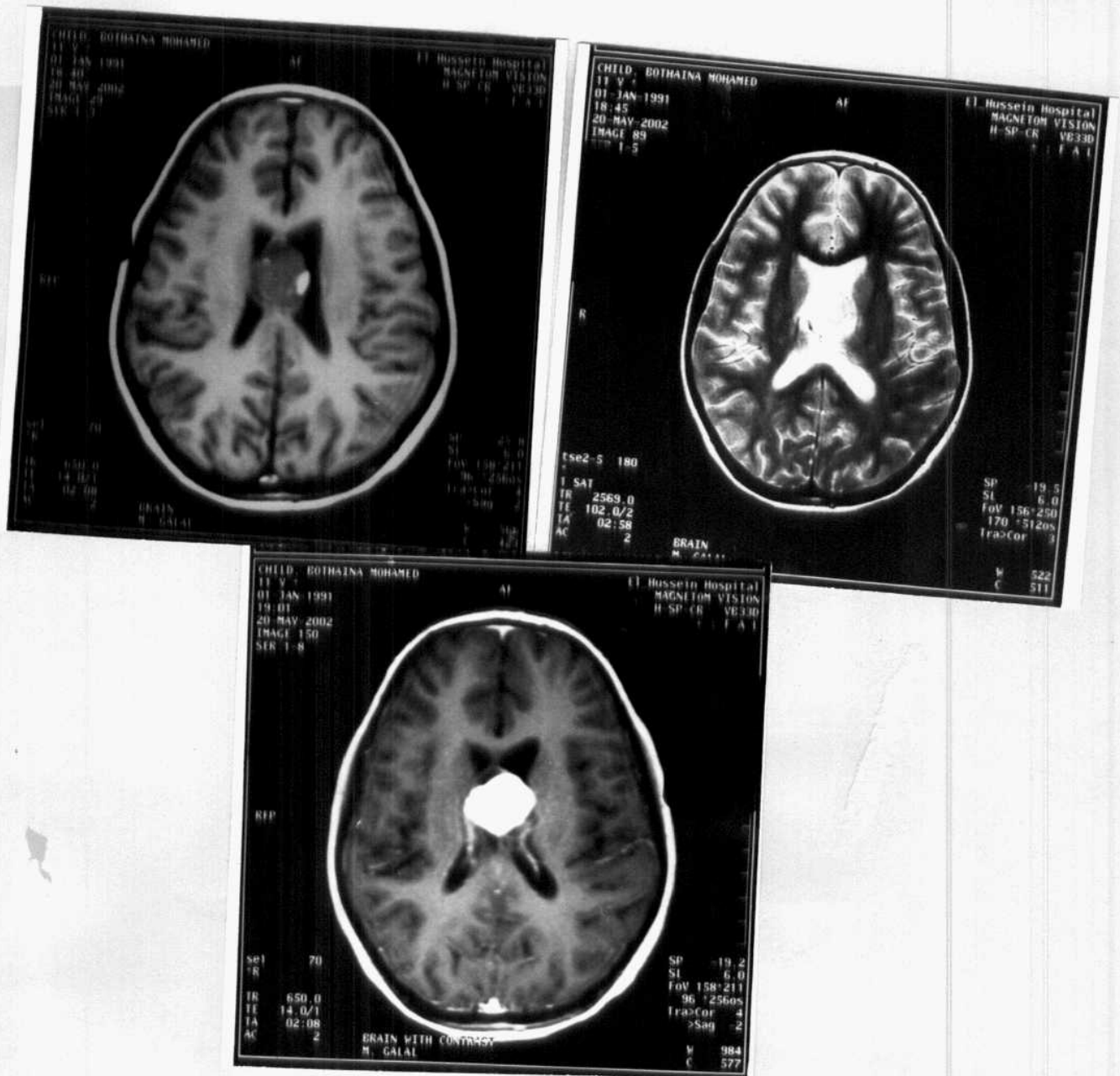


Fig. (37) Intraventricular choroide papilloma.

Discussion

In the diagnostic work up of intracranial tumors, the primary goals of imaging studies are to detect the abnormality, localize and determine the extent of the lesions, and provide a list of differential diagnosis or if possible the specific diagnosis (Ann et al, 1990).

Greenberg et al(1988) summarized the advantages of MRI in comparison to CT in the following: first, the ability to directly image in multiple planes. Second, the visualization of vascular structures without the need for injection of contrast agents. Third, there is no ionizing radiation involved.

Hessilink et al (1989) stated that Gd- DTPA increase both sensitivity and the specificity of MR. It does not cross the intact BBB, but when the BBB is absent or deficient, Gd- DTPA enters the interstitial space to produce enhancement(increase signal) on T1-weighted images.

Glial origin tumors account for 70 to 80 percent of primary intracranial neoplasms in the pediatric population, and astrocytomas account for 21 to 45 percent of this group [Watanabe et al, 1992].

Astrocytomas, are a large group of gliomas and comprise up to 35% of all primary intracranial tumors, they are graded

according to the degree of anaplasia into, low grade astrocytoma (G1 and II) and high grade astrocytoma (GIII and IV) Burge et al., 1994.

Astrocytomas of grade 3 and 4 correspond to the age-honored term (glioblastoma multiform). Some authors favor dividing glioblastomas into two categories : 1) anaplastic astrocytomas or secondary glioblastomas and 2) primary glioblastomas. [Huro Okazaki].

In our study we met 23 cases of gliomas, 11 cases were supratentorial astrocytomas, 4 cases were cerebellar astrocytomas, 7 cases were brain stem gliomas and 1 case was thalamic glioma, 12 cases were females and 11 cases were males, their age ranged between 1 month and 16 years.

Supratentorial low grade astrocytomas are usually slowly growing tumors and demonstrate low signal intensity on T1-weighted images and high signal intensity on T2-weighted images with little mass effect. there is only patchy or no enhancement [Hesselink et al., 1989].

11 cases of supratentorial astrocytomas were encountered in our study, they were isointense to the brain tissue on T1-weighted images with slight heterogenous hypointensity

representing cystic changes and hyperintense on T2- weighted images.

Edema is absent or little with minimal mass effect, contrast enhancement (I.V. Gd – DTPA in 8 cases) revealed faint enhancement in 2 cases, heterogenous enhancement in 4 cases and thin regular ring enhancement in 2 cases.

Johnson et al.(1989) and Black et al. (1991) reported that supratentorial high grade astrocytomas include grade III, and grade IV, are irregular, poorly defined heterogenous masses, demonstrate varying degree of low signal intensity on T1 – weighted images and high signal intensity on T2- weighted images. Associated moderate oedema and mass effect.

The pattern of enhancement is variable from fine rim enhancement, dense thick irregular wall to ring like with central no enhancement representing necrosis or cyst formation [Dean et al, 1990].

Two cases of supratentorial high grade astrocytomas were encountered in our study [with tumor recurrence].

Postoperative MRI with contrast was very important since postoperative gliosis and encephalomalacia may be difficult to differentiate from residual tumor on non contrast MRI.

Cerebellar astrocytomas :

Cerebellar astrocytoma may occur in the cerebellar vermis or hemispheres in children, older patients tending to have eccentric hemispheric lesions. The mass and its cystic components are commonly iso-to hypointense on T1- weighted image and hyperintense to normal tissues on T2- weighted image. Cysts have intermediate signal intensities depending on the protein content of the fluid within, and hemorrhagic cysts are a typical in these low- grade tumors [Zimmerman,1992].

Multiphannar MRI allows differentiation between intra- and extra- axial components with greater clarity than with CT. [Lee et al., 1984].

We have met with 4 cases, they showed the characteristic appearance of the tumor, iso-to hypointense on T1- weighted images and hyperintense on T2- weighted images.

Enhancement with gadolinium -DTPA results in superior differentiation of tumor margins from associated oedema. Enhancement aids the recognition of cystic components that may mimic solid neoplasia on non contrast studies, and allow localization of the mural nodule in tumors composed primarily of a solitary cyst [Bird et al., 1988].

Cystic masses with a mural tumor nodule are typical of cerebellar astrocytoma, however, in older pediatric patients, hemangioblastoma may have similar appearance. [Bird et al., 1988].

Brain stem glioma, MRI is exquisitely sensitive in detecting brain stem pathology, and allows recognition and characterization of lesions that may be totally inapparent on CT. This is particularly true for brain stem tumors that have little associated mass effect or fail to enhance after contrast medium administration. MRI is markedly sensitive for intraparenchymal pathology, eliminates artifact from bone, and can be performed in any plane [Multiplanner]. [Han et al., 1984].

Most brain stem neoplasms are of astrocytic origin, and fibrillary or pilocytic types are common [Cohen, 1984].

Up to 40% [percent] are frankly malignant, as in glioblastoma multiforme. Brain stem gliomas may be eccentric or may involve virtually the entire brain stem diffusely. Those involving the pons and medulla tend to be more aggressive than those of the midbrain. [Smith, 1990].

During our study 7 cases of brain stem gliomas were encountered and MRI provides better visualization of the tumor

extension, displacement of the fourth ventricle and associated cyst formation.

Gadolinium – DTPA enhancement is useful for defining tumor margins apart from oedema analogous to iodinated contrast and CT [powers et al., 1988].

Gadolinium- DTPA was given in 4 cases, three cases revealed heterogenous contrast enhancement and one case revealed no contrast enhancement.

Thalamic gliomas, primary tumors of the deep structures of the brain excluding the relatively benign hypothalamic-chiasmal group are uncommon, accounting for approximately 6 percent of primary brain tumors in children. The biologic behaviour and patient survival rates vary with the degree of malignancy, although these generally are more aggressive than their midline counterparts arising in the hypothalamus and optic chiasma. [Kollias, et al, 1991].

In our study we have met with one case of left thalamic glioma, MRI provides better visualization of the tumor extension.

There was no evidence of contrast injection and no evidence of mass effect or associated brain edema.

Craniopharyngioma has a variable MRI appearance depending on the constituent solid, cystic and cholesterol

components of the mass, variable intensities are noted on T1-weighted images from hypointense [solid] to hyperintense [cyst with cholesterol content]. On T2-weighted images, the tumor appears hyperintense with signal void representing calcification. [Pusey et al., 1987].

It is a primarily tumor of childhood and the most common supratentorial tumor of non glial origin in children. Fifty percent of suprasellar tumors in the paediatric age are craniopharyngioma (Halod et al, 1992).

With MR imaging, a distinct plane is virtually always detected between suprasellar and sellar structures, thus, classic craniopharyngioma is depicted as a mass of the suprasellar cistern distinct from the pituitary gland. The normal pituitary gland is recognized on MRI on the basis of its morphologic appearance and intensities similar those of normal brain parenchyma. It may be obscured or destroyed by extensive intrasellar extension of craniopharyngioma, or by craniopharyngioma arising in the sella. [Pusey1987].

During our study 8 cases of craniopharyngioma were encountered, they showed variable MR signal intensities as follows:

Hypointense signals on T1- weighted images noticed in 6 cases, 4 of them showed areas of hyperintensity which represent lipid or cholesterol content.

Hyperintense signals on T1—weighted images demonstrated on 2 cases

Heterogenous intensity on T1 with multiple focal areas of signal void in 2 cases, mostly due to calcifications.

Compared with CT, coronal and sagittal MRI better demonstrate the extent of the tumor and its relationship to adjacent structures. In particular, the relationship of the tumor to the third ventricle, optic chiasm, hypothalamus, and pituitary gland is better seen with MRI than with CT. [Freeman et al,1987].

Gadolinium – DTPA was administered in 6 cases, ring enhancement noticed in 1 cases, intense enhancement of the solid component noticed in 3 cases with no enhancement of the cystic component, heterogenous enhancement with multiple focal areas of signal void due to calcification noticed in 2 cases.

MR imaging of medulloblastoma demonstrates a midline posterior fossa mass arising in or adjacent to the fourth ventricle with variable eccentricity. On T1- weighted images, medulloblastoma results in a well- defined mass that is iso-or hypointense compared with normal parenchyma. Multiplanar T1-

weighted images provide excellent contrast between soft tissues and CSF, and thus anatomic details of posterior fossa structures and tumor growth within the fourth ventricle are well seen. The signal intensities of both tumor and associated parenchymal oedema are increased on proton density and T2 weighted images in comparison with normal brain, so that tumor margins and oedema are often difficult to differentiate. [Powers et al., 1988].

MR studies of patients with medulloblastoma both at presentation and at follow-up should be performed with intravascular contrast enhancement. Medulloblastoma enhances moderately to markedly on T1-weighted images after administration of gadolinium – DTPA owing to enhancement of areas of blood-brain barrier disruption [Agerlin N, et al., 1999].

This enhancement permits gross definition of tumor margins apart from secondary parenchymal oedema, which is problematic on non-contrast MR studies. Gadolinium-DTPA enhancement is also helpful for differentiation of tumor from postoperative changes. Leptomeningeal seeding that may be entirely hidden on non-contrast studies enhances with gadolinium – DTPA and is readily recognizable [Davis et al., 1987].

Two subgroups of medulloblastomas are identified :

1-Midline tumors (the most frequent type, about 75% occurring mostly in children.

2-Lateral tumors (the minority, about 25% occurring mainly in adults).

8 cases of medulloblastomas were encountered in our study, the most common appearance is of a hypointense mass compared with normal brain on short TR/TE images and hyperintense on long TR/TE images.

Obstructive hydrocephalus is frequent [4cases].

Gadolinium – DTPA was given in 8 cases, the enhancement pattern was mostly heterogenous in 6 cases and homogenous in 2 cases.

Ependymoma, multiplanar MR images demonstrate those arising in the posterior fossa either within or directly involving the fourth ventricle, with variable lateral and cranio caudal extension. Those arising low in the fourth ventricle, adjacent to the medulla, or extending into the upper cervical spine are better defined on MRI than on CT. Calcifications, although common on CT, are infrequently recognizable on MRI, resulting in difficulty

in differentiation of medulloblastoma from ependymoma [Barkovich, Edwards, 1990].

Calcifications, although common, are often inapparent on MRI. This MR limitation is relatively minor, since calcifications are common in other supratentorial neoplasms and not specific for this tumor. Multiplanar MRI is superior to CT for delineation of the relationship of the neoplasm to the ventricular system and for surgical and radiation planning. An aggressive infiltrating supratentorial tumor with ill defined borders and associated edema favors the diagnosis of a more aggressive malignant ependymoma or ependymoblastoma, but on MRI, these may be indistinguishable from each other and from more benign forms of ependymoma. Gadolinium contrast enhancement should be routinely included in the MR evaluation of these tumors because it permits better differentiation of tumor margins from associated edema and from postradiation and postoperative abnormalities [Akyuz C, et al, 2000].

In addition, gadolinium markedly improves the sensitivity of MRI both intracranially and in the spinal canal for detection of metastasis to the leptomeninges, a relatively common occurrence in both ependymoma and ependymoblastoma. [Sze et al., 1988].

During our work, 4 cases were encountered and proved to be ependymomas, variable hypointensity on T1 and hyperintensity on

T2 are typical findings in all cases, foci of low intensity [signal void] in long TR/TE images were noticed within the tumor mass in one case [due to calcifications or hemorrhage]. Gadolinium – DTPA was given in all cases, it showed homogenous enhancement of the tumor in 3 cases and heterogenous enhancement in one case.

Choroid plexus papilloma, Radkowski, et al, 1988 described a neonatal papilloma as a large lobulated tumor of mixed intensity. Tumor intensities in the absence of hemorrhage should be similar to those of other neoplasms on MRI, hypo- to isointensity on T1- weighted and hyperintensity on T2- weighted images. Choroid plexus papilloma not commonly hemorrhage spontaneously, resulting in foci of hyperintensity on T1- weighted images and variable hypointensity on T2- weighted images peripherally [hemosiderin] or centrally [deoxyhemoglobin]. Associated intraventricular or subarachnoid hemorrhage may not be seen on CT. Multiplanar imaging with MRI provides detailed localization of these intraventricular masses relative to the choroid plexus and periventricular tissues. Malignant choroid plexus papillomas may mimic aggressive intra- and periventricular masses, but, multiplanar MR imaging facilitates a correct diagnosis by demonstrating an epicenter within the choroid plexus.

Large or dense calcifications are recognizable on MRI, although small calcifications are more apparent with CT. Gadolinium enhancement assists definition of the mass itself, differential diagnosis, and recognition of CSF seeding, it thus should be routinely included in the MR examination of these patients. Gadolinium- DTPA enhancement is helpful postoperatively for evaluation of recurrent or residual tumor apart from surgical abnormalities. [Radkowski, et al., 1988].

During our work one case of choroid plexus papilloma was encountered, it was isointense to the brain tissue on T1- weighted images and slightly hyperintense on T2- weighted images with hemorrhagic foci seen within the mass. Gadolinium – DTPA revealed intense uniform enhancement.

Pineal region masses, the role of MRI in imaging pineal masses thus far has been to provide excellent anatomic definition of the mass itself and its adjacent tissues for surgical planning and follow- up examination. In children with hydrocephalus, MRI may demonstrate small tumors that are not detected by CT. Pineal masses are homogenously or inhomogenously isointense to hypointense relative to normal parenchyma on T1- weighted sequences. Infrequently, focal areas of increased signal suggest fatty elements of previous hemorrhage. On T2- weighted studies, pineal lesions are variable in intensity. Heavily calcified masses

may be mildly hypointense, although most pineal masses are hyperintense compared with brain. Smaller calcifications are inapparent on MRI. Ill-defined tumor margins and associated secondary edema suggest aggressive or malignant tumor, but, both benign and malignant masses may be well circumscribed on MRI. [Edwards, et al., 1988].

Gadolinium administration should be included for initial study of a pineal mass to define the primary lesion, distinguish between cystic and solid masses, exclude an associated suprasellar lesion [Edwards, et al., 1988].

In our work 2 cases of pineal region masses were encountered, one case of pineal germinoma and the other case was pinealoma, pineal germinoma showed isointensity on T1-weighted images and hyperintense on T2-weighted images with intense contrast enhancement on administration of gadolinium-DTPA, pineoblastoma appeared as a large heterogeneously enhancing mass following administration of gadolinium DTPA.

Meningiomas This is rare in children with an incidence of 2.4% of all primary intracranial tumors, with many of them arising in arachnoidal granulation (Erdinler et al, 1998). They occur mainly above the tentorium cerebelli in relation to venous sinuses and occasionally they occur within a lateral ventricle (one quarter of paediatric meningiomas are intraventricular). The absence of

dural attachment is more common in children than in adults. [Davis,1990].

Pediatric meningiomas tend to be larger and more aggressive than the adult tumors. Childhood meningiomas occur in the same location as adult meningiomas [calvarial surface, skull base, tentorium, orbit], but there is a higher incidence of intraventricular meningiomas in children and a higher incidence of cystic meningiomas. Children also have a higher incidence of malignant degeneration of meningiomas. [Davis, 1990].

In contrast to adult meningiomas, which are common in women, pediatric meningiomas have an equal sex incidence. The MR appearance of meningiomas is a mass that is isointense to hypointense on T1- weighted scans and bright on T2-weighted scans. The tumor enhances brightly. Dense calcifications are better seen on CT. Hyperostosis related to meningioma is also better demonstrated by CT. Edema surrounding meningioma is variable. In our study, one case of meningioma was encountered, it appeared slightly hypointense on T1 and hyperintense on T2 with intense contrast enhancement following gadolinium DTPA administration.

Aneurysms, are most commonly found in middle aged women and usually present with sign more indicative of a mass lesion [Nathal et al.,1992].

Aneurysm of the vein of galen, this is in fact another manifestation of cerebral angioma, the dilated vein being secondary to AV shunting through an angioma usually in the brain stem or medial temporal lobes, some cases presenting in infancy, however, seem to be due to a congenital malformation of the venous system. The hugely dilated central nervous structure is a persistent embryonic vein known as the median vein of the prosencephalon. The AV shunt is from choroidal arteries opening directly into the vein. Heart failure or irreversible brain damage may occur and also a form of hydrocephalus in which ventricular shunting may be detrimental and is to be avoided [David sutton, 1998].

In our study one case of aneurysm of the vein of galen was encountered, it appeared hyperintense on T1 and T2 weighted images with a central hypointense thrombus formation and revealed intense contrast enhancement following gadolinium DTPA administration, the aneurysm was proved by MRA and MRV.

Metastatic disease accounts for 15% to 25% of intracranial tumors. The involvement of the brain takes many forms, ranging from hematogenous metastases to the brain meninges, direct spread to the brain and meninges from primary tumors of the

skull base and face, or intracranial dissemination of primary and secondary brain tumors via CSF pathways (Russell et al, 1989).

Hematogenous metastasis to brain parenchyma are uncommon in the pediatric population, most commonly resulting from hematopoietic malignancies. Skull metastasis to the bone or adjacent dura arise in neuroblastoma, lymphoma and leukemia

. Uncommon skull primary tumors and tumors arising adjacent to the skull base (orbit, nasopharynx, middle ear) may invade the CNS, as in chondrosarcoma, osteosarcoma, rhabdomyosarcoma and nasopharyngeal malignancy.

Leptomeningeal seeding in the intracranial space or spinal canal results from systemic disorder generally of the hematopoietic system, e.g, leukemia and lymphoma, or from other CNS tumors [Uchino A, et al, 1993].

Two cases of pediatric intracranial metastasis were encountered, they appeared isointense on T1 and T2 weighted images with heterogenous contrast enhancement following gadolinium DTPA administration in one case and intense enhancement at the other one [the last case was potoperative removal of pineoblastoma].

Summary And Conclusion

MRI is a sensitive technique for delineation of brain morphology in the axial, coronal and sagittal planes [multiplanar] without changing patient position or any biological hazards.

In this work, we study the role of MRI in the evaluation of pediatric intracranial tumors. The study was divided into many chapters. The first chapter demonstrate the anatomy and MR sectional anatomy of the brain. The next chapter dealt with the pathological features of the most important and common brain tumors after their histological classifications. The third chapter mention a small hint on the other modalities of diagnosis of pediatric intracranial tumors. The fourth chapter mention a small hint on the physical principles of MRI. The fifth chapter dealt with the materials and methods used in this work and mention the MRI technical aspect, followed by the results, this chapter ends by a series of illustrated cases to the most common pediatric intracranial tumors. The study is supported by many figures which help in the explanation and by a lot of references which collected and alphabetically rearranged at the end of the work as a single chapter followed by the Arabic summary. Fifty cases of pediatric intracranial tumors were selected in this study. 26 cases were females, and 24 cases were males, their age ranged between 30 days and 16 years.

The selected cases were subjected to full clinical history, radiological examination as CT scanning, finally the MRI examination.

The selected cases were classified into 10 groups according to the final diagnosis.

MRI, provides information about intrinsic tumor vascularity, as well as the effects of tumors on the adjacent arterial and venous channels, this information can be of great value to the neurosurgeon in the preoperative planning.

MRI with contrast enhancement, IV- Gd – DTPA, is valuable in more accurately defining the anatomic boundaries of the tumors, distinguishing it from the surrounding edema and detection of residual or postoperative recurrence.

The use of MR angiography is greatly valuable in the diagnosis of vascular lesion such as aneurysm and arteriovenous malformation.

The superiority of MRI over CT is prominent in the following Situations;

- Tumors that contain cystic components

- Determination of blood vessels affection.
 - Detection of edema.
 - Tumors of the posterior fossa.
 - Tumors in contact with CSF.

However, CT at the present time remain superior in:

Bone eroding and pathological calcifications producing tumors.

Scanning facility including time, availability and price.

From our study we can conclude that MRI with its multiplanar capabilities, availability of various pulse sequences, high contrast resolution and superior contrast enhancement pattern provide high diagnostic capabilities in identification and characterization of intracranial tumors. Moreover, the application of new technique as MR angiography and MR venography well lead to more accurate diagnosis.

REFERENCES

- Adamas Hume J, Graham D. I. And Harriman D. G. F (1988). In An introduction to neuropathology, pp44 – 56 and 227-265.
- Agerlin N, Gjerris F, Brincker H et al. (1999) : Childhood medulloblastoma in denmark 1960-1984. A population-based retrospective study, Childs Nerve Syst, Jan 15: 129-36.
- Ambrosino MM, Genieser NB, Roche KJ : Infant cranial sonography. Appl Radiol 21:14 46, 1992.
- A. James Barkovich, MD, et al : Neuroimaging Clinics of North America, Pediatric Neuroradiology, May 1994.
- Allen JC, Miller DC, Bodzilovich GN, et al : Brain and spinal cord hemorrhage in longterm survivors of malignant pediatric tumors : Neurology 41 : 148 – 150, 1991.
- Altman NR, Purser RK and Post MDJ (1988): Tuberos sclerosis : characteristics at CT and MR imaging Radilogy:167 : 527-523.
- Akyuz C, Emir S, Akalan N et al. (2000) Intracranial ependymomas in childhood a retrospective review of

sixty two children, Acta Oncol 39 : 1 97 – 100.

Anderson JE (1983) : The head in Grants atlas of anatomy, 8 th edition section 7, Wilkins, Baltimor, london.

Anne C Price, Val M Runge and Gregory V Babigian(1990) : Brain neoplastic disease, 4 th ed., clinical MRI, philadelphia, J.B Lippincott Co., 3 : 113-176.

Aoki S, Barkovich Aj, Nishimura K et al. (1989) : Neurofibromatosis type 1 and 2 : cranial MR findings.

Balakrishnan Rajan, Sue Ashley, David G. T. Thomas, et al : Craniophayngioma:Improving outcome by early recognition and treatment of acute complications. Int. J. Radiation Onchology Biol. Phys. Vol. 37,No 3,517-521,1997.

Bakovich AJ, Kjos BO, Jackson DE, et al : Normal maturation of the neonatal and infant brain : MR imaging at 1.5 T. Radiology 166:173 180, 1988.

Bakovich AJ, Edwards MSB : Brain tumors in childhood. In Barkovich AJ, (ed) : Pediatric Neuroimaging. New York, Raven Press, 1990, pp 149-204.

Barnes PD, Urion DK, Share JC: Clinical principles of pediatric neuroradiology. In Wolpert SM, Barnes PD (eds) : MRI

in pediatric neuroradiology. St. Louis, Mosby,1992,pp
41-82

Benitez WI, Glasier CM, Husain M, et al : MR findings in
childhood gangliogliomas. J Comput Assist Tomogr 14 :
712, 716,1990.

Bilaniuk T, Zimmerman RA, Littman P,et al : Computed
tomography of brain stem gliomas in children. Radiology
134 : 89 95, 1980.

Bird CR, Drayer BP, Median M, et al. Gd DTPA – enhanced MR
imaging in pediatric patients after brain tumor resection.
Radiology 1988, 169 : 123-126.

Black KL, Mazziotta JC and Becker DP(1991): Brain tumors,
west J.Med.,154-186.

Blickman JG, Jaramillo D, Cleveland RH : Neonatal cranial
ultrasonography. Curr Probl Diagn Radiol 20:91-
119,1991].

Bloom H. J. G., Gless J. , and Bell J. (1990). The treatment and
long term prognosis of children with intracranial tumors.
A study of 610 cases, 1950 1981. Int. J. Radiation
oncology Biol. Phys., 18 : 723 – 745.

Boyko OB, Curnes JT, Oakes W J et al. (1991) : Hamartomas of

the tuber cinereum CT, MR and pathogenic findings.
AJNR, 12, 309.

Braffman BH, Bilanuik LT, Naidich TP et al.(1992): MR imaging of tubrous sclerosis : pathogenesis of this phakomatosis, use of gadopentetate dimeglumine and literature review, Radiology,183:227.

Burger PC and Scheithauer BW (1994) : Tumors of the central nervous system Washington, DC : Armed factors institute of pathology.

Bydder GM, Kingsley DP, Brown J et al. (1985) : MR imaging of meningioma including studies with and without Gd DTPA J comput Assist Tomogr., 9 : 690-697.

Byrne JV, Kendall BE, Kingsley DP et al : Lesions of the brain stem, Assessment by MR imaging, Neuroradiology, 31 : 129-133, 1989 .

Carpenter MB, Sutin J : The cerebellum. In Human neuroanatomy, ed 8, Baltimore, 1983, Williams Wilkins.

Castillo M, Davis PC Takei Y, Hoffman JC. Intracranial ganglioglioma : MR and CT findings in 18 patients. ANJR 1990. 11 : 109-114.

Castillo M (1994): Contrast enhancement in primary tumors of

the brain and spinal cord. Neuroimaging clinics of North America,4:63.

Centeno PS, Lee AA, Winter J, et al : Supratentorial ependymomas. J Neurosurg 1986 : 64 : 209 - 215.

Chiechi M V, Smirniotopoulos JG and Mena H (1995) : Pineal Parenchymal tumors CT and MR features. J Comput Assist tomogr., 19 : 509- 517.

Cohen ME, Duffner PK. Brain tumors in children. Principles of diagnosis and treatment. New York : Raven press, 1984.

Colt JS and Blair A (1998). Parental occupational exposures and risk of childhood cancer. Environ – Health Perspect. Jun. 106 suppl 3: 909 – 25.

Cordier S, Lefeurve B, Fillipini G,et al : Parental occupation, occupational exposure to solvents and polycyclic aromatic hydrocarbons and risk of childhood brain tumors (Italy, France, Spain). Cancer – Causes Control. Sep, 8(5) :688 –97, 1997 .

Courchesne E, Press GA. Murakami J, et al : The cerebellum in sagittal plane : anatomic – MR correlation. 1. The vermis, AJNR 10:659 - 656, 1989.

Curnes JT, Laster DW, Ball MR, et al : Magnetic resonance

imaging of radiation injury to the brain. AJNR 1986;7:
389 - 394.

David Sutton (1998) MD FRCP (Hon). Consulting Radiologist, St
Marys Hospital and the National Hospital for Neurology
and Neurosurgery, London, UK.

Davis PC, Friedman NC, Fry SM, et al. Leptomeningeal metastasis
: MR imaging. Radiology 1987, 163 : 449-454.

Davis PD : Tumors of the brain. In Cohen MD, Edwards MK(eds)
: Magnetic Resonance Imaging of children. Philadelphia,
BC Decker, 1990,pp 155-220.

Dean BL, Draver BP, Bird CR et al. (1990) : Gliomas
classification with MR imaging, Radiology, 174: 111-
115.

Denasy R, Vanpachterbeke T, Toppet V, et al : Prediction of
cerbral palsy in high risk neonates :A technetium -99m -
HMPAO SPECT study. J Nucl Med 34: 1223 1227,
1993].

Deutsch M : Medulloblastomas : Staging and treatment outcome.
Radiat Oncol Biol Phys 14 : 1103-1107, 1988.

Devi BI, Shukla D, Bhat D et al (2001). Hypothalamic tumor with
haemorrhage, Childs Nerv Syst Sep 17:9 567- 9.

- Diebler C, Dulac O. Pediatric neurology and neuroradiology. Cerebral and cranial diseases. Berlin : Springer Verlag, 1987.
- Doumalin CL (1992) : Phase contrast magnetic resonance angiography. Neuroimaging, Clinics of North America, 2 : 801-817.
- Drayer B, Burger P, Darwin R et al. (1986) : MRI of brain iron., AJNR, 7 : 373-380.
- Drophco EJ (1989) : The remote effects of cancer on the nervous system, Neurol clin., 7 :579-604.
- Duffner PK, Cohen ME, Freeman AL. Pediatric brain tumors : an overview. CA 1985 : 35 : 287 -301
- Duffner P.K and Cohen M.E (1986). Recent developments in pediatric Neuro Oncology. Cancer 58 : 561-568.
- Edwards MSB, Hudgins RJ, Wilson CB, et al. Pineal region tumors in children. J neurosurg 1988, 68 : 689-697.
- Elster AD, Challa VR, Gilbert TH et al.(1989): Meningiomas MR and histopathologic features. Radiology, 170:857-862.
- Epstein F, Wysoff JH: Intrinsic brain stem tumors in childhood: Surgical indications. J Neuro oncol 6:309-317, 1988.

- Erdincler P, Lena G, Sarioglu A C, et al (1998). Intracranial meningiomas in children: review of 29 cases. Surg Neurol. Feb,49(2) : 136 -40.
- Eric N. Faerber, MD, and Nancy V. Roman, MD: Radiological clinics of North America Volume 35. Number b. November 1997.
- Fitz CR (1985) : Neoplastic diseases, in Gonzalez CF, Grossman CB, Masdeu JC (Eds) : Head and spine imaging : New York, John Wiely & Sons, 483-521.
- Flodmark O, Jan JE, Wong PK : Computed tomography of the brains of children with cortical visual impairment. Dev Med Child Neurol 32 :6611 620, 1990.
- Freeman MP, Kessler RM, Allen JH,et al : Craniopharyngioma : CT and MR imaging in nine cases. JCAT 1987; 11 : 810-814.
- Gado MH and Tobben PJ (1992) : Supratentorial anatomy in Stark DD and Bradly WG, (eds) MRI, CV Mosby Lovis,557-572.
- Gerber CJ, Neil, Dwyer G and Evans BT (1989) : An alternative surgical approach to aneurysms of the posterior cerebral artery. Neurosurgery, 19 : 689-723.

- Ghika JA, Bogousslavsky J and Regli F (1990) : Deep perforator from the carotid system. Arch. Neurid, 47 : 1097-1110.
- Glasier GM, Husain MM, Chadduk W et al : Meningiomas in children : MR and histopathologic findings. AJNR, 14:237-241, 1993 .
- Gray H (1977) : The blood vascular system, in Pick TP and Howden R (eds) : Anatomy descriptive and surgical, Bounty Books, New York.
- Grossman CB, Masdeu JC, Marvilla KR et al (1985) : Intracranial Tumors of the adult : In Gonzalez CF (eds) : Head and spine imaging, New York, John Wiley & Sons, 225-281.
- Gusnard DA : Cerebellar neoplasms in children. Semin Roentgenol 25 : 263- 278, 1990.
- Han JS, Bonstelle CT, Kaufman B, et al. Magnetic resonance imaging in the evaluation of the brain stem. Radiology 1984; 705-712.
- Harlod J. Hoffman, Marcia De Silva, et al (1992). Aggressive surgical management of craniopharyngiomas in children. J. Neurosurg 76:47 - 52.
- Hauro Okazaki, MD. Fundamental of Neuroradiology. Morphological basis of Neurologic Disorders, second

edition. Mayo Medical school. 347. 038 1989.

Hesselink JR and Press GA (1989) : MR contrast enhancement of intracranial lesions with Gd DTPA, Radiol., Clin. North Am., 26: 873.

Higano S, S Takahashi, N. Kurihara, et al (1997). Supratentorial primary intra axial tumors in children. Acta Radiologica 38,945 952.

Hicks RJ, Hesselink JR, Wismer GL et al : Brain vascular diseases in Edelman, RR(eds): Clinical MRI, WB Saunders, Philadelphia, 516-544,1990 .

Hirsch WL, Kemp SS, Martinez AJ. et al : Anatomy of the brainstem : correlation of in vitro MR images with histologic sections. AJNR 10:923 928. 1989.

Horvath E. and Kovacs K. (1986). Identification and classification of pituitary tumors. In : Recent advances in Neuropathology, vol. 3, pp75 93. Edited by J. B. Cavanagh. Edinburgh: Churchill Livingstone.

James E. Hector and Edwards S. B Michael(1985). Sytemic staging of supratentorial extra axial brain tumors in children. Cancer56:1800 1803.

Ji BT, Shu XO, Linet MS, Zheng W, et al (1997). Paternal

cigarette smoking and the risk of childhood cancer among offspring of non smoking mothers. J Natl Cancer Inst. Feb 5,89(3):238 4.

Johnson PC, Hunt SJ and Drayer BP (1989) : Human cerebral gliomas, correlation of postmortem MR imaging and neuropathologic findings, Radiology, 170:211.

Kaba SE and Kyritsis AP(1997). Recognition and management of gliomas. Drugs. Feb: 53(2):235- 44.

Keler PJ (1992) : Time of flight, MR angiography. Neuroimaging clinics of North America, 639-656.

Kollias SS, Barkovich AJ, Edwards MSB : Magnetic resonance analysis of suprasellar tumors of childhood Pediatr Neurosurg 17 : 284 – 303, 1991.

Kortman KE, Bradley WG(1988): Supratentorial neoplasm in stark DD, Bradley WG (eds) : MRI, CV Mosby ST, Louis.

Kouwenhoven M, Baker CJ and Harthamp MJ (1994) : Current MR angiographic imaging techniques. Vascular diagnosis, Springvelag , Heideberg.

Kristensen P, Andersen A, Irgens LM, et al : Cancer in offspring of parents engaged in agricultural activities in Norway:

incidence and risk factors in the farm environment. Int J Cancer Jan 3,65 (1):39-50, 1996 .

Kune LE, Kovnar EH, Sanford RA : Ependymomas in children. Pediatr Neurosci 14 : 57-63, 1988.

Latchaw RE and Nadell J (1976) : Intra and extracerebral arachnoid cyst. AJR, 126: 629-633.

Lea JS, Pinto RS, Huiiat GF et al. (1979): Computed tomography of arachnoid cyst. Radiology, 130: 675-680.

Lee BCP, Kneeland JB, Deck MDF, et al : Posterior fossa lesions : magnetic resonance imaging. Radiology 1984; 153 : 137-143.

Lee BCP, Kneeland JB, Chill P et al : MR recognition of supratentorial tumors. AJNR, 6: 871-878, 1985.

Leibel A. Steven and Sheline E. Glenn(1987). Radiation therapy for neoplasms of the brain. J. Neurosurg. 66: 122.

Lenart Hardell, Bo Holmberg, Hans Malker, et al : What is the the aetiology of human brain tumors? Cancer. March 1, vol. 77 Number 5: 1006-1009, 1996.

Liao MF, Chaou WT, Taso LY, et al : Ultrasound measurement of the ventricular size in newborn infants. Brain Dev 8:262

268, 1986.

Lockhart RD, Hamilton GF, Fyle FW : anatomy of the human body, London, 1974, JB Lippinco H.

Makow LS (1989) : MRI, brief review of image, Radiology Clin. North America, 227(2) : 195-218.

Malluci CL, Parkers SE, Barber P et al, (1996). Pediatric meningeal tumors. Childs Nerv Syst. Oct, 12(10):582-8.

Martin JH (1989) : Vasculature of the central nervous system. In Neuro anatomy Text & Atlas, Elseiver, New York .

Maroldo TV, Barkovich AJ: Pediatric brain tumors. Semin Ultrasound CT MRI 13:412-448,1992.

Mauricio Castillo, Peckers SE (1998). MR Characteristics of pediatric intracranial tumors. 13 : 212-224.

McArdle CB, Richardson CJ, Hayden CK et al: Abnormalities of the neonatal brain :MR imaging. Part 1. Intracranial hemorrhage. Radiology 163:387-394,1987.

Mc Girr SJ, Ebersold MJ, Scheithauer BW, et al. Choroid plexus papillomas : Long term follow up results in a surgically treated series. J. Neurosurg 1988 : 69 : 843-849.

Mc Kean Cowdin R, Preston Martin S, et al, (1998). Parental

occupation and childhood brain tumors: astroglial and PNETs. J Occup Environ Med. Apr,40(4):332-40.

Medlock MD, Olivero WC, Hanigan WC, et al : Children with cerebral venous thrombosis diagnosed with magnetic resonance imaging and magnetic resonance angiography. Neurosurgery 31: 870-876, 1992.

Meyers SP, Kemp SS, Tarr RW : MR imaging features of medulloblastoma. AJR Am J Roentgenol 158 : 859-865, 1992.

Miki Y, Mastuo M and Nishizawa S et al. (1990) : Pituitary adenomas and normal pituitary tissue enhancement pattern on enhanced MRI, Radiology, 177:35.

Naidich TP, Daniels DL, Houghton VM et al. (1987) : Hippocampal formation and related structures of the limbic lobe, Anatomic MR correlation, Part1, surface features and coronal sections, Radiology, 162 : 747 – 754.

Naidich TP, Zimmerman RA, Primary brain tumors in children. Semin Roentgenol 19 : 10 : 100-114, 1984.

Nakagawa H, Iwaski S, Kichikawa K et al. (1990) : MR imaging of pineocytoma, report of two cases, AJNR, 11 : 195-

198.

Nathal E, Yasui N, sampei T and Suzuki A (1992) : Intraoperative anatomical studies in patients with aneurysms of the anterior communicating artery complex. J. Neurosurg., 76 : 629-634.

Osborn AG (1994) : Normal vascular anatomy. In : Patterson, AS. (ed.) Diagnostic Neurosurgery, Mosby.

Paker DR, Yuan C and Blatter DD (1991) : MR angiography by multiple thin slab 3D a quisation. Mag. Reso. Med., 17 : 434-451

Paley RJ, Persing JA, Doctor A et al. (1989) : Multiple sclerosis and brain tumor : a diagnostic challenge, J. Emerg. Med., 7 (3) : 241-244.

Pieree Yves Dietrich, Paul R. Walker, Philippe Saas, et al : Immunobiology of gliomas : New perspectives for therapy. Ann N Y Acad Sci. Sep. 17:824:124-140,1997.

Potchen EJ and Perncione ES (1996): Intracranial vascular anatomy in MRA, concept and applications potchen EJ, sibert JE and Gottschalk A (eds). Mosby, St. Louis, 33 363-380.

Powers TA, Partain CL, Dessler RM, et al. Central nervous

system lesions in pediatric patients: Gd DTPA enhanced MR imaging. Radiology 1988; 169 : 723-726.

Press GA, Murakami J, Courchesne E, et al : The cerebellum in sagittal plane ; anatomic – MR correlation.2. The cerebellar hemispheres, AJNR 10 : 667-676,1989.

Press GA, Murakami JW, Courchesne E, et al : The cerebellum. 3. Anatomic – MR correlation in the coronal plane, AJNR 11 : 41-50, 1990.

Pusey E, Kortman KE, Flannigan BD et al. (1987) : MR of craniopharyngiomas, tumor delineation and characterization, AJNR, 8 : 439-444.

Radkowski MR, Naidich TP, Tomita T, et al. Neonatal brain tumors : cT and MR findings. JCAT 1988; 12 : 10-20.

Rodriguez LA, Edwards MSB, Levin VA (1990) : Management of hypothalamic gliomas in children, an analysis of 33 cases. Neurosurgery, 26:242-247.

Russell DS, Rubinstein LJ. Pathology of tumors of the nervous system. 5th ed. Baltimore : Williams & Wilkins, 1989.

Schneider JH, Raffel C, Mc Comb G : Benign cerebellar astrocytomas of childhood. Neurosurgery 30 : 58 – 63, 1992.

- Scheithauer, B. W. (1984). Surgical pathology of the pituitary: part 1 and 2. In : pathology annual. Vol. 19 parts 1 and 2. pp 317-374 and 269-329. Edited by S. C. Sommers and pp. Rosen.
- Schrittlein HN and Murlagh FR (1990) : Imaging anatomy of the head and spine. Blatimore, Urban Schwarzenburg.
- Schwaighofer BW, Hesselink JR, Press CA et al. (1989): Primary intracranial CNS lymphoma. MR manifestation. AJNR, 10: 725-729.
- Scotti G, Yu CY and Dillon WP et al. (1988) :MR imaging of cavernous sinus involvement by pituitary adenomas. AJR, 151 : 799-806.
- Shalet SM, Brennan BM, and Reddingius RE (1997). Growth hormone therapy and malignancy. Horm Res, 48 Suppl 4:29-32.
- Sibert JE, Perinico JR and Potchen EJ (1992) : Physical principles and application of MR angiography. Seminar in ultrasound, CT and MRI, 13 (4) : 227-245.
- Smith AS, Benson JE, Bloser SI (1991) : Diagnosis of ruptured intracranial dermoid cyst : Value of MR over CT. AJNR, 12 : 175.

- Smith RR : Brain stem tumors. *Semin Roentgenol* 25: 249 – 262, 1990.
- Sze G, Abramson A, Krol G, et al. Gadolinium DTPA in the evaluation of intradural extramedullary spinal disease, *AJNR* 1988; 9 : 153-164.
- Teele RT, Share JC: Crainal Ultrasonography. In Teel RT (ed) : *Ultrasonography of infants and children*. Philadelphia, WB, Saunders, 1991, pp 156.
- Teresi LM and Davis SJ (1992) Cerebrovascular malformations in magnetic resonance angiography in Stark DD and Bradley WG (eds). *Mosby*, 29 : 963-985.
- Tampieri D, Melanson D, Ethier R (1989) : MR imaging of epidermoid cysts. *AJNR*, 10 : 351-356.
- Tice H, Barnes PD, Goumnerova I, et al (1993): Pediatric and adolescent oligodendrogliomas, *AJNR*, 14: 1293.
- Tien RD, Barkovich AI and Edward MSR (1990) : MR imaging of pineal tumors. *AJNR*, 11 : 557.
- Truwit CL, Lempert TE (1994) : High resolution atlas of cranial neuroanatomy. Baltimore, Williams and Wilkins.
- Uchino A, Hasuo K, Matsumoto S, et al: MRI of dorsal

mesencephalic lipomas. Clin Imag 17 : 12-16, 1993. .

Vats T.S. (1997). Adjuvant chemotherapy of pediatric brain tumors. Ann N Y Acad Sci Sep. 17 :824 :156-166.

Waggenspack GA and Guinto FC jr. (1989): MR and CT of masses of the anteriosuperior third ventricles, AJR, 152: 609.

Watanabe M, Tanaka R, Takedan : Magnetic resonance imaging and histopathology of cerebral gliomas. Neuro radiology 34 : 463-469, 1992.

Wehrli FW (1988) : Principles of MR in : Stark DD, Bradyley WG (eds) : MRI ST Louis, Mosby 3 : 22.

William F. Regine and Simon Kramer (1992). Pediatric craniopharyngiomas : Long term results of combined treatment with surgery and radiation. I. J. Radiation Onchology Biol. Phys. Vol. 24:611-617.

Wisoff H. Jeffery (1995). Tumors of the cerebral hemispheres. In Paediatric neurosurgery. Surgery of the developing system, 3rd ed. Chapter 30, pp 392-402.

Yachins A T (1997). Neuropathology of pediatric brain tumors. Semin paeditar – Neurol. Dec, 4 (4):282-91.

- Young IR, Bailes D, Burl M, Collins A et al. (1982) : Initial clinical evaluation of a whole body NMR, J. Comput. Assist. Tomogr., 6 : 118.
- Yuh WTC, Tali ET, Nguyen HD et al. (1995) : The effect of contrast dose, imaging time and lesion size in the MR detection of intracranial metastasis. AJNR, 16 : 373-380.
- Zimmerman RA, Bilaniuk LT, Brunol, Rosenstock J : Computed tomography of cerebellar astrocytoma. AJR AM J Roentgenol 130 : 929-933, 1978.
- Zimmerman RD, Fleming CA et al. (1985): MRI of meningiomas, AJNR, 6: 149-157.
- Zimmerman RA (1990) : Imaging of intrasellar, suprasellar and parasellar tumors, Semin, Roentgenol, 25 : 174.
- Zimmerman RA, Bilaniuk LT, Rebsamen S: Magnetic resonance imaging of pediatric posterior fossa tumors. Pediatr Neurosurg 18:58-64, 1992.
- Zulch KJ, Medulloblastoma. In: Zulch KJ, ed. Brain tumors. Their biology and pathology. 3rd ed. Berlin: Springer Verlag, 1986: 324-340.

ARABIC SUMMARY

المخلص العربى

تناولت هذه الرسالة دراسة دور الفحص بالرنين المغناطيسى فى تشخيص اورام المخ عند الأطفال .

تم تقسيم الرسالة إلى عدة فصول :

* تناول الفصل الأول شرح تفصيلى للناحية التشريحية للمخ وأجزاءه كما تظهر بواسطة الفحص بالرنين المغناطيسى .

* أما الفصل الثانى فيتضمن تقسيم وتوضيح للمظاهر الباثولوجية لمعظم وأهم أورام المخ عند الأطفال .

* وفى الفصل التالى تم اعطاء فكرة مبسطة عن الطرق الأخرى فى التشخيص .

* وفى الفصل التالى تم إلقاء الضوء على الأساس الفيزيائى للرنين المغناطيسى وكيفية تكوين الصورة .

* وفي الفصل التالى تناولت الرسالة بالعرض عدد الحالات المستخدمة مع إلقاء الضوء على النواحي الفنية والعملية وكيفية الفحص الذى تم إجراءه للحالات التى تضمنتها رسالته .

* وقد أيدنا الجانب النظرى فى هذا العمل بفصل منفصل يحتوى على عرض صور لأهم حالات أورام المخ عند الأطفال كما تظهر بالفحص بالرنين المغناطيسى .

* وقد أضيف فى نهاية الرسالة قائمة للمراجع الخاصة التى أستخدمت فى موضوع البحث بعد ترتيبها أبجدياً .

* اشتملت الرسالة على ٥٠ حالة جميعها تعاني من أورام المخ عند الأطفال, ٢٦ حالة من الإناث و ٢٤ حالة من الذكور, أعمارهم تتراوح بين ٣٠ يوم - ١٦ سنة .

* تم تقسيم الحالات إلى ١٠ مجموعة حسب التشخيص النهائى لكل مجموعة .

* من الدراسة تبين أن الفحص بالرنين المغناطيسى يتفوق على الأشعة المقطعية فى حالات أورام المخ بصفة عامة يضاف إلى ذلك عدم استخدام أشعة

مؤينة وتوضيح الرشح الداخلى للمخ من الورم الرئيسى ولكن الأشعة المقطعية تتفوق على الرنين المغناطيسى فى الحالات الآتية :

- الأورام المصاحبة بتكلس أو الأورام المصاحبة بتآكل فى العظام المجاورة يضاف إلى ذلك قصر مدة إجراء الفحص ورخص ثمنة مع كثرة انتشار أماكن الفحص .

- وفى النهاية نستنتج أن الفحص بالرنين المغناطيسى أكثر حساسية فى تشخيص أورام المخ عند الأطفال وأورام المخ بصفة عامة مع الأخذ فى الاعتبار طول مدة الفحص واستبعاد المرضى الذين تحتوى أجسامهم على أشياء معدنية وتركيبات صناعية مثل منظمات ضربات القلب أو أى شرائح معدنية. يضاف إلى ذلك وهو الأهم عدم استخدام أشعة مؤينة .

دراسة دور الرنين المغناطيسي فى تشخيص أورام المخ عند الأطفال

رسالة مقدمة من

الطبيب / مختار رجب رمضان محمود

مدرس مساعد الأشعة بكلية الطب جامعة الأزهر

توطئة للحصول على درجة الدكتوراة فى الشعبة التشخيصية

تحت إشراف

أ.د / هشام عبد الرازق أحمد جلال

أستاذ الأشعة التشخيصية كلية الطب - جامعة الأزهر

أ.د / صلاح الدين محمد كريم

أستاذ مساعد الأشعة التشخيصية كلية الطب جامعة الأزهر

أ.د / شهاب محمد الخضراوى

استاذ جراحة المخ والأعصاب كلية الطب جامعة الأزهر

كلية الطب جامعة الأزهر

٢٠٠٣